



Durham E-Theses

Synthesis and application of cyclodextrin conjugates.

Skinner, Phillip J.

How to cite:

Skinner, Phillip J. (1999) *Synthesis and application of cyclodextrin conjugates.*, Durham theses, Durham University. Available at Durham E-Theses Online: <http://etheses.dur.ac.uk/4542/>

Use policy

The full-text may be used and/or reproduced, and given to third parties in any format or medium, without prior permission or charge, for personal research or study, educational, or not-for-profit purposes provided that:

- a full bibliographic reference is made to the original source
- a [link](#) is made to the metadata record in Durham E-Theses
- the full-text is not changed in any way

The full-text must not be sold in any format or medium without the formal permission of the copyright holders.

Please consult the [full Durham E-Theses policy](#) for further details.

**Synthesis and Application
of
Cyclodextrin Conjugates.**

Philip J. Skinner

A thesis submitted for the degree of Doctor of Philosophy

Department of Chemistry
University of Durham
1999

The copyright of this thesis rests
with the author. No quotation
from it should be published
without the written consent of the
author and information derived
from it should be acknowledged.



27 JAN 2000

Abstract.

Synthesis and Application of Cyclodextrin Conjugates.

Cyclodextrins, a family of compounds formed from a cyclic array of glucose monomers, contain a hydrophobic cavity which displays selective complexation of size specific guests. This selective molecular recognition is critical to the development of successful chemosensors. A selection of cyclodextrin-conjugates have been designed to report complexation of guests into the cyclodextrin cavity by optical and electrochemical means.

Alkylated cyclodextrins containing a single linker group have been synthesised allowing the development of two cyclen-appended cyclodextrin conjugates and their lanthanide complexes. The tetraamide ligand (**25**) displayed a high rigidity, assessed by ^1H NMR and luminescence methods. The Tb complex of the monoamide ligand [**Tb.26**] displayed long lived luminescence arising from energy transfer from cyclodextrin-complexed naphthalene to the lanthanide. The association constant, K_{11} , between naphthalene and the cyclodextrin [**Tb.26**], was calculated as $10,200\text{ M}^{-1}$. K_{11} between the Gd complex [**Gd.26**] and GdDOTAPh (**40**) was determined to be 1740 M^{-1} by NMRD. These association constants are *ca* 14 and 7 times greater respectively than for the corresponding complexes with β -cyclodextrin (**1**).

Bromonaphthalenes exhibit long lived phosphorescence when complexed within cyclodextrins. Four bromonaphthalene-appended cyclodextrins (**57-60**) were designed to form intramolecular self-complexes. Competitive complexation of optically transparent guests was expected to reduce the lifetime of phosphorescent emission. The four conjugates were successfully synthesised, although luminescence studies revealed no evidence for complex formation and no response upon competitive guest complexation was observed.

The rotaxane (**95**) and corresponding thread (**92**) of a hydrophilic ferrocene-cyclodextrin conjugate were made and structurally assessed by CD, ^1H NMR and MALDI-TOF MS. The hydrophilic per-O-ethyl conjugates (**93** & **100**) were also synthesised. A lipophilic quinoline-cyclodextrin conjugate (**94**) was made, which, when incorporated into an optode membrane, allowed the detection of acetylcholine at micromolar concentrations.

Philip John Skinner, 1999.

Declaration.

The work described herein was carried out in the Department of Chemistry, University of Durham, between October 1996 and September 1999. The contents of this thesis represents the work of the author unless indicated to the contrary or indicated by reference. This work has not been submitted for a higher degree in any other academic institution.

Statement of Copyright.

The copyright of this thesis rests with the author. No quotation from it should be published without prior consent and information derived from it should be acknowledged.

Acknowledgements.

I would like to thank my supervisor, Professor David Parker, for his kind help, support, encouragement and advice throughout these three years. Without David, this would have come to nothing. I would also like to thank Dr. Andrew Beeby for all his constructive advice and practical help with the luminescence work, Dr. Ritu Katakya and Stephanie Blair for the membrane studies, Prof. Silvio Aime and Prof. Mauro Botta for the NMRD profiles, Dr. Alex Drake and Dr. Giuliano Siligardi for the circular dichroism studies, and Prof. D. Games and the EPSRC National Mass Spectrometry Service Centre for accurate mass-mass spectrometry.

I am also grateful to all the staff in the department, without whom this work would not have been possible; including Alan Kenwright, Ian MacKeag and Catherine Hefferman for NMR, Lara Turner and Mike Jones for Mass Spectrometry, Lenny Lauchlin for HPLC and Ray, Gordon and Malcolm for glassblowing.

I am especially grateful to all members of the Wolfson laboratory (CG27), past and present, without whom I would have been totally lost. I would especially like to thank Dr Linda Govenlock and Dr Stephen Faulkner, and my 'partner in arms' Ian Clarkson.

Financial support from the BBSRC is gratefully acknowledged.

I would like to thank Mum and Dad for supporting me this far and always believing in me. Finally, my greatest thanks are for Sarah who has kept me sane, happy and provided love, friendship and a continual shoulder for me. Without her, I would not have believed in myself.

Thank you all.

Abbreviations.

amu	Atomic mass units.
ax	Axial.
BET	Back energy transfer.
br	Broad.
Bu	Butyl.
CD	Circular dichroism.
CD	Cyclodextrin
Cyclen	1, 4, 7, 10-Tetraazacyclododecane.
CHN	Carbon, hydrogen, nitrogen combustion analysis.
d	Doublet.
dd	Doublet of doublets.
ddd	Doublet of doublet of doublets.
DCM	Dichloromethane.
DMAP	4-Dimethylaminopyridine.
DMF	N, N-Dimethylformamide.
DMP	Dess-Martin periodinane.
DMSO	Dimethylsulfoxide.
DO3A	1, 4, 7, 10-Tetraazacyclododecane triacetate.
DOS	Bis(2-ethylhexyl) sebacate.
DOTA	1, 4, 7, 10-Tetraazacyclododecanetetraacetate.
DTPA	Diethylenetriaminepentaacetic acid.
EDC	1-(3-Dimethylaminopropyl)-3-ethylcarbodiimide hydrochloride.
EI	Electron impact ionisation.
en	Ethylenediamine.
eq	Equatorial.
ESMS	Electrospray mass spectrometry.
ET	Energy transfer.
Et	Ethyl.
EtOH	Ethanol.
FTIR	Fourier transform infra-red.
HOBt	1-Hydroxybenzotriazole.
Inc	Including.

IR	Infra-red.
ISE	Ion selective electrode.
J	Coupling constant.
K ₁₁	1:1 Binding constant.
lit.	Literature.
Ln	Generic symbol for lanthanide.
M	Generic symbol for metal.
M	Mol dm ⁻³ .
m	Multiplet.
MALDI-TOF	Matrix assisted laser desorption ionisation-time of flight.
Me	Methyl.
Mesyl (Ms)	Methanesulfonyl.
MeOH	Methanol.
<i>m</i>	Meta.
m	Multiplet.
mp	Melting point.
MRI	Magnetic resonance imaging.
MS	Mass spectrometry.
NMR	Nuclear magnetic resonance.
NMRD	Nuclear magnetic resonance dispersion.
<i>o</i>	Ortho.
<i>p</i>	Para.
PES	Phosphorescence emission spectrum.
psi	Pounds per square inch.
Ph	Phenyl.
PGSE	Pulsed gradient filed spin echo.
PVC	Polyvinyl chloride.
pyr	Pyridine.
q	Quartet.
RMM	Relative molecular mass.
s	Singlet.
<i>t</i>	Tertiary
t	Triplet.
td	Triplet of doublets.

TES	Total emission spectrum.
TFA	Trifluoroacetic acid.
THF	Tetrahydrofuran.
tlc	Thin layer chromatography.
2, 6-TNS	2- <i>p</i> -Toluidino-6-naphthalenesulfonate.
Triflate	Trifluoromethanesulfonate.
tris	Tris(hydroxymethyl)aminomethane.
Tosyl (Ts)	<i>p</i> -Toluenesulfonyl.
tt	Triplet of triplets.
UV	Ultra violet.
VT	Variable temperature.

Contents

Chapter 1. Introduction.

1. Introduction	1
1.1 Chemosensor Design.	2
1.2. Cyclodextrins As Neutral Synthetic Receptors.	3
<i>1.2.1 Structural Properties Of Cyclodextrins.</i>	3
<i>1.2.2 Guest Binding In Cyclodextrins.</i>	5
<i>1.2.3. Nomenclature of Functionalised Cyclodextrins.</i>	6
<i>1.2.4. Functionalisation of Cyclodextrins.</i>	7
<i>1.2.5 Selective Functionalisation of Cyclodextrins.</i>	8
1.3. Luminescence and the Lanthanides.	12
<i>1.3.1 Photophysics Of Luminescence.</i>	12
<i>1.3.2 Luminescence From Europium (III) And Terbium (III).</i>	14
<i>1.3.3 Sensitised Luminescent Emission.</i>	15
<i>1.3.4 Yb Luminescence.</i>	19
1.4 References.	19

Chapter 2. Lanthanide-appended Cyclodextrin Systems.

2. Lanthanide-appended Cyclodextrin Systems.	22
2.1 Introduction	23
<i>2.1.1 Lanthanides as Luminescent Reporters.</i>	23
<i>2.1.2 Existing Cyclodextrin-lanthanide-appended Systems.</i>	24
2.2 Design of Novel Lanthanide-cyclodextrin-appended Detection Systems.	27
2.3 Synthetic Methodology.	32
<i>2.3.1 Synthesis of a Monofunctionalised Cyclodextrin Linker.</i>	32
<i>2.3.2 Synthesis of Lanthanide Complexes of a Cyclodextrin Tetraamide Ligand</i>	36
<i>2.3.3 Synthesis of Lanthanide Complexes of a Cyclodextrin Monoamide Ligand.</i>	38
2.4 Structural Studies on Lanthanide Complexes.	39
<i>2.4.1 ¹H NMR Conformational Studies on Lanthanide Complexes of the Tetraamide.</i>	39

2.4.2 <i>¹H NMR Conformational Studies on Lanthanide Complexes of the Monoamide.</i>	42
2.4.3 <i>Luminescence of the Lanthanide Complexes.</i>	45
2.4.4 <i>Determination of Bound Water By Lifetime Measurement of the Monoamide Complexes.</i>	49
2.4.5 <i>Determination of Bound Water by Lifetime Measurement of the Tetraamide Complexes.</i>	50
2.5 <i>Relaxivity and Paramagnetic Ions.</i>	52
2.5.1 <i>NMRD Profiles of the Monoamide Complex [Gd.26].</i>	53
2.5.2 <i>Interactions Of The Monoamide [Gd.26] With The Paramagnetic DOTAPh-Gd (III) Complex [Gd.40].</i>	54
2.6 <i>Luminescence Properties.</i>	56
2.6.1 <i>Detection Properties of the Tetraamide Complexes [Eu.25] & [Tb.25].</i>	56
2.6.2 <i>Detection Properties of the Monoamide Complexes [Eu.26], [Tb.26] & [Yb.26].</i>	58
2.7 <i>Photokinetic Studies.</i>	62
2.7.1 <i>Variable Temperature Luminescence.</i>	64
2.7.2 <i>Flash Photolysis Of Naphthalene-cyclodextrin-lanthanide Conjugates</i>	66
2.8 <i>References.</i>	69

Chapter 3. Bromonaphthalene-appended Cyclodextrin Systems.

3. <i>Lanthanide-appended Cyclodextrin Systems.</i>	71
3.1. <i>Introduction.</i>	72
3.1.1. <i>Chromogenic Indicators.</i>	72
3.1.2. <i>Fluorescence Change Indicators.</i>	74
3.1.3. <i>Phosphorescent Enhancement of Bromonaphthalenes in Cyclodextrin.</i>	77
3.2. <i>Aims.</i>	80
3.3. <i>Synthetic Methodology.</i>	82
3.3.1. <i>Synthesis of [6'-(2'-Bromonaphthyl)methylcarbamoyl]-per-O-methyl-β-cyclodextrin (57).</i>	82
3.3.2. <i>Synthesis of [5'-(1'-Bromonaphthyl)ethylcarbamoyl]-per-O-methyl-β-cyclodextrin (58).</i>	84

3.3.3. Synthesis of Mono-[2'-(1'-bromonaphthyl)ethylcarbamoyl]-per-O-methyl- β -cyclodextrin (59).	87
3.3.4 Synthesis of Mono-{1'',3''-bis-[2'-(1'-bromonaphthyl)]-2''-butylcarbamoyl}-per-O-methyl- β -cyclodextrin (60).	89
3.4. Luminescence Studies.	90
3.5. Further Work.	93
3.6. References.	94

Chapter 4. Detectors for Flow and Membrane Inclusion.

4. Detectors for Flow and Membrane Inclusion.	95
4.1 Introduction.	96
4.1.1 <i>Cyclodextrins in Ion Selective Electrodes.</i>	96
4.1.2 <i>Ferrocene-cyclodextrin Conjugates.</i>	97
4.1.4 <i>Optodes.</i>	97
4.1.4 <i>Cyclodextrins in Capillary Electrophoresis.</i>	98
4.2 Aims.	99
4.3. Synthetic Methodology.	101
4.3.1. <i>Synthesis of Hydrophilic Ferrocene-cyclodextrin Conjugates (92 & 95)</i>	101
4.3.2 <i>Synthesis of Monofunctionalised Lipophilic Cyclodextrins.</i>	103
4.3.3. <i>Synthesis of Lipophilic Ferrocene-cyclodextrin Conjugates (93 & 100).</i>	104
4.3.4. <i>Synthesis of a Lipophilic Cyclodextrin For Optometry (94).</i>	105
4.4. Detection Properties.	107
4.4.1 <i>Detection Properties of the Quinoline-appended Cyclodextrin (94).</i>	107
4.5 References.	110

Chapter 5. Experimental Methods.

5 Experimental Methods.	111
5.1 Methods.	112
5.2 Experimental for Chapter 2.	115
5.3 Experimental for Chapter 3.	131

5.4 Experimental for Chapter 3.	147
5.5 References.	153

Appendices

Appendix A. Calculation of Binding Constants by Benesi-Hildebrand Analysis	156
Appendix B. Research Colloquia and Lectures.	159
Appendix C. Conferences.	164

Chapter 1

Introduction.

1 Introduction.

The concept of molecular recognition was first proposed by Fischer in the late 19th century when he discussed the idea of a "lock and key" system.¹ He identified the concepts of molecular recognition as analogous to a lock and key, the molecular receptor acting as a lock and the key being a substrate that is selectively recognised by the receptor to form a receptor-substrate complex. Since then chemists have striven to replicate the ability of biological systems to select and signal the presence of specific chemical species.

This thesis describes attempts to develop a range of novel selective chemical signalling systems utilising cyclodextrin derivatives as molecular recognition sites. Chapter 1 describes the concepts of chemosensor design, concentrating on the use of cyclodextrins as molecular recognition sites and on the properties and derivatisation of cyclodextrins. The photophysics of phosphorescence and long-lived lanthanide luminescence as a convenient mechanism for reporting molecular recognition are then discussed. Chapter 2 describes the development of cyclodextrin systems appended to lanthanide binding sites which were designed to report molecular recognition through long-lived lanthanide emission. Existing cyclodextrin-lanthanide conjugates are described, as are the structural and detection properties of the systems developed. Chapter 3 outlines the synthesis and properties of bromonaphthalene-appended cyclodextrin systems, designed to report molecular recognition through enhanced phosphorescence. Chapter 4 describes the synthesis of cyclodextrin-based detectors designed for use in capillary flow systems or for inclusion into polymer membranes. The final chapter details the experimental methods used throughout this work.

1.1 Chemosensor Design.

The design of chemosensors, detectors designed for the recognition of specific chemical species, has long been of interest to chemists. Sensors for pH, pO₂, pCO₂ and concentrations of glucose and common alkali and alkaline earth ions have been

developed, particularly for clinical monitoring. However the development of chemosensors for other industrially or biologically important chemical species, such as amino acids, neurotransmitters, coenzymes or nucleotides, has proved more difficult.²

A chemosensor must possess two distinct components. Firstly, a chemosensor must contain an appropriate receptor subunit for molecular recognition of the species to be detected. Ideally this receptor should display a large selectivity for the substrate of interest over similar species. Binding of the desired substrate must also be strong enough to allow a useful limit of detection, but not so strong that equilibrium is slow to be restored. Secondly, the chemosensor must report the binding event to the observer in a useful format.

1.2. Cyclodextrins As Neutral Synthetic Receptors.

Molecular recognition is critical to all life systems. The clinical role of enzymes and antibodies relies on their ability to recognise a particular substrate in preference to any other molecules. Since their discovery, chemists have attempted to replicate the behaviour of existing natural systems with synthetic analogues. Amongst these attempts, the family of cavitands, molecules which provide a cavity which is able to hold and complex a suitable guest, have proven remarkably successful as models of natural systems. Within this broad family are the families of crown ethers and cryptands, cyclophanes, calixarenes, cyclotrimeratrylenes and cryptophanes, carcerands and hemicarcerands and cyclodextrins.³ Of particular interest in this thesis is the structure and properties of cyclodextrins.

1.2.1 Structural Properties Of Cyclodextrins.

Cyclodextrins are a family of compounds formed from a cyclic array of α -1,4-linked glucose monomers (Figure 1.1). The most common members of the family, in order of decreasing availability, are β -cyclodextrin (1), α -cyclodextrin (2) and γ -cyclodextrin (3), macrocycles containing 7,6 and 8 glucose units respectively.^{4a} The

cyclodextrin family are generally synthesised through degradation of starch by the enzyme glucosyltransferase. This gives rise to a variety of cyclic and acyclic dextrans from which the α -, β - or γ -cyclodextrins can be selectively extracted. α -Cyclodextrin (2) has also been synthesised from maltose in 21 steps with an overall yield of 0.3%^{3b} although this doesn't offer a useful route into cyclodextrin chemistry.

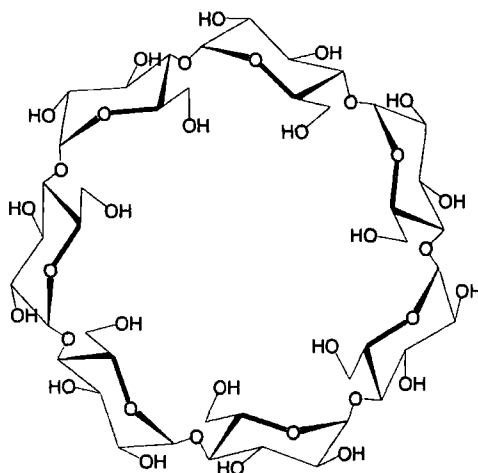


Figure 1.1. Looking down the primary face of β -cyclodextrin (1).

The conformation of the glucose subunits in cyclodextrins gives rise to a structure resembling a 'molecular bucket.' Each glucose subunit contains a primary hydroxy group on the 6-position, and two secondary hydroxy groups on the 2- and 3-positions. The cyclic compounds form into a hollow truncated cone shape with the primary (6-) hydroxyls located on the narrow face of the torus and the secondary (2- and 3-) hydroxyls at the wider face. The non-bonding electrons of the glycosidic oxygens are directed into the centre of the cavity formed, as are the 3- and 5-hydrogen atoms. This gives the molecule a hydrophobic cavity with Lewis-base character and two polar hydrophilic rims (Figure 1.2).^{*.4}

* The hydrophilic rims of the cavity are also referred to as the primary, or secondary faces.



Figure 1.2. Molecular models of β -cyclodextrin (**1**) showing the hydrophobic cavity. The secondary and primary faces respectively are shown.

1.2.2 Guest Binding In Cyclodextrins.

Cyclodextrins have been found to act as hosts for binding size-matched guests. The hydrophobic cavity of β -cyclodextrin (**1**) has a volume of 346\AA^3 , a depth of 7.9\AA and a diameter at the widest (secondary) face of 7.8\AA .⁵ β -Cyclodextrin (**1**) has been found to form stable 1:1 complexes with single, double and triple aromatic ring (eg phenyl, naphthyl and anthryl) derivatives with preferential binding towards larger substrates. Preferential binding is also shown towards non-charged species (see Table 1.1).

Substrates larger than the cyclodextrin cavity can partially insert, where the part of the molecule which interacts most strongly with the cavity will be inserted with the remainder of the molecule sitting outside.⁶ In such cases 2:1, 3:1 and higher order host:guest complexes can also be formed.⁷ Guests substantially smaller than the cyclodextrin cavity can form association dimers (1:2 host:guest complexes)⁸ or lower order complexes.

The chirality of the glucose subunits which define the cavity also allows chiral recognition: the complexes of the methyl esters of tryptophan and phenylalanine

have been shown to exhibit preferential binding with a selectivity of greater than 5:1 for the D-isomer over their respective enantiomers.⁸

Host	Guest	Binding constant K_{11}/M^{-1}	Ref.
β -cyclodextrin (1)	Benzene	169	3c, 9
β -cyclodextrin (1)	Naphthalene	685	3c, 10
β -cyclodextrin (1)	Anthracene	3870	3c, 11
β -cyclodextrin (1)	Phenanthrene	1500	3c, 10
β -cyclodextrin (1)	$C_6H_5CO_2H$	794	3c, 12
β -cyclodextrin (1)	$C_6H_5CO_2^-$	60	3c, 12
β -cyclodextrin (1)	2,6-TNS* (4)	1980	4, 13
Per-OMe- β -cyclodextrin (5)	2,6-TNS (4)	2180	4, 14

Table 1.1. 1:1 Binding constants for some host-guest cyclodextrin complexes (H_2O , 293K).

1.2.3. Nomenclature of Functionalised Cyclodextrins.

Naming of perfunctionalised cyclodextrins, where functionalisation occurs in an identical manner on all of the glucose residues, is fairly trivial. The nomenclature of cyclodextrins which have been selectively functionalised to alter one or more of the glucose monomers uniquely is less simple. The glucose residue containing the largest substituent is named A, the others are named B, C, D etc anticlockwise looking down on the primary hydroxyl face (Figure 1.3).⁴ Thus the naming of the molecule reflects not only the position of a substituent on the glucose residue, but also the residue which has been substituted.

* 2-*p*-Toluidino-6-naphthalenesulfonate

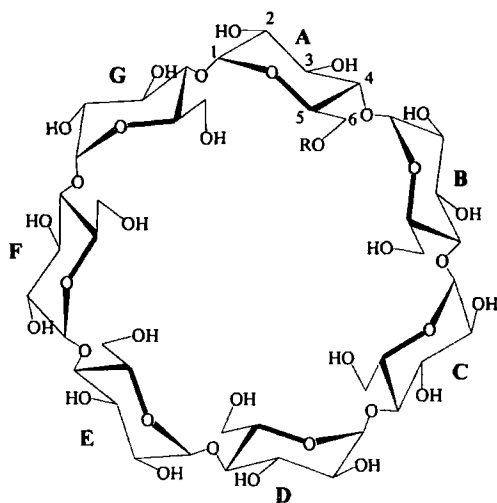


Figure 1.3. Looking down at the primary face of a mono-6-O-functionalised β - cyclodextrin

1.2.4. Functionalisation of Cyclodextrins.

Functionalisation of the hydroxyl groups of cyclodextrin can significantly alter the nature of cyclodextrin host-guest chemistry. Permethylation of the hydroxyl groups causes the two previously hydrophilic faces to become more hydrophobic in character. For β -cyclodextrin this essentially increases the length of the cavity from 7.9Å to about 11Å.^{3d} The increased hydrophobicity of the cavity also slightly increases the stability of complexes with some hydrophobic guests, as is shown by the increase in the 1:1 binding constant with 2-*p*-toluidino-6-naphthalenesulfonate (2,6-TNS, **5**) (see Table 2.1).⁴

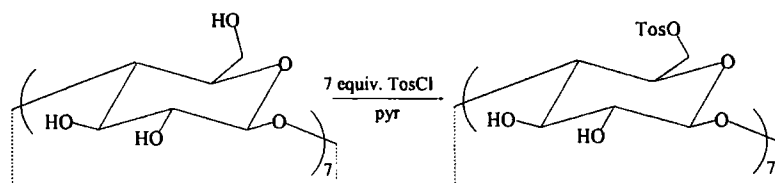
Functionalisation of the cyclodextrin hydroxyl groups can also alter the physical properties of the host. Perhaps the most dramatic change is the increase in aqueous solubility observed on methylation of the C(2) and C(6) hydroxyls of β -cyclodextrin. A strong intermolecular hydrogen bonding network exists for solid β -cyclodextrin that is maintained in solution. Solvation requires disruption of this network hence β -cyclodextrin has a low water solubility (1.85 g/100 cm³/25°C) despite its strongly polar character. Methylation of all but the C(3) hydroxyls increases the solubility in cold water to approximately 50% w/v. Conversely, permethylation of all the

hydroxyl groups reduces the solubility compared to the C(2,6)-O-methyl cyclodextrin, although the permethylated derivative is still significantly more water soluble than the parent β -cyclodextrin.⁴

1.2.5 Selective Functionalisation of Cyclodextrins.

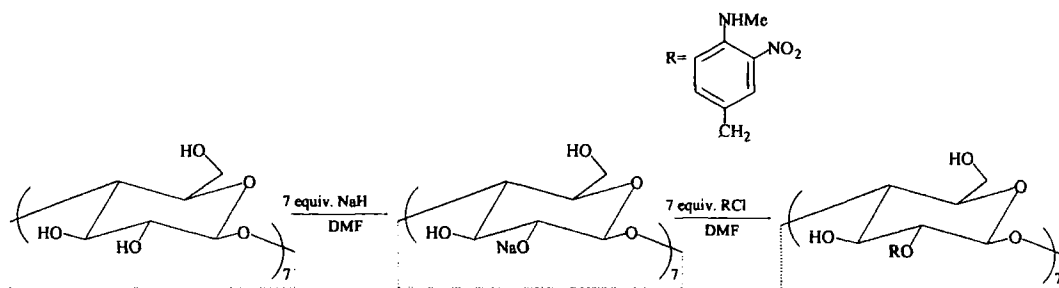
The readily available cavity of cyclodextrins have made them obvious targets for binding studies with a range of guests. This work has led to the development of more advanced systems, such as enzyme mimics,¹⁵ containing both binding and active sites. Such work has demanded selective functionalisation of the cyclodextrins to control both solubility and reactivity requirements. An obvious route into the functionalisation of the cyclodextrins utilises the primary and secondary hydroxyl groups on the lower and upper rims. The relative reactivities of the C(2), C(3) and C(6) hydroxyls can be used to provide per-functionalised systems. However more subtle methodology is required to give selective functionality.

Hydroxyls on the primary face of cyclodextrins, at the C(6) position, are the least sterically crowded and most solvated of the cyclodextrin hydroxyl groups. They are also the most nucleophilic and least acidic positions. Deprotonation with a weak base, such as pyridine, will selectively occur at the C(6) hydroxyl. Nucleophilic substitution, for example with *p*-toluenesulfonyl chloride (1), will also selectively occur at C(6) before the C(2) and C(3) positions (Scheme 1.1).



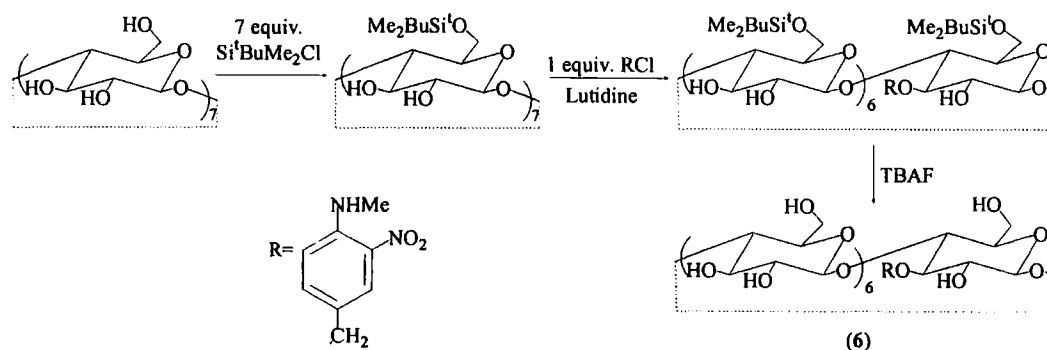
Scheme 1.1. Selective reaction of the C(6) hydroxyl.¹⁶

The proximity of the C(2) hydroxyl to two acetal linkages makes it the most acidic group, with a pK_a of *ca* 12.4.⁴ Deprotonation with strong bases, such as sodium hydride, and subsequent electrophilic attack by species such as methyl iodide¹⁷ occurs preferentially at the C(2) hydroxyl before the remaining sites (Scheme 1.2).



Scheme 1.2. Selective reaction of the C(2) hydroxyl.¹⁷

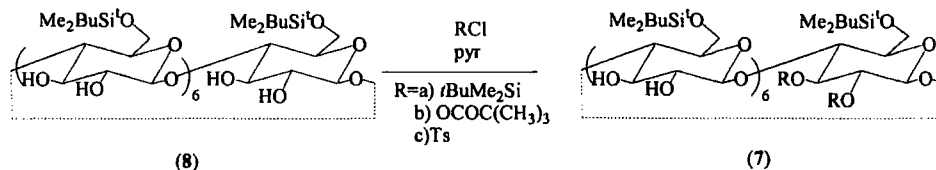
Selective reaction of the C(3) hydroxyls of cyclodextrin is more problematic and the general approach is to protect the C(6) hydroxyls using the aforementioned methodology. The C(3) position can then be selectively functionalised with a weak base and a non-labile electrophile, followed by removal of the protecting C(6) groups (Scheme 1.3) to yield a C(3) modified product (6).¹⁸



Scheme 1.3 Selective reaction of the C(3) hydroxyl.¹⁸

It can be seen from this synthesis that addition of a single equivalent of the electrophile yields a monosubstituted species. Indeed the synthesis of mono-functionalised cyclodextrins has remained a synthetic target, allowing the coupling of cyclodextrins to a variety of species to render them suitable for use in situations such as enzyme mimics, catalysts, monolayer generation and chiral separation gas chromatography.¹⁹ A similar approach has been used for synthesis of a mono-2-O-modified β -cyclodextrin (7) (Scheme 1.4). Use of a per-6-O-protected- β -cyclodextrin (8) allows addition of the *t*-butyldimethylsilyl, 2,2,2-trimethylacetyl or toluenesulfonyl moiety to a C(2) hydroxyl group.²⁰ In this case however

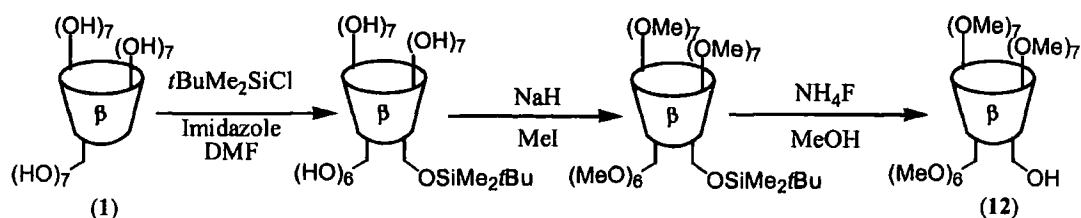
monomodification occurs despite use of a large excess (5-30 equivalents) of the electrophile, the lack of more extensive substitution has not been explained.



Scheme 1.4 Monomodification of the C(2) hydroxyl.²⁰

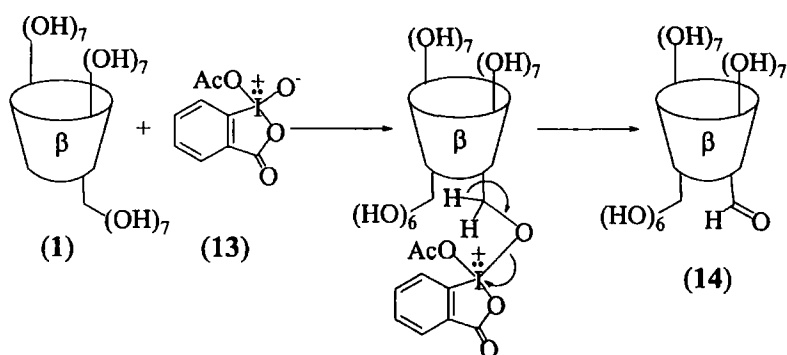
Most other examples of monosubstituted cyclodextrins have been selectively functionalised on the primary face. Of these, most preparations start with addition of a single tosyl group onto a C(6) hydroxyl. Nucleophilic substitution of the monotosylate (9) allows the synthesis of mono-azido (10),^{19,21} halo^{22, 23} and amino (11)^{24,25,26} cyclodextrins and thereafter a variety of tethered species. Low yields during tosylation (ca 20%⁴) have inhibited the suitability of this route yet its use remains common. A recent improvement to the procedure has been reported by Bittman *et al.*²⁷ In contrast to typical procedures where tosyl chloride is reacted with cyclodextrin in anhydrous pyridine, Bittman allows an association complex to form between tosyl anhydride and cyclodextrin in aqueous solution. Addition of base then forms 6-tosyl- β -cyclodextrin (9) in 61% yield.

An alternative to the tosylation route has been reported by Bradshaw *et al.*²⁸ (Scheme 1.5). In the synthesis of a mono-unfunctionalised cyclodextrin derivative, a single 6-hydroxy group is protected with *t*-butyldimethylsilyl chloride; Permethylolation of the remaining hydroxyls is then effected in a ‘one-pot’ reaction. Removal of the protecting group yields mono-hydroxy-per-O-methyl- β -cyclodextrin (12) in a relatively high yield (43%). The single remaining hydroxyl is then open to further functionalisation without danger of competitive reaction from remaining functionality within the cyclodextrin. Use of a greater excess (3.5 equivalents) of *t*-butyldimethylsilyl chloride also allowed synthesis of the di-unfunctionalised 6^A,6^B-, 6^A,6^C and 6^A,6^D-dihydroxy-per-O-methyl- β -cyclodextrins in 7.6%, 8.3% and 8.9% yields, respectively.²⁹



Scheme 1.5 Preparation of mono-6-hydroxy-per-O-methyl- β -cyclodextrin (12).²⁸

Another route to 6-monofunctionalised cyclodextrins has been reported by Bieniarz *et al.*³⁰ (Scheme 1.6). In this synthesis a 6-hydroxyl group of cyclodextrin is oxidised to an aldehyde in a single step using the Dess-Martin periodinane reagent (DMP, 13). The authors report that further oxidation of remaining hydroxyls is suppressed by the presence of the aldehyde functionality. Yields are reported to be between 80 and 100%, the yield being largely dependent on the quality of the DMP (13). This synthesis suffers from the commercial unavailability of DMP (13), although a straightforward synthetic route to DMP (13) has recently been reported.³¹



Scheme 1.6 Synthesis of β -cyclodextrin-mono-6-aldehyde (14).³⁰

A more comprehensive review of selective cyclodextrin modification strategies has been given by D'Souza *et al.*³²

1.3. Luminescence and the Lanthanides.

1.3.1 Photophysics Of Luminescence.

Luminescence may be defined as the emission of light which is not caused by a thermal population of an excited state. Of particular interest is photoluminescence, the emission of light caused by the absorption of light of equal or greater energy. Photoluminescence can be separated into two distinct phenomena, fluorescence, the direct and rapid emission of light of equal or lower energy than the light absorbed, and phosphorescence, the slower emission of light of lower energy than the light absorbed.

Both fluorescence and phosphorescence result from an excitation from the substrate's electronic ground state (commonly S_0 for organic systems) to a higher excited state (commonly S_1). In fluorescence, the substrate rapidly relaxes to the various vibrational energy levels of the ground state, hence emitting light of approximately equal energy to that absorbed (Figure 1.4). The lifetime (defined as the reciprocal of the rate constant for non-radiative decay, k_{ns}) for the process is generally between 10^{-12} and 10^{-8} seconds.³³ In contrast, during phosphorescence the substrate relaxes by a process of intersystem crossing to a lower energy level with a higher spin state (commonly T_1). Relaxation to the ground state is a spin forbidden transition and therefore occurs more slowly than fluorescence. The lifetime of phosphorescence is generally between 10^{-6} and a few seconds.³³

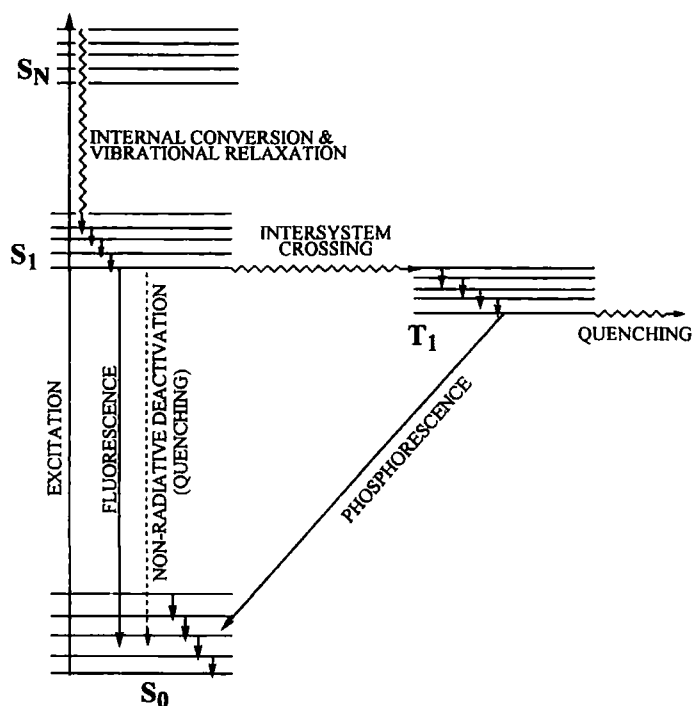


Figure 1.4. Simplified Jablonski diagram illustrating processes of fluorescence and phosphorescence.

The ease of monitoring luminescent emission renders it ideal for use as a reporting mechanism for intended chemosensors. One significant problem with detecting luminescent emission however is that of background fluorescence which can mask the luminescent signal under observation. This is particularly significant for detection of species in clinical samples where a number of naturally occurring compounds are also found to display 'autofluorescence'. The long emission lifetimes of phosphorescent systems can be used to avoid this problem. Phosphorescence experiments can be 'time gated,' where the collection of data is delayed for a short time after the initial stimulation, allowing the background fluorescence to subside before collection of results starts (Figure 1.5).

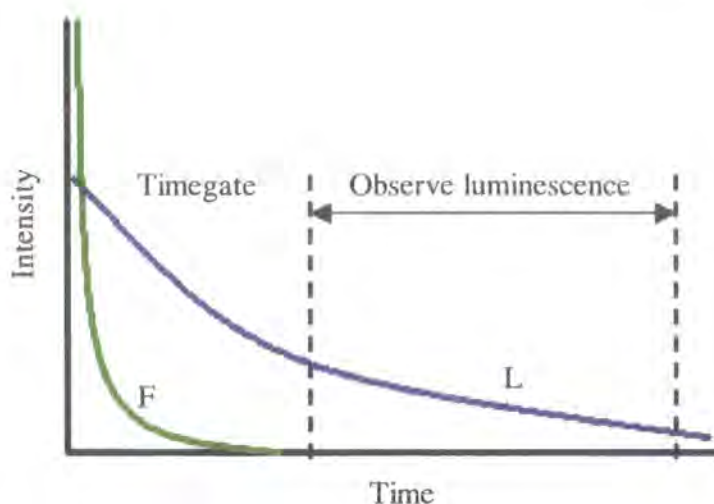


Figure 1.5 Time-gating' of luminescence to selectively detect long lived luminescence (L) against a background fluorescence (F).

1.3.2 Luminescence From Europium (III) And Terbium (III).

Of all the lanthanide(III) ions, it is the photophysical properties of complexes of the central lanthanides, samarium(III), europium(III), terbium(III) and dysprosium(III) that have generated the most interest. The gadolinium(III) system has too large an energy gap between the emissive and ground states to be of practical use, the wavelength of emission being too far into the uv (312nm).³⁵ The remaining ions have a small energy gap between the ground and excited states and hence the excited state is easily deactivated by H-O and D-O oscillators before phosphorescence can occur.³⁶

The larger energy gaps of europium(III) and terbium(III) are deactivated by higher harmonics of the H-O and D-O oscillators than the remaining lanthanide(III) ions. This gives rise to poor Franck-Condon overlap with the metal excited state. This in turn leads to increased lifetimes, the observed lifetimes of europium and terbium being of the order of milliseconds.³⁴ The energy gaps of europium(III) and terbium(III) can also be seen to overlap very inefficiently with higher harmonics of D-O compared to H-O oscillators, thus deactivation of the lanthanide excited states is found to be less in D₂O than in H₂O (Figure 1.6). Indeed it has been shown that, for

the case of europium(III) and terbium(III), X-D oscillators* were at least 200 times less effective at vibronic quenching than the corresponding X-H oscillators.³⁶

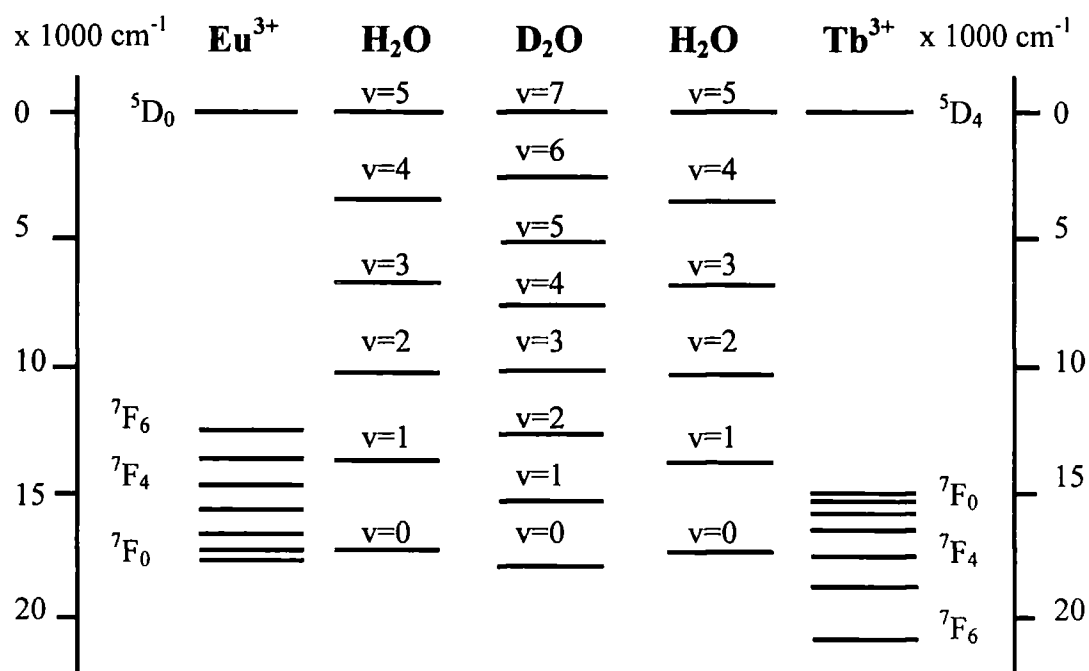


Figure 1.6 The deactivating effect of H-O and D-O oscillators.

Emission from the lowest luminescent level of europium(III) is from the ⁵D₀ to the ⁷F_J levels (J=0-6), whilst emission from terbium is from the ⁵D₄ to the ⁷F_J levels (J=6-0).³⁷ Excitation spectra are usually generated by monitoring the emission frequency of one of the ion's strongest emissive bands, thus the ⁵D₀ - ⁷F₂ (ca 618nm) emission for europium and the higher energy ⁵D₄ - ⁷F₅ (545nm) emission for terbium

1.3.3 Sensitised Luminescent Emission.

Measurement of the luminescence from Eu³⁺ and Tb³⁺ is not without its own practical difficulties. The extinction coefficients of lanthanide ions are low, due to the formally disallowed nature of the transitions and poor orbital penetration. Deactivation by water also serves to reduce luminescent intensities. It has been

* X = O, N or C.

shown however that both ions are able to absorb energy via energy transfer (ET) from the triplet state of an excited chromophore (Figure 1.7).^{39,40,41}

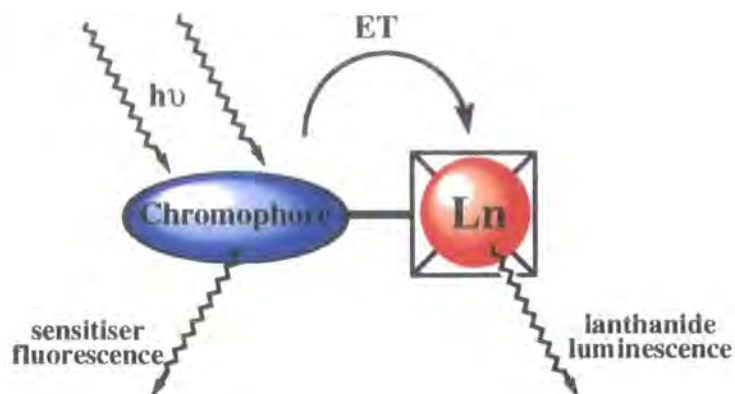


Figure 1.7. Sensitised lanthanide emission by energy transfer.

This 'sensitisation' of the ions allows the development of molecular probes, the ions can be used to report the presence of suitable chromophores. For efficient energy transfer to occur, the triplet state energy of the chromophore should be slightly higher in energy than the lanthanide energy gap. This effect is complicated when the relative energy difference between the triplet state and the excited lanthanide state is too small, less than *ca* $1,700\text{ cm}^{-1}$ for sensitisation at 298K. It is then possible for a thermally initiated back energy transfer to occur from the excited lanthanide ion to the chromophore (Figure 1.8). This triplet state is then open to deactivation by triplet oxygen in aerated solutions, or through phosphorescence in degassed solutions. This effect is particularly important for terbium where the emissive state is high in energy, limiting the possible range of energies of suitable chromophores.³⁵

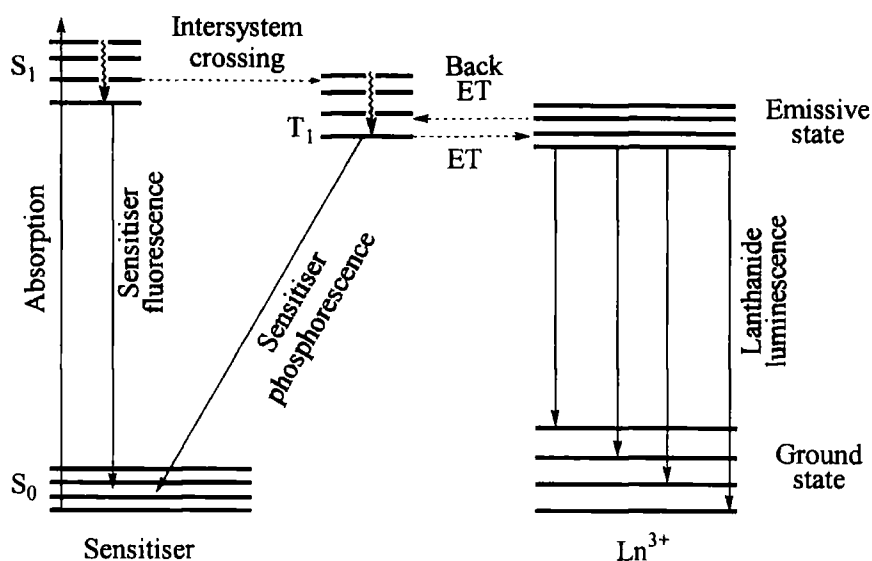


Figure 1.8. Jablonski diagram for sensitised lanthanide emission.

Sensitised luminescence of europium(III) and terbium(III) may occur through one of two possible mechanisms. Energy transfer via the Förster mechanism⁴¹ is due to a coulombic interaction arising when the dipole of the excited sensitiser induces a dipole in the acceptor. This 'through space' process does not require physical contact between the sensitiser and acceptor. The rate of energy transfer via the Förster mechanism is generally accepted to exhibit a r^{-6} distance dependence, where r is the intermolecular distance between the sensitising chromophore and the metal centre.

The Dexter mechanism arises from an exchange interaction involving mutual electron exchange between the sensitiser and the acceptor, with conservation of the total spin multiplicity of the system (Figure 1.9). Energy transfer via the Dexter mechanism occurs via the overlap of the electron clouds of the sensitiser and metal and hence requires physical contact between the two components.

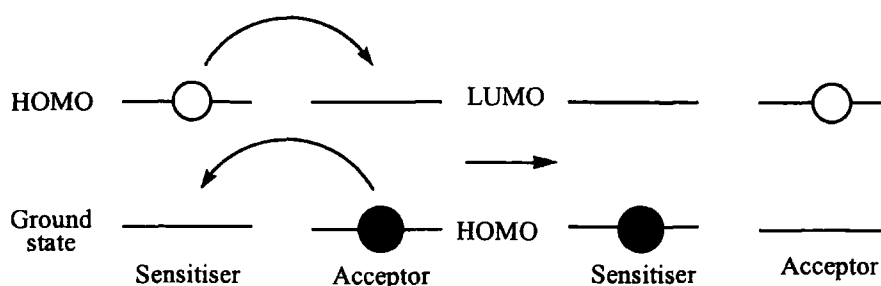


Figure 1.9 Energy transfer from sensitiser to acceptor via the Dexter mechanism (mutual electron exchange).

The use of free lanthanide ions is also problematic. The solvent shell of the free aqueous ions contains 9 water molecules leading to significant deactivation of the excited state and thereby causing a decrease in luminescent intensity and lifetime. The toxicity of free ions also inhibits their suitability for clinical applications. Development of specific lanthanide ionophores has allowed the synthesis of lanthanide complexes that shield the ion from solvent interactions, or that can be targeted for specific *in vivo* use.³⁴ Such complexes are commonly based on a 1,4,7,10-tetraazacyclododecane (cyclen) modified with N-carboxymethyl or N-phosphinoxyalkyl units (Figure 1.10). This provides a pre-organised octadentate ligand with a size specific cavity highly suitable for binding lanthanide ions. The mixture of hard O and N donors also suits the hard, polarising lanthanides.

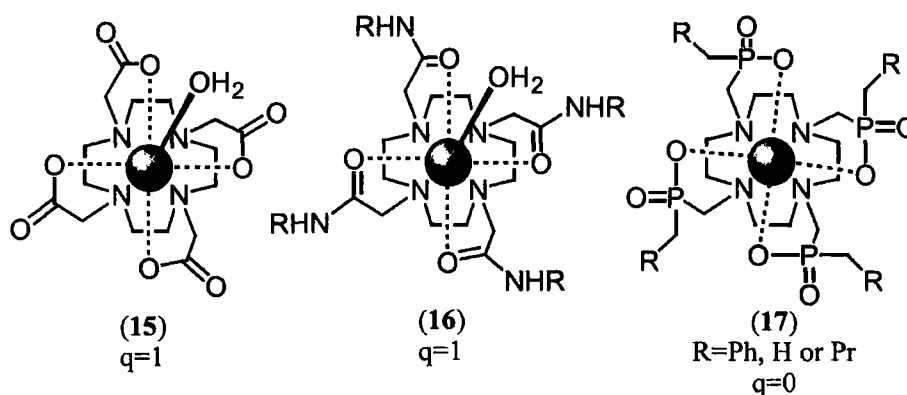


Figure 1.10. Complexes of 1,4,7,10-tetraazacyclododecanetetraacetate (DOTA, 15), 1,4,7,10-tetraazacyclododecanetetraamide (16) and 1,4,7,10-tetraazacyclododecanetetraphosphinate (17).

1.3.4 Yb Luminescence.

Of the remaining lanthanides, luminescence from ytterbium ions has also recently generated interest. Ytterbium(III) can also exhibit sensitised luminescence, although the emission lies within the near infra-red ($\lambda_{em}=980$ nm, $^2F_{5/2}-^2F_{7/2}$ manifold), in contrast to emission from europium(III) and terbium(III) which occurs within the visible range of the electromagnetic spectrum. The lowest luminescent level of ytterbium(III) is also of a relatively low energy ($10,200$ cm⁻¹), allowing sensitisation from chromophores with low triplet state energies. This can avoid competitive sensitisation by biological chromophores which tend to exhibit higher triplet state energies. Sensitised luminescence has been attributed to be due to either a long range electron transfer process,⁴³ or to involve energy transfer from the triplet excited state of the aromatic antennae.⁴⁴

1.4 References.

¹ E. Fischer, *Ber.*, 1894, **27**, 2985.

² A. W. Czarnik, *Chemistry & Biology*, 1995, **2**, 423.

³ *Comprehensive Supramolecular Chemistry: Volume 2, Molecular Recognition: Receptors for Molecular Guests*. Editors: J.L. Atwood, J.E.D. Davies, D.D. Macnicol, F. Vögtle, J.-M. Lehn, J. Szejtli, T. Osa, Pergammon, 1996.

⁴ *Comprehensive Supramolecular Chemistry: Volume 3; Cyclodextrins*. Editors: J.L. Atwood, J.E.D. Davies, D.D. Macnicol, F. Vögtle, J.-M. Lehn, J. Szejtli, T. Osa, Pergammon, 1996, a) Chapter 1, J. Szejtli, b) Chapter 2, J. Szejtli, c) Chapter 6, K. A. Connors, d) Chapter 4, L. Jicsinszky, E. Fenyvesi, H. Hashimoto, A. Ueno.

⁵ Erik van Dienst, Ph.D. Thesis, University Twente, Netherlands, 1994.

⁶ P. Cescutti, D. Garozzo, R. Rizzo, *Carbohydr. Res.*, 1996, **290**, 105.

⁷ K. A. Udachin, J. A. Ripmeester, *J. Am. Chem. Soc.*, 1998, **120**, 1080.

⁸ A. Ueno, I Suzuki, T. Osa, *J. Am. Chem. Soc.*, 1989, **111**, 6397.

- ⁹ N. Davey, D.A. Leigh, J. P. Smart, L. W. Tetler, A. M. Truscello, *Carbohydr. Res.*, 1996, **290**, 117.
- ¹⁰ E. E. Tucker, S. D. Christian, *J. Am. Chem. Soc.*, 1984, **106**, 1942.
- ¹¹ I. Sanemasa, T. Takuma, T. Deguchi, *Bull. Chem. Soc. Jpn.*, 1989, **62**, 3098.
- ¹² L. Blyshak, K. Y. Dodson, G. Patonay, I. M. Warner, W. E. May, *Anal. Chem.*, 1989, **61**, 955.
- ¹³ K. A. Connors, T. W. Roasanske, *J. Pharm. Sci.*, 1980, **69**, 173.
- ¹⁴ A. Nakamura, K. Saitoh, F. Toda, *Chem. Lett.*, 1989, 2209.
- ¹⁵ G. C. Catana, F. V. Bright, *Anal. Chem.*, 1989, **61**, 905.
- ¹⁶ R. Breslow, S. D. Dong, *Chem. Rev.*, 1998, **98**, 1997.
- ¹⁷ A. P. Croft, R. A. Bartsch, *Tetrahedron*, 1983, **39**, 1417.
- ¹⁸ D. Rong, V. T. D'Souza, *Tetrahedron Lett.*, 1990, **31**, 4275.
- ¹⁹ S. Tian, P. Forgo, V. T. D'Souza, *Tetrahedron Lett.*, 1996, **37**, 8309.
- ²⁰ G. Yi, W. Li, J. S. Bradshaw, A. Malik, M. L. Lee, *J. Heterocyclic Chem.*, 1995, **32**, 1715.
- ²¹ S. -H. Chiu, D. C. Myles, *J. Org. Chem.*, 1999, **64**, 332.
- ²² H. Parrot-Lopez, F. Djedaïni, B. Perly, A.W. Coleman, H. Galons, M. Miocque, *Tetrahedron Lett.*, 1990, **31**, 1999.
- ²³ L.D. Melton, K.N. Slessor, *Carbohydr. Res.*, 1971, **18**, 29.
- ²⁴ R.P. Bonomo, V. Cucinotta, F. D'Alessandro, G. Impellizzeri, G. Maccarrone, G. Vecchio, E. Rizzarelli, *Inorg. Chem.*, 1991, **30**, 2708.
- ²⁵ C. Henke, C. Steinem, A. Janshoff, G. Steffan, H. Luftmann, M. Sieber, H.-J. Galla, *Anal. Chem.*, 1996, **68**, 3158.
- ²⁶ S. E. Brown, J. H. Coates, D. R. Coghlan, C. J. Easton, S. J. van Eyk, W. Janowski, A. Lepore, S. F. Lincoln, Y. Luo, B. L. May, D. S. Schiesser, P. Wang, M. L. Williams, *Aust. J. Chem.*, 1993, **46**, 953.
- ²⁷ H. Ikeda, M. Nakamura, N. Ise, N. Oguma, A. Nakamura, T. Ikeda, F. Toda, A. Ueno, *J. Am. Chem. Soc.*, 1996, **118**, 10980.
- ²⁸ N. Zhong, H.-S. Byun, R. Bittman, *Tetrahedron Lett.*, 1998, **39**, 2919.
- ²⁹ Z. Chen, J. S. Bradshaw, M. L. Lee, *Tetrahedron Lett.*, 1996, **37**, 6831.
- ³⁰ Z. Chen, J. S. Bradshaw, Y. -F. Shen, Y. Habata, M. L. Lee, *J. Org. Chem.*, 1997, **62**, 8529.
- ³¹ M. J. Cornwell, J. B. Huff, C. Bieniarz, *Tetrahedron Lett.*, 1995, **36**, 8371.

-
- ³² P.J. Stevenson, A. B. Treacy, M. Nieuwenhuyzen, *J. Chem. Soc., Perkin Trans. 2*, 1997, 589.
- ³³ A. R. Khan, P. Forgo, K. J. Stine, V. T. D'Souza, *Chem. Rev.*, 1998, **98**, 1977.
- ³⁴ Luminescent Probes, J.- C. G. Bünzli, Chapter 7, in *Lanthanide Probes In Life, Chemical and Earth Sciences: Theory and Practice*, J.-C. G. Bünzli, G. R. Choppin, Elsevier, 1989.
- ³⁵ D. Parker, J. A. G. Williams, *J. Chem. Soc., Dalton Trans.*, 1996, 3613.
- ³⁶ W. DeW. Horrocks, jr., D. R. Sudnick, *Acc. Chem. Res.*, 1981, **14**, 384.
- ³⁷ Y. Haas, G. Stein, *J. Phys. Chem.*, 1972, **76**, 1093.
- ³⁸ G. Stein, E. Würzberg, *J. Chem. Phys.*, 1975, **62**, 208.
- ³⁹ D. Parker, J.A.G. Williams, *J. Chem. Soc., Perkin Trans. 2*, 1996, 1581.
- ⁴⁰ A. Beeby, D. Parker, J. A. G. Williams, *Chem. Soc., Perkin Trans. 2*, 1996, 1565.
- ⁴¹ M. Murru, D. Parker, G. Williams, A. Beeby, *J. Chem. Soc., Chem. Commun.*, 1993, 1116.
- ⁴² T. Förster, *Discuss. Faraday Soc.*, 1959, **27**, 7.
- ⁴³ W. D. Horrocks Jr., J. P. Bolender, W. D. Smith, R. M. Supkowski, *J. Am. Chem. Soc.*, 1997, **119**, 5972.
- ⁴⁴ A. Beeby, R. S. Dickens, S. Faulkner, D. Parker, J. A. G. Williams, *J. Chem. Soc., Chem. Commun.*, 1997, 1401.

Chapter 2

Lanthanide-appended Cyclodextrin Systems.

2 Lanthanide-appended Cyclodextrin Systems.

2.1 Introduction.

2.1.1 Lanthanides as Luminescent Reporters.

The use of lanthanides, specifically europium and terbium, as luminescent reporters has recently generated significant interest. Long lived emission allows detection of a signal without undue interference from background autofluorescence or Rayleigh scattering as may be observed in biological systems. Commonly, the metal is constrained within a protective ligand which fulfils a dual role. Firstly the ligand is generally designed to form stable complexes with the metal, preventing the metal from dissociating and hence avoiding toxicity effects when used in vivo. Secondly, as metal emission is quenched by interaction by water, the emission lifetime from the metal is maximised by removing water from the environment immediately surrounding the metal. Ligands such as DOTA (15) and its derivatives (Figure 2.1) have become widely used.

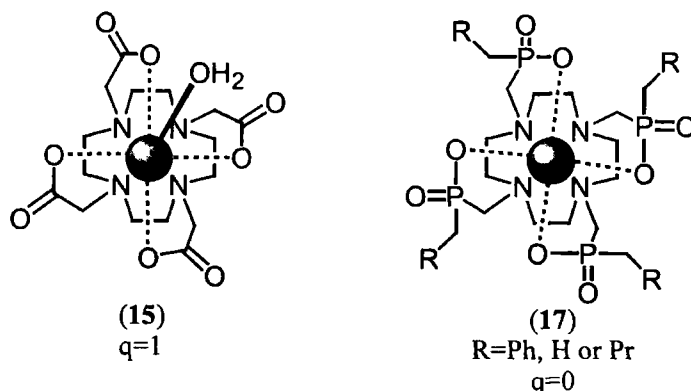


Figure 2.1. Lanthanide complexes of 1, 4, 7, 10-tetraazacyclododecane tetraacetate (DOTA) (15) and tetraphosphinate analogues (17).

Metal emission can also be enhanced by appending the ligand with a light harvesting moiety with a triplet excited state above that of the emissive lanthanide excited state (such as 5D_0 Eu, 5D_4 Tb or $^2F_{5/2}$ Yb). Such species include naphthalene, phenanthridine and quinoline. Irradiation of the aromatic chromophore generates the triplet state, following intersystem crossing from the singlet excited state. The

excited chromophore can then transfer energy to the metal, which reverts to its ground state by emitting characteristic luminescence. This approach avoids problems with low overall quantum yields associated with direct excitation of the metal. Use of chromophores with excited states which are perturbed by changes in acidity or ion concentration has allowed development of systems which are able to report concentrations of species such as protons, chloride ions, oxygen or hydrogencarbonate ions.¹

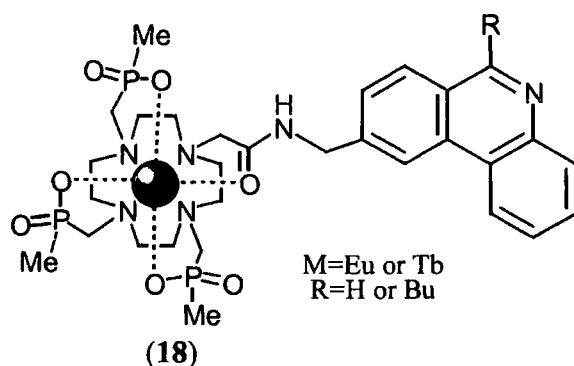


Figure 2.2. Luminescent sensor for pH developed by Parker *et al* (18).¹

2.1.2 Existing Cyclodextrin-lanthanide-appended Systems.

The use of lanthanides as reporters for the detection of aromatic chromophores themselves remains an area which has been little explored. An obvious approach to the problem is to append a stable lanthanide cage with a site suitable for binding such chromophores. Binding of the chromophore would then allow excitation of the chromophore and following intramolecular energy transfer, lanthanide emission would result, observable by time-gated methods.

This approach has been explored by Nocera *et al.*, in three systems utilising a cyclodextrin as an aromatic binding site. The first system developed² incorporated an 'aza-crown swing' appended to the primary face of β -cyclodextrin (19).

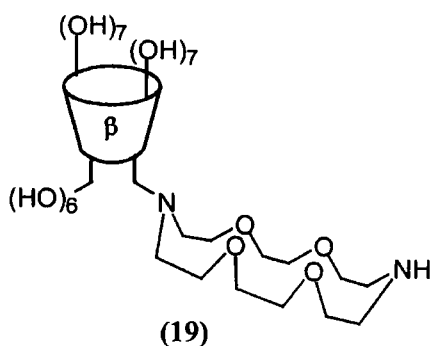


Figure 2.3. Cyclodextrin - 'swing-aza-crown' conjugate (19).

Lanthanide ions form weak 1:1 complexes with $18N_2O_4$ aza-crowns, which are kinetically unstable with respect to lanthanide decomplexation in polar media. It is therefore unsurprising that inefficient energy transfer occurs upon inclusion of benzene into the cyclodextrin cavity. The authors attributed the poor energy transfer to the large distance between the receptor and the lanthanide: poor energy transfer reflecting both the compounds preferred conformation with the crown facing away from the cavity (shown above) and the attenuating effect of the r^{-6} distance dependence for efficiency of energy transfer.

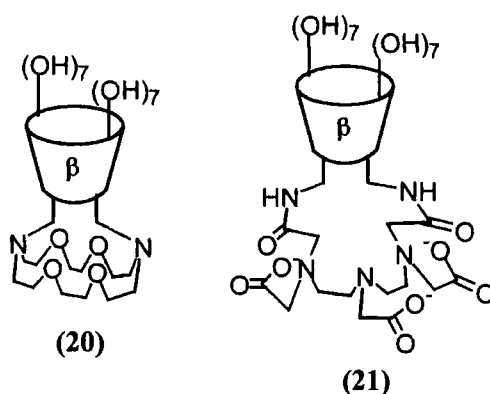


Figure 2.4. Cyclodextrin based lanthanide ligands* (20 & 21) developed by Nocera *et al.*^{3,4}

Synthesis of a cyclodextrin with a europium complexed aza-crown tethered at both ends to form a capped cyclodextrin (20) was expected to reduce the distance needed for energy transfer and hence improve sensitivity. It was reported that although the efficiency of energy transfer was improved in the cradle cyclodextrin (20), the proximity of the Eu^{3+} charge centre to the cavity reduced the hydrophobicity of the

* Remaining primary hydroxyls have been omitted for clarity.

cavity and severely reduced the degree of guest association.³ The competitive binding of the counter-ion into the cyclodextrin cavity offered a more plausible explanation for reduced guest binding.

Synthesis of a cyclodextrin (**21**) appended with a charge neutral complex was more successful.⁴ In this case, charge neutrality was achieved by incorporation of a binding site derived from diethylenetriaminepentaacetic acid (DTPA) with three pendant carboxylate groups which increase the strength of binding to lanthanides. This substrate has the additional advantage of exhibiting stronger binding to lanthanides than the previous systems. Markedly enhanced emission upon addition of naphthalene or 1,2,4,5-tetramethylbenzene was observed. The 1:1 binding affinity (K_{11}) of naphthalene into the cyclodextrin (**21**) was calculated as 18000 M^{-1} , circa 25 fold greater than observed for the binding of naphthalene into β -cyclodextrin (**1**) ($K_{11}=760\text{M}^{-1}$).⁵ The increased binding affinity was attributed to a greater rigidity inherent in the capped system (**21**), probably associated with a more favourable entropy of complexation term.

A more flexible cyclodextrin-lanthanide conjugate (**22**) was developed by Wenzel *et al.*,⁶ in this case the ligand formed a binding site for dysprosium (Figure 2.5). Of the lanthanides, dysprosium, terbium and praseodymium give the largest enhanced shifts in ^1H NMR spectrometry. Guests complexed into the cavity were subject to enhanced lanthanide induced shifts. The system thus operated as a probe for elucidating optical purity, the enantiomeric resolution of a number of biologically important species such as aspartame, tryptophan and propranolol were reported, albeit with modest chemical shift non-equivalence

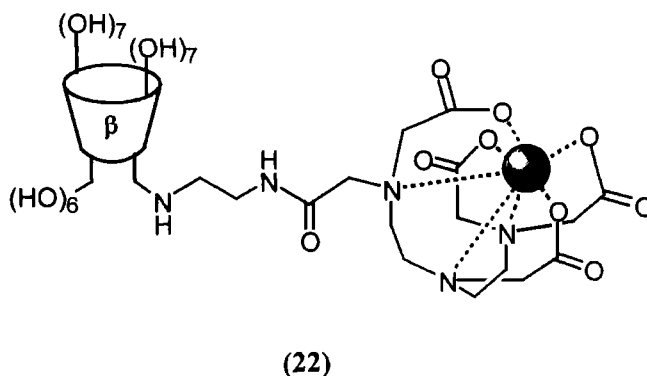


Figure 2.5. Lanthanide-cyclodextrin conjugate (**22**) as described by Wenzel *et al.*⁶

The synthesis of two further ligands was recently reported by Marsura *et al.*⁷ In these systems, four or three cyclodextrins are appended onto the aza-cycles 14N₄ and 9N₃ respectively (Figure 2.6). Although the synthesis of the europium complex of the tetramer was reported, the photophysics of the system was not investigated beyond metal emission due to direct excitation. Both ligands are also expected to coordinate weakly to lanthanide ions. This arises because the direct bond from the ring nitrogens to the carbonyl moieties results in the urea oxygen atoms being poorly disposed for coordination to the lanthanide ion. The appended tri-azacycle (**24**) also only provides only 3 coordination sites to the metal, severely limiting the stability of the metal complex in 1:1 ML complexes.

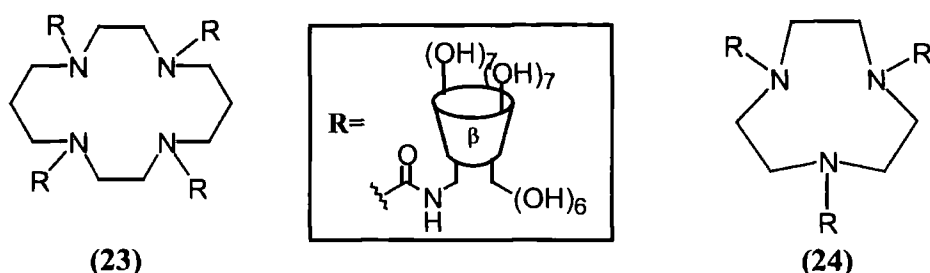


Figure 2.6. Cyclodextrin appended lanthanide ligands (**23** & **24**) developed by Marsura *et al.*⁷

2.2 Design of Novel Lanthanide-Cyclodextrin Appended Detection Systems.

This project set out to develop a molecular sensing system based on β -cyclodextrin linked to a stable lanthanide complex. It was envisaged that in the presence of a suitable guest, the cyclodextrin host will selectively bind the guest within its cavity. Photoexcitation of the guest to a higher electronic state should allow energy transfer through the cyclodextrin macrocycle, and its tether, to the lanthanide ion. Characteristic lanthanide phosphorescence emission should thus signal the binding of the guest into the cyclodextrin host (Figure 2.7).



Figure 2.7. Lanthanide luminescence sensitised by irradiation of a cyclodextrin included fluorophore and subsequent energy transfer.

Two substrates have been designed for this purpose. The first, (**25**), consists of four β -cyclodextrin derivatives arranged in a C_4 symmetric pattern around a cyclen (1,4,7,10-tetraazacyclododecane) ring. It was proposed to synthesise both the europium and terbium complexes of this system. It should be observed that a number of features peculiar to this substrate are anticipated to increase its suitability as a molecular probe over systems previously reported.^{2,3,4} These features are discussed below.

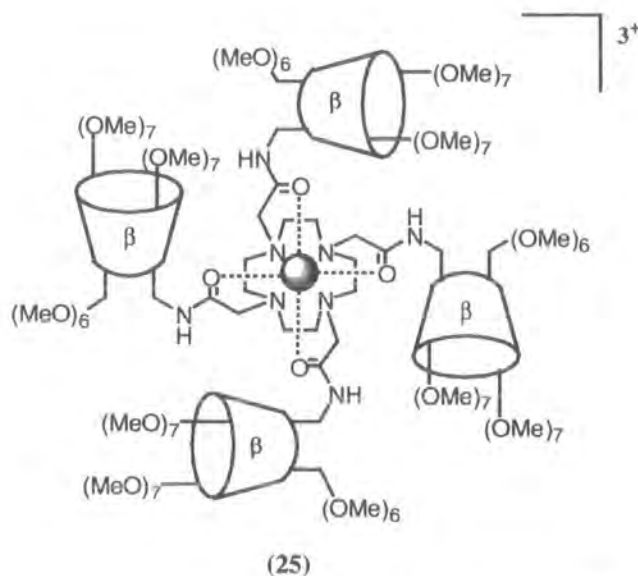


Figure 2.8. Tetra substituted 1,4,7,10-tetraazacyclododecane (**25**) lanthanide complexes.

The lanthanide binding site is based on a tetra-(*N*- β -carbamoyl)-1,4,7,10-tetraazacyclododecane system. This system has been shown to form very stable complexes with lanthanide (III) ions.⁸ In this complex the lanthanide binding site is offset from the primary face of the cyclodextrin cavity. This should prevent interference of the charged lanthanide (III) ion with the cyclodextrin cavity, systems

with the lanthanide ion sited in close proximity to the primary face of cyclodextrin have suffered from a reduction of the hydrophobicity of the cavity,³ and hence a reduction in the strength of binding to included guests.

Despite the offset of the lanthanide complex to the primary face of the cyclodextrin, the through-space distance between the lanthanide ion and the cyclodextrin cavity is reasonably short (*circa.* 9Å). It was anticipated that such a distance, while inevitably being far from optimal for efficient energy transfer, would still be not too long as to inhibit the process.

The cyclodextrin moieties are considerably more sterically demanding than the cyclen ring to which they are tethered. Although their steric demands should not prevent their addition to the cyclen ring, addition to the primary face of the cyclodextrin will enforce a degree of spacing from the macrocycle. The presence of four such units around the lanthanide complex may inhibit coordination of water molecules to the lanthanide ion. Since H-O oscillators efficiently quench the excited states of lanthanide (III) ions, the removal of water from the primary lanthanide complexation shell should increase the lifetime and intensity of lanthanide emission and hence improve the sensitivity of the molecular probe.

It was also anticipated that the steric bulk of the cyclodextrin moieties would inhibit pendant arm rotation of the cyclen ring (Figure 2.9.). Such a process would maintain the cyclodextrin units in reasonably close proximity. Thus of the four possible conformational isomers, it was hoped that the steric bulk of the cyclodextrin moieties would favour the formation of a single pair of diastereomers.

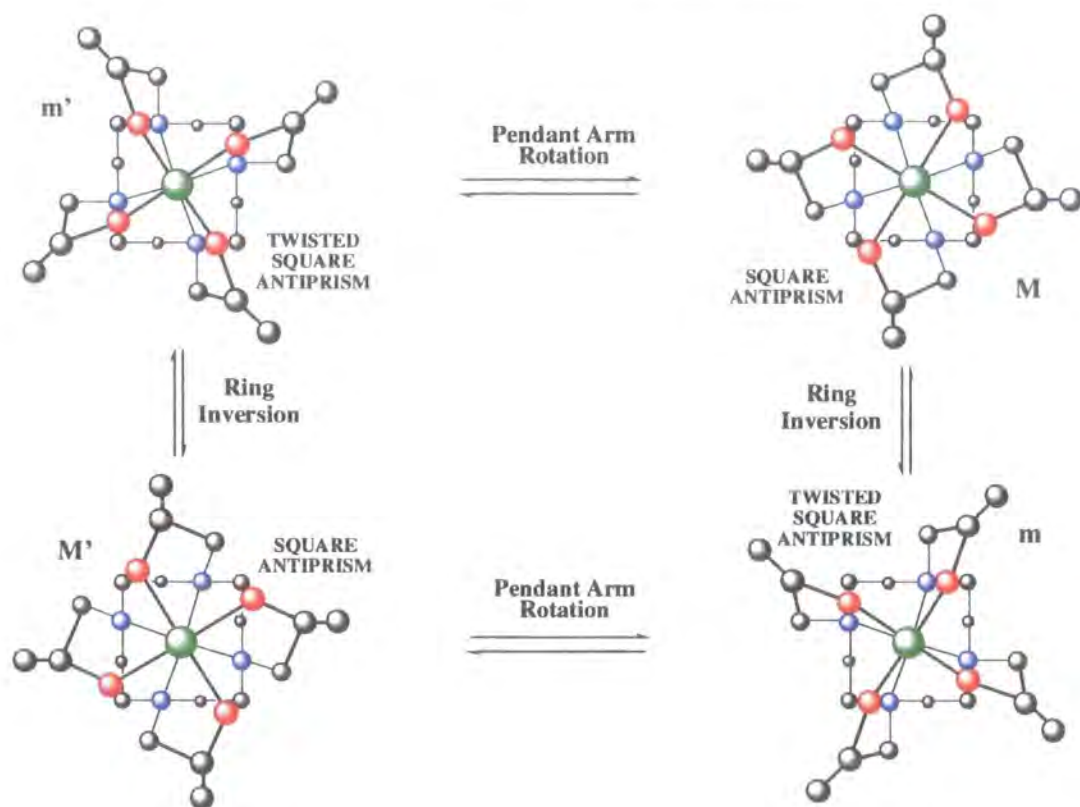


Figure 2.9. Schematic representation of the coordination geometries adopted by the lanthanide (III) complexes of 1,4,7,10-tetracarbamoyl-1,4,7,10-tetraazacyclododecane systems in solution. Their interconversion pathways of pendant arm rotation and ring inversion are also shown.

Permethylation of hydroxyl groups on cyclodextrin has been shown to greatly increase water solubility and also to increase the hydrophobicity of the cyclodextrin cavity.⁹ It was intended to functionalise the cyclodextrin hosts so that 20 out of the 21 hydroxyl units are converted to their methyl ethers, the remaining hydroxyl group being selectively functionalised to link to the cyclen ring.

Despite the increased hydrophobicity of the cavity, typical adamantane and phenol derivatives have been shown to afford weaker complexes with per-O-methyl- β -cyclodextrin (**5**) compared to the parent β -cyclodextrin (**1**).¹⁰ The reduced binding affinity is attributed to unfavourable entropy changes. A reduced binding affinity relative to the parent cyclodextrin is not always the rule: 2-*p*-toluidino-6-naphthalenesulfonate (2,6-TNS, **4**) shows a greater binding affinity to per-O-methyl- β -cyclodextrin (**5**) ($K_{11}=2180 \text{ M}^{-1}$)¹¹ than to the parent β -cyclodextrin (**4**) ($K_{11}=1980 \text{ M}^{-1}$).¹² Increased binding of oversized guest molecules, such as 4-

methylbenzoic acid, into substituted α -cyclodextrins over the parent α -cyclodextrin (**2**) have also been observed.¹⁰ It is clear that although binding affinities of guests are expected to differ between methylated and the parent cyclodextrins, the effect is likely to be small and it is difficult to predict which would show the strongest binding.

In the tetraamide system (**25**) the ligand has no overall charge so that a lanthanide (III) complex develops a tripositive charge. It was foreseen that the effects of this charge on the binding capabilities of cyclodextrin to charged and neutral species may not be beneficial. Therefore a second ligand (**26**) has also been designed. This substrate has a single β -cyclodextrin derivative attached to a cyclen ring, the remaining three ring nitrogens being functionalised with acetate units. Complexation with lanthanide (III) ion should yield an uncharged complex. Again it was planned to synthesise both the europium and terbium complexes of this system.

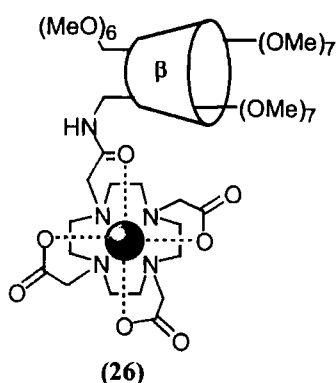


Figure 2.10. Charge neutral mono-substituted 1,4,7,10-tetraazacyclododecane (**26**) lanthanide complexes.

This substrate shares many features with the tetra substituted product (**25**) outlined above. Permethylation of the single cyclodextrin moiety is again expected to improve solubility and increase the hydrophobicity of the cavity. The lanthanide binding site is close to the cyclodextrin macrocycle, aiding efficient energy transfer, but not situated directly below the primary face so as to prevent substrate binding. The mono-substituted product has less steric bulk around the lanthanide binding site however, and provided a useful comparison allowing the importance of conformational mobility to be assessed.

Both substrates are linked to β -cyclodextrin derivatives rather than their α - or γ - analogues. β -Cyclodextrin (**1**) is the most common of the cyclodextrins, and hence also the cheapest, but also perhaps has the most useful guest binding characteristics. The cavity of β -cyclodextrin (**1**) is a suitable size to bind both phenyl, naphthyl and anthryl derivatives (including heteroatom analogues). The chiral nature of cyclodextrin also affords the possibility of enantiomeric discrimination of chiral aryl guests.

2.3 Synthetic Methodology.

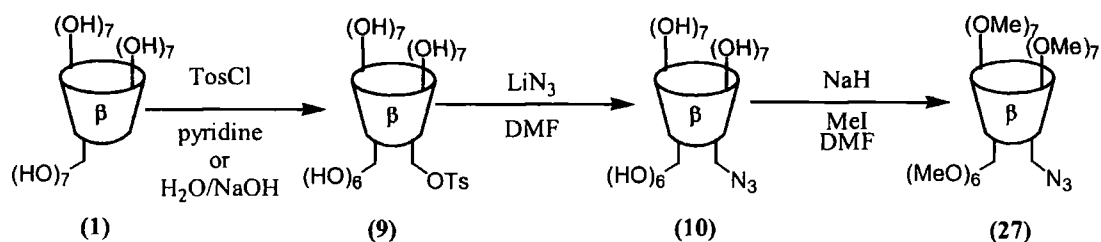
2.3.1 Synthesis of a Monofunctionalised Cyclodextrin Linker.

The synthesis of the two lanthanide ligands discussed above relies on successful selective functionalisation of β -cyclodextrin (**1**). Strategies for per- and mono-O-functionalisation of cyclodextrins have previously been discussed in detail.

Two approaches were examined for the selective monosubstitution of β -cyclodextrin (**1**) at the primary face. The first method (Scheme 2.1) commenced with formation of mono-O-tosyl- β -cyclodextrin (**9**), a common starting point for cyclodextrins mono substituted on the primary face.

Mono-O-tosyl- β -cyclodextrin (**9**) was initially prepared as described by Easton et al¹³ by reaction of dried β -cyclodextrin with *p*-toluenesulfonyl chloride in anhydrous pyridine. This approach proved to be less than satisfactory. Yields for this reaction were low (17%) and although similar to those reported elsewhere (*circa* 17%),¹⁴ the reaction also proved to be highly capricious. Difficulties encountered with the removal of pyridine suggested an affinity of the solvent for the cyclodextrin cavity which inhibited its removal. The low aqueous solubility of the product did however allow facile purification by recrystallisation from water.

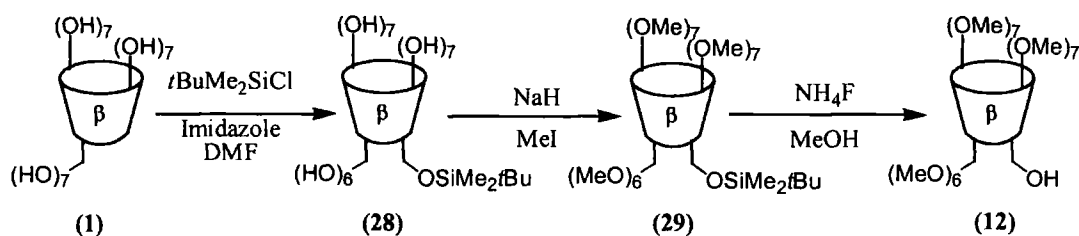
An alternative method for the preparation of mono-O-tosyl- β -cyclodextrin (**9**) was investigated subsequent to a publication by Bittman *et al.*¹⁵ Bittman presented a preparation where a suspension of β -cyclodextrin (**1**) and toluenesulfonyl anhydride was stirred at room temperature for 2 hours before addition of base (aqueous sodium hydroxide) leading to formation of the desired tosyl- β -cyclodextrin (**9**). Bittman proposed that the mechanism involved a solubilising complex between the cyclodextrin and the toluenesulfonyl anhydride which placed the two species in close proximity, hence susceptible to reaction upon addition of the base. Although the results reported by Bittman were not repeated here, substitution of *p*-toluenesulfonyl chloride for *p*-toluenesulfonyl anhydride afforded mono-O-tosyl- β -cyclodextrin in a moderate yield (40%).



Scheme 2.1. Preparation of mono-azido-per-O-methyl- β -cyclodextrin (**27**).

Conversion of mono-O-tosyl- β -cyclodextrin (**9**) to mono-azido- β -cyclodextrin (**10**) using LiN₃ in DMF occurred in good yield (93%). β -Cyclodextrin (**1**), formed by competitive hydrolysis of the tosylate, constituted the major impurity and was removed following purification by recrystallisation. Methylation of the remaining hydroxyls proved to be more problematic. Reaction with dimethyl sulfate in the presence of potassium hydroxide as described by Perly *et al.*¹⁶ was incomplete, leading to formation of a mixture of partially methylated cyclodextrins observable by electrospray mass spectrometry. Reaction with sodium hydroxide and methyl iodide in anhydrous DMF proved to be more successful, although yields were still low (22%). Removal of per-O-methyl- β -cyclodextrin (**5**), the major side product formed by hydrolysis of the azide (**10**), also proved to be problematic due to the similar polarities of the two products. This method ultimately afforded mono-azido-per-O-methyl- β -cyclodextrin (**27**) in an overall yield of 3.5% from β -cyclodextrin (**1**).

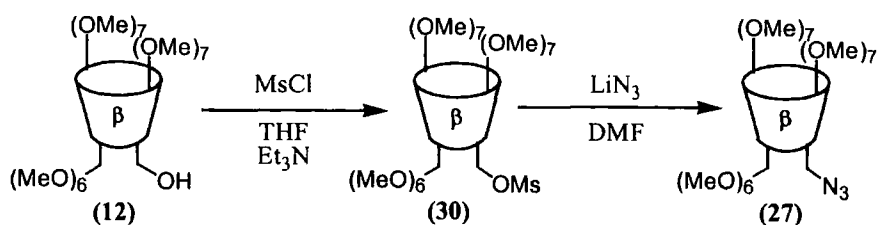
The second method examined for selective modification of β -cyclodextrin (**1**) followed the approach outlined by Bradshaw *et al.*¹⁷ In a 'one pot' reaction, β -cyclodextrin (**1**) was protected once on the primary face by use of *t*-butyl-dimethyl silyl chloride, leaving the remaining 20 hydroxyl groups available for reaction with sodium hydride and methyl iodide. The silyl protecting group was then readily cleaved with ammonium fluoride to give cyclodextrin with one hydroxyl group available for subsequent modification, the remainder being protected as their methyl ethers (**12**) (Scheme 2.2).



Scheme 2.2. Preparation of mono-hydroxy-per-O-methyl- β -cyclodextrin (**12**).

Mono-hydroxy-per-O-methyl- β -cyclodextrin (**12**) was successfully prepared as described, although yields proved to be lower than reported (20% *cf* 43% reported¹⁷). Removal of the major side product, per-O-methyl- β -cyclodextrin (**5**), also proved to be less facile than reported due to the similar polarities of the two species.

Derivatisation of the mono unprotected species was expected to occur readily towards generation of a species suitable for attachment onto a cyclen backbone (Scheme 2.3). Conversion of mono-hydroxy-per-O-methyl- β -cyclodextrin (**12**) to mono-methanesulfonyl-per-O-methyl- β -cyclodextrin (**30**) proceeded in quantitative yield using methanesulfonyl chloride in anhydrous THF. Mono-azido-per-O-methyl- β -cyclodextrin (**27**) was readily prepared by subsequent nucleophilic substitution with lithium azide in anhydrous DMF. Purification by column chromatography gave the product in good yield (62%, 12.4% from β -cyclodextrin (**1**)).

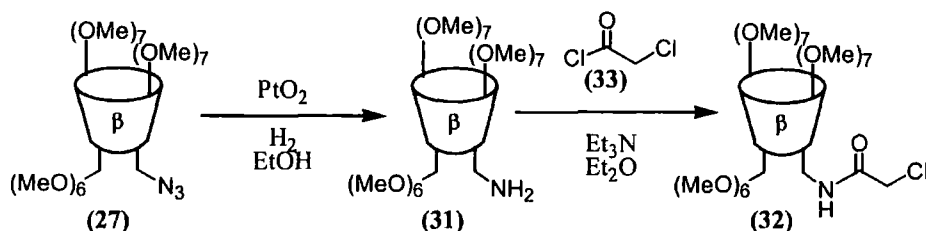


Scheme 2.3. Alternative preparation of mono-azido-per-O-methyl- β -cyclodextrin (**27**).

Of the two routes to mono-azido-per-O-methyl- β -cyclodextrin (**27**) described here, it can be seen that the two problematic, and hence lowest yielding steps, are the monofunctionalisation of cyclodextrin and the methylation of the remaining hydroxyl moieties. By effectively combining these two in a single 'one pot' reaction to mono-hydroxy-per-O-methyl- β -cyclodextrin (**12**), the yield of the process can be increased relative to that starting with mono-O-tosyl- β -cyclodextrin (**b14**). Analysis of the intermediates by ^1H NMR is also aided by their increased solubility in common polar solvents, allowing easy reaction monitoring. The high solubility however does preclude the use of recrystallisation as a purification procedure and the repeated use of column chromatography does make the route described more laborious. Removal of other similar cyclodextrin side products, such as per-O-methyl- β -cyclodextrin (**5**), is also difficult due to their similar polarities.

Both parallel synthetic routes converged with the synthesis of mono-azido-per-O-methyl- β -cyclodextrin (**27**). Reduction of this species to mono-amino-per-O-methyl- β -cyclodextrin (**31**) occurred readily by a variety of procedures. Transfer hydrogenation with aqueous ammonia solution and triphenylphosphine in DMF occurred readily in 20 hours at room temperature. However the resulting product could not be easily separated from residual triphenylphosphine, ^1H NMR analysis suggested that the formation of a 1:2 complex with the cyclodextrin had occurred. Catalytic hydrogenation as described by Bradshaw *et al.*¹⁸ using platinum oxide readily gave total conversion to the amine (**31**) and purification by column chromatography allowed a good recovery (93%). Interestingly, the low polarity of the amine relative to the other cyclodextrin products described allowed species such as per-O-methyl- β -cyclodextrin (**5**) to be removed easily. Conversion of the amine

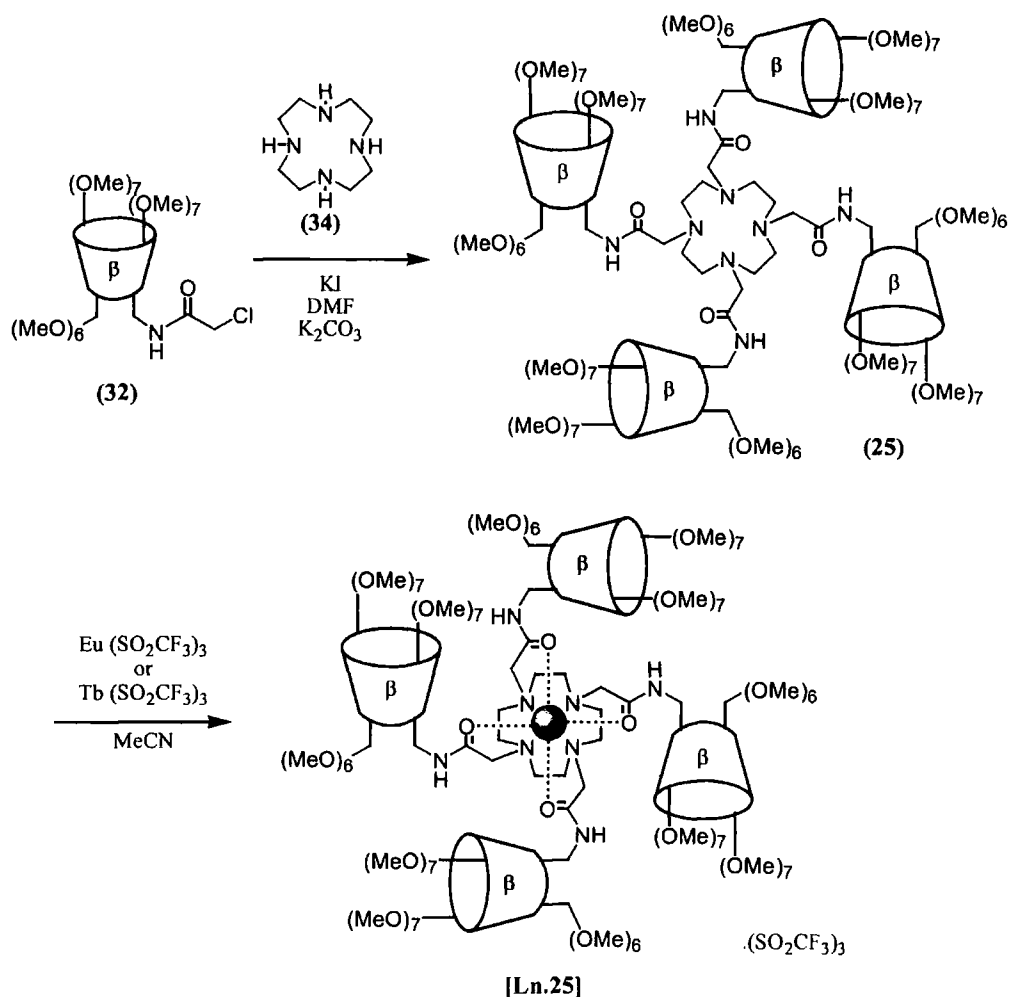
(31) to the chloroamide mono-(chloromethylcarbonylamino)-per-O-methyl- β -cyclodextrin (32) occurred readily on reaction with chloroacetylchloride (33) in ether (Scheme 2.4).



Scheme 2.4. Preparation of mono-(chloromethylcarbonylamino)-per-O-methyl- β -cyclodextrin (32).

2.3.2 Synthesis of lanthanide complexes of a cyclodextrin tetraamide ligand.

Reaction of the chloroamide (32) with 1,4,7,10-tetraazacyclododecane (34) occurred readily in anhydrous DMF in the presence of potassium carbonate at 60°C. The presence of a slight excess of the chloroamide (32) allowed complete conversion to the tetraamide (25) without partially substituted products or quaternisation of any of the ring nitrogens. Recovery of the product was low (18%) however, and loss of the product seemed to occur during purification by column chromatography. This suggested binding of the ligand (25) onto impurities in the silica, possibly Ca²⁺ ions, may have led to loss of product as immobile complexes. Similar problems have been observed in the purification of related tetraamide ligands.



Scheme 2.5. Preparation of lanthanide complexes of the tetraamide (**25**).

Characterisation of the product (**25**) was also rendered more difficult due to its high molecular mass (RMM=5990). Analysis by electrospray mass spectrometry only proved possible by addition of yttrium ions and observation of the resulting doubly and triply charged species. Analysis by matrix assisted laser desorption ionisation - time of flight (MALDI-TOF) mass spectrometry did allow simultaneous observation of both product and potential impurities. The mass resolution proved to be less than satisfactory however, variation of up to 50 amu was observed for the parent ion peak for the ligand (**25**) absorbed on to a selection of matrices.

The relatively high molecular mass of the product did allow the development of alternative purification methods. Benzoylated dialysis tubing, with a molecular mass cut off of 1200-2000 amu, was used to purify the product. Small 'holes' in the dialysis membrane allow compounds of lower molecular mass free movement

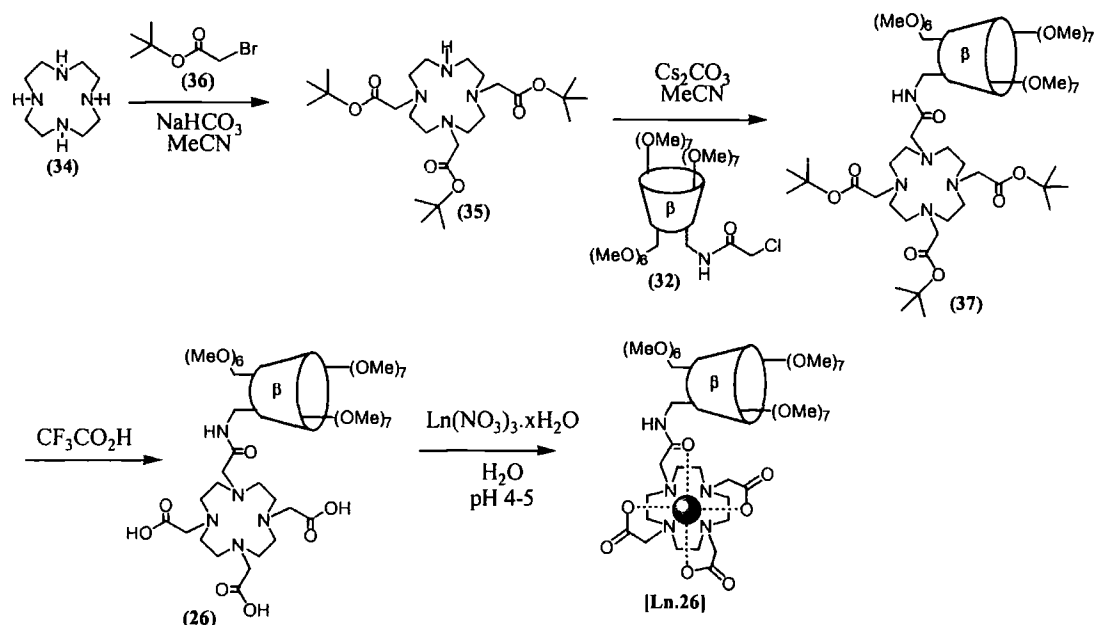
through the tubing, allowing their concentrations to equilibrate inside and outside the tubing. Compounds of a higher molecular mass are unable to pass through the membrane and so are retained inside. Use of the tubing allowed retention of an aqueous solution of the tetraamide (**25**) within the tubing, lower molecular mass impurities, such as potassium salts, DMF, and to a lesser extent residual chloroamide (**32**) were able to diffuse through the dialysis membrane into a large reservoir. Another similar approach involved the use of dialysis membrane filters. Here filters of a set molecular mass cut-off, such as 1000, 2000 or 6000 amu, were used to separate two chambers, one of which contained an aqueous solution of the tetraamide and the other a dynamic flow from a reservoir (generally 1000 cm³) of water. Again the high molecular mass tetraamide (**25**) was retained by the filter, lower molecular mass impurities pass through.

Complexation of europium (III) and terbium (III) ions with the tetraamide occurred on heating the tetraamide with europium or terbium trifluoromethanesulfonate in anhydrous acetonitrile. Complexation was easily followed by thin layer chromatography and purification readily achieved by the use of the dialysis method described above.

2.3.3 Synthesis of lanthanide complexes of a cyclodextrin monoamide ligand.

Synthesis of the analogous charge neutral complexes of the monoamide ligand was achieved by reaction of the cyclodextrin chloroamide (**32**) and the tri-*t*-butyl ester of DO3A (**35**) (Scheme 2.6). The triester (**35**) was synthesised as described by Woods¹⁹ following the stoichiometric addition of 3 equivalents of *t*-butyl bromoacetate (**36**) with 1,4,7,10-tetraazacyclododecane (**34**) in anhydrous acetonitrile. Careful column chromatography allowed removal of doubly and tetra functionalised species to yield the trisubstituted aza-cycle. Addition of the chloroamide (**32**) to a stirred solution of the triester (**35**) in acetonitrile yielded an aza-cycle functionalised with a single cyclodextrin moiety (**37**). Hydrolysis of the *t*-butyl esters occurred at room temperature in a solution of trifluoroacetic acid and was monitored by ¹H NMR, observing the disappearance of the *t*-butyl singlets at *circa* 1.4 ppm.

Complexation of europium (III), terbium (III), gadolinium (III) and ytterbium (III) ions with the monoamide (**26**) occurred following addition of the lanthanide nitrate to an aqueous solution of the monoamide (**26**) adjusted to a pH of 4-5. Complexation was followed by the use of MALDI-TOF mass spectrometry. Purification was readily achieved by the use of the dialysis method described earlier.



Scheme 2.6. Preparation of lanthanide complexes of the monoamide (**26**).

2.4 Structural Studies on Lanthanide Complexes.

2.4.1 ^1H NMR conformational studies on lanthanide complexes of the tetraamide (**25**).

Lanthanide complexes of ligands based on the 1,4,7,10-tetraazacyclododecanetetraacetate skeleton have been shown to form two diastereomers, described as having a square antiprismatic and a twisted square antiprismatic geometry. The processes of pendant arm rotation and ring inversion allow interconversion. A C_4 symmetric system, with four identical achiral pendant arms, will be transformed into its stereoisomer by the successive processes of pendant arm rotation and ring inversion (Figure 2.11). If the pendant arms are chiral

and possess the same absolute configuration, such as the cyclodextrin units of the tetraamide complexes [Ln.25], then the four species obtainable by these interconversions will be diastereomeric.

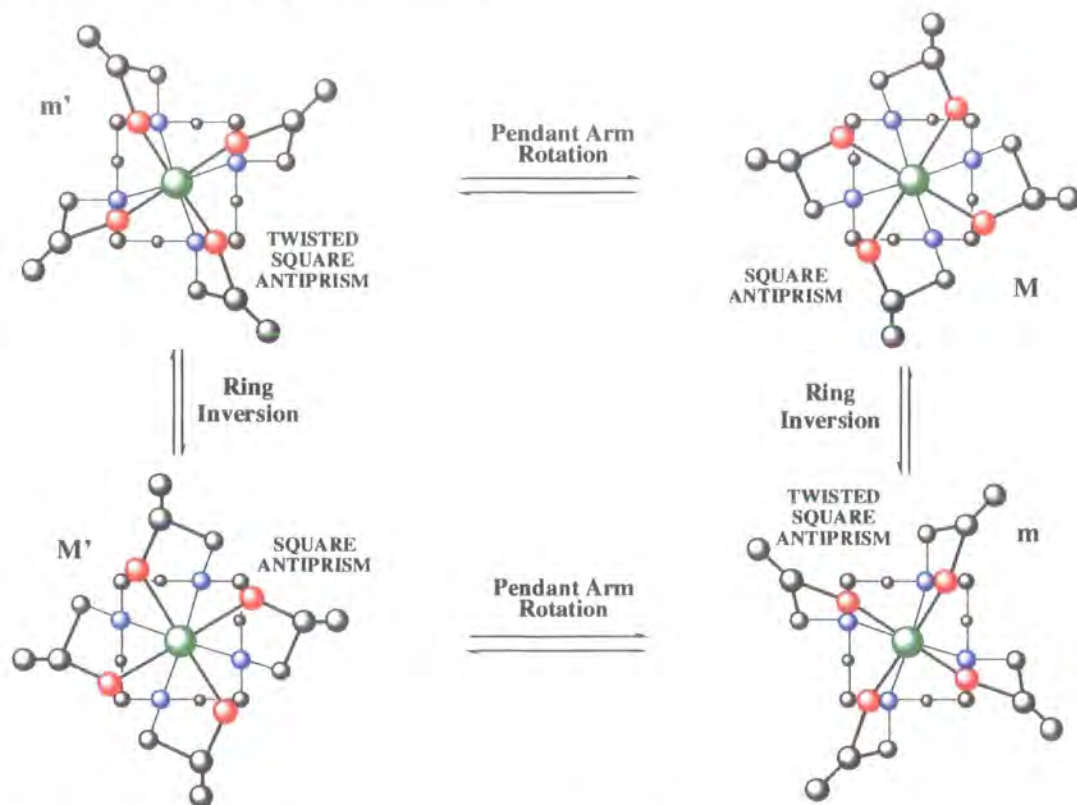


Figure 2.11. Schematic representation of the coordination geometries adopted by the lanthanide (III) complexes of 1,4,7,10-tetracarbamoyl-1,4,7,10-tetraazacyclododecane systems in solution. Their interconversion pathways of pendant arm rotation and ring inversion are also shown. For systems with achiral pendant arms successive pendant arm rotation and ring inversion ($M \leftrightarrow M'$ or $m \leftrightarrow m'$) interconverts between stereoisomers. For pendant arms with chirality of a specific absolute configuration, all four conformers are diastereomers.

In such lanthanide complexes each N-CH₂-CH₂-N unit contains two axially and two equatorially disposed protons. Although both equatorial protons (H_{eq} and H'_{eq}) and one axial proton (H'_{ax}) can be seen to be pointing away from the paramagnetic centre (Figure 2.12), one axial proton is disposed towards the metal centre. In the case of europium (III) complexes the pseudocontact shift, δ_p , is positive for the axial proton disposed towards the metal centre (a more detailed discussion of pseudocontact shifts is given by Sherry and Gerald²⁰) hence resonances resulting from H_{ax} are shifted to

higher frequency. The nature of the resonances arising from the shifted protons correlates to the distribution of each of the four possible diastereomers in solution.

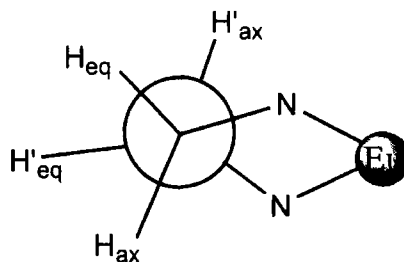


Figure 2.12. Newman projection of the NCCN bond in 1,4,7,10-tetracarbamoyl-1,4,7,10-tetraazacyclododecane systems. The relative position of H_{ax} , H'_{ax} , H_{eq} and H'_{eq} are shown.

Analysis of the C_4 symmetric europium complex [Eu.25] by 1H NMR showed significant line broadening due to complexation of the paramagnetic europium ion. Significantly, a peak corresponding to four of the eight axial protons from the cyclen ring occurs as a broad singlet at 23.1 ppm at room temperature (Figure 2.13). This shows two significant properties of the complex. First it confirms that the ring is fully (tetra) substituted; partial substitution to the mono, di or tri substituted analogues would result in loss of C_4 symmetry and hence lead to greater multiplicity.

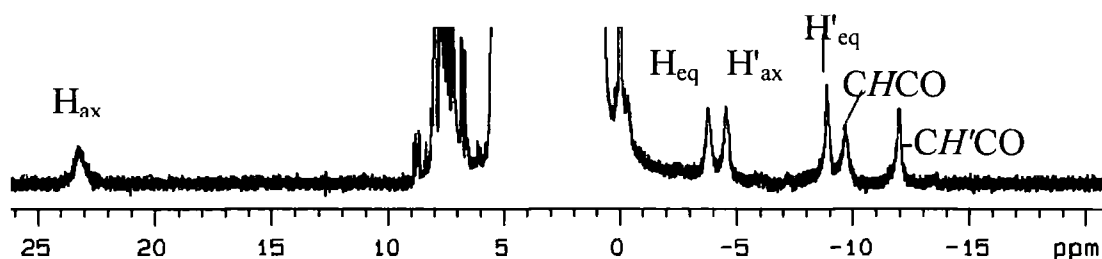


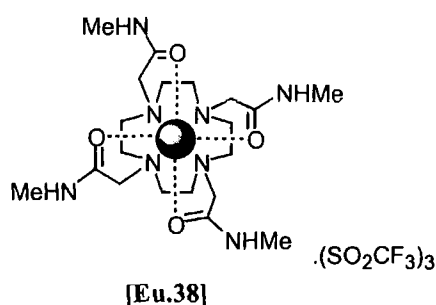
Figure 2.13. 1H NMR of the tetraamide complex [Eu.25] (293K, 300 MHz, CD_3OD).

The singlet observed for the axial protons also suggests that the complex is unable to interconvert between different diastereomers through the processes of pendant arm rotation and ring inversion described above. Such interconversions would give rise to

a signal for each of the four diastereomers present in solution. The broad singlet observed therefore suggests formation of a single diastereomer.

A broad singlet would also be observed if the diastereomers were in fast exchange on the NMR timescale at 293 K. That this isomer was not simply in fast exchange with other species was probed by a variable temperature NMR study. Over the temperature range of 233 K (CD₃OD) to 333 K (D₂O) no additional resonances appeared. Further evidence is given by the presence of two separate singlets for the am protons (NCH₂CO) appearing at -9.3 ppm and -12 ppm. Fast exchange would also cause these two signals to coalesce, the presence of two distinct resonances confirms the predominant formation of a single isomeric species.

The chemical shift of the H_{axial} proton is characteristic of the geometry surrounding the metal centre. In this case, the shift of the H_{axial} proton occurs at 23.1 ppm (293 K, CD₃OD). This is typical of a square antiprismatic conformation, H_{axial} for the twisted square antiprismatic conformation would be expected to resonate at a lower frequency. The analogous tetraamide complex [Eu.38] has previously been shown to display resonances for H_{axial} at *circa* 27 ppm and 5 ppm for the square antiprismatic and twisted square prismatic conformations respectively.²¹



2.4.2 ¹H NMR conformational studies on lanthanide complexes of the monoamide (26).

Lanthanide complexes of the charge neutral monoamide ligand (26) do not possess the C₄ symmetry shown by the tetraamide analogues. Thus each of the eight axial protons on the cyclen ring are unique, four of these eight being shifted to higher frequency by the paramagnetic ion. It can be assumed that for each of the four

conformations of the complex, four separate signals should exist for the higher frequency axial protons.

The ^1H NMR of the europium complex **[Eu.26]** in CD_3OD shows 8 prominent H_{axial} proton resonances in the region 42-32 ppm, with four of the signals resonating together to give two signals (Figure 2.14). These signals correspond to the complex in its two possible square antiprismatic forms, the relative peak areas suggesting the two conformations exist in an approximately 55:45 ratio. A further set of broadened axial protons are discernible in the region 13-17 ppm, corresponding to the twisted square antiprismatic isomers. The integral of the resonances show that the ratio of the square:twisted square antiprismatic isomers is *circa* 19:1. These observations are consistent with slow interconversion between these diastereomers at 293 K, with the square antiprismatic isomers predominating in solution.

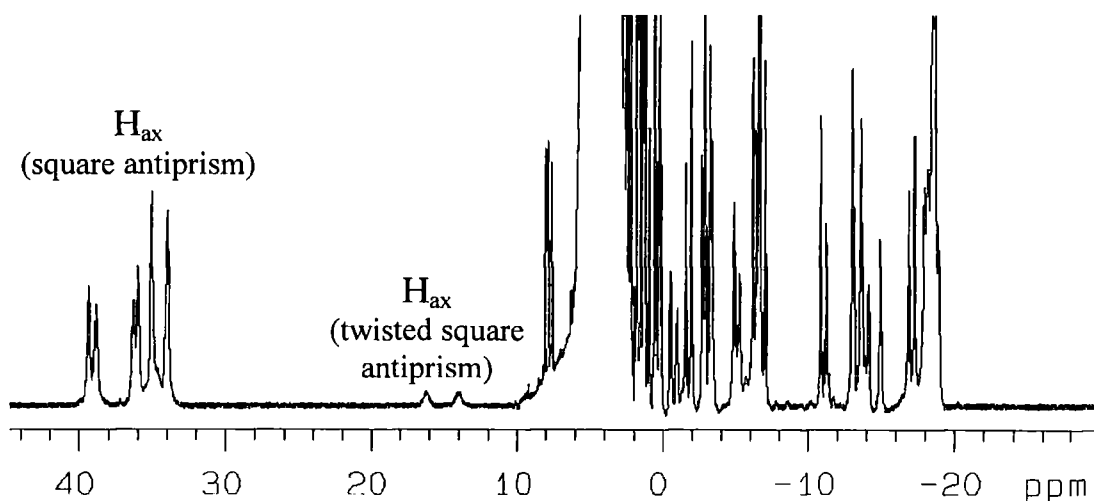


Figure 2.14 ^1H NMR of the monoamide complex **[Eu.26]** (293 K, 300 MHz, CD_3OD).

The spectrum of the europium complex warmed to 313 K showed little discernible change in the form of the resonances suggesting that interconversion of the diastereomers was occurring slowly on the NMR timescale at room temperature. Cooling of the sample to 213 K resulted in significant broadening of all of the signals. This is probably due to reduced motion of the complex caused by an increased viscosity of the solvent.

A ^1H NMR spectrum recorded at 65 MHz of the corresponding Tb complex [Tb.26] showed significant broadening of the paramagnetically shifted axial protons. In contrast to the situation with europium, for terbium the axial ring protons disposed towards the metal centre (H_{ax}) are shifted to lower frequency and appear between -370 and -440 ppm. Both sets of equatorial protons (H_{eq} and H'_{eq}) are also shifted to lower frequency, although to a lesser extent than the axial protons, appearing between -40 and -150 ppm. The remaining axial protons (H'_{ax}) and the pendant arm protons ($-\text{CHCO}$) are all shifted to higher frequency (Figure 2.15).

The H_{ax} resonances for the square anti prismatic and twisted square antiprismatic conformations of the terbium complex of DOTA [Tb.15] at 301K have previously been observed at *circa* -410 ppm and -240 ppm respectively.¹⁹ The chemical shift of the H_{ax} resonances (-370 to -440 ppm) of the monoamide complex [Tb.26] is consistent with the formation of two diastereomers in the square antiprismatic conformation. No evidence for the presence of two twisted square antiprismatic conformations was found.

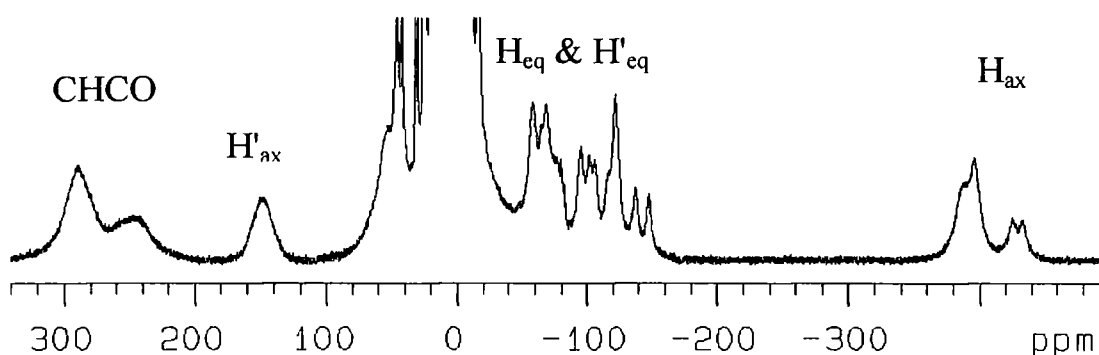


Figure 2.15 ^1H NMR of monoamide complex [Tb.26] showing paramagnetically shifted axial protons (293 K, 65 MHz, CD_3OD).

^1H NMR analysis at 65 MHz of the corresponding ytterbium complex [Yb.26] displayed significant line broadening of the most shifted proton resonances. This is attributed to the presence of the complexed paramagnetic ytterbium ion (Figure 2.16). Trace amounts of uncomplexed ytterbium ions would also broaden the proton resonances, however in this case the less shifted proton resonances retain a narrow peak width which is not consistent with the presence of free ytterbium ions. Heating

of the sample of [Yb.26] to 60°C did not noticeably reduce the line broadening observed.

Similar to the europium complexes shown above, the axial protons disposed towards the metal centre (H_{ax}) are shifted to higher frequency, appearing between 140 and 110 ppm. The remaining axial protons (H'_{ax}) and the pendant arm protons ($CHCO$) are shifted to lower frequency. The ytterbium complex of DOTA [Yb.15] displays H_{ax} resonances at 134 ppm and 82 ppm at 293K corresponding to the square and twisted square antiprismatic conformations respectively in a ratio of 15:2. The chemical shift of the H_{ax} resonances (120 to 140 ppm) of the monoamide complex [Yb.26] is consistent with the formation of two diastereomers in the square antiprismatic conformation. Resonances corresponding to the twisted square antiprismatic conformation are detectable at *circa* 67 ppm. The integral of the resonances show that the ratio of the square:twisted square antiprismatic isomers is greater than 19:1.

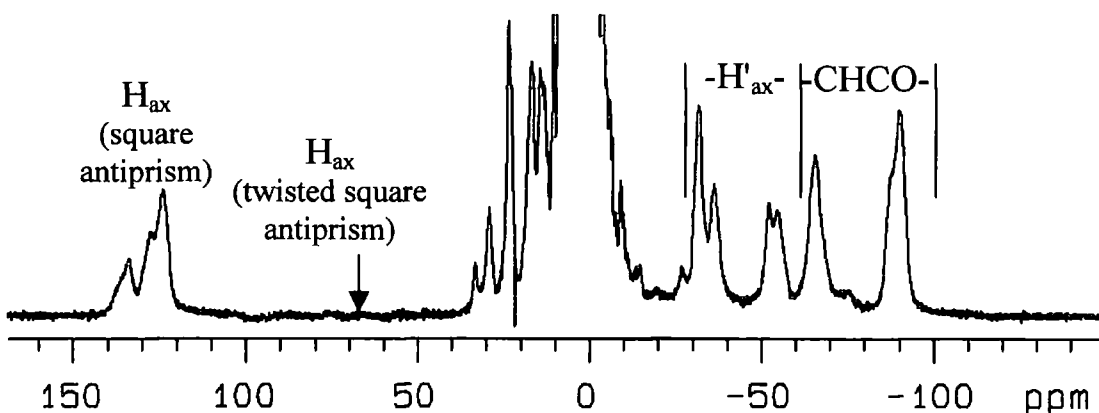


Figure 2.16 1H NMR of [Yb.26] showing paramagnetically shifted axial protons (293 K, 65 MHz, CD_3OD).

2.4.3 Luminescence of the Lanthanide Complexes.

Structural information relating to the hydration state of the metal centre can be obtained from photophysical studies on complexes of europium(III) and terbium(III) ions. The results from such studies are given below, a more detailed discussion of lanthanide luminescence has previously been given (Chapter 1, pages 12-14).

Analysis of the phosphorescence spectra of the europium monoamide complex **[Eu.26]** in D₂O showed the characteristic emission from europium (III) ions. Emission from the ⁵D₀ to the ⁷F_n electronic levels gave rise to the different bands (Figure 2.17). The relative intensity of each band is determined by the Frank-Condon overlap of the two levels. The europium excited state was generated by direct excitation of the metal ion at 397 nm. Excitation at wavelengths below 300nm was also possible by excitation of the ligand-metal charge transfer band.

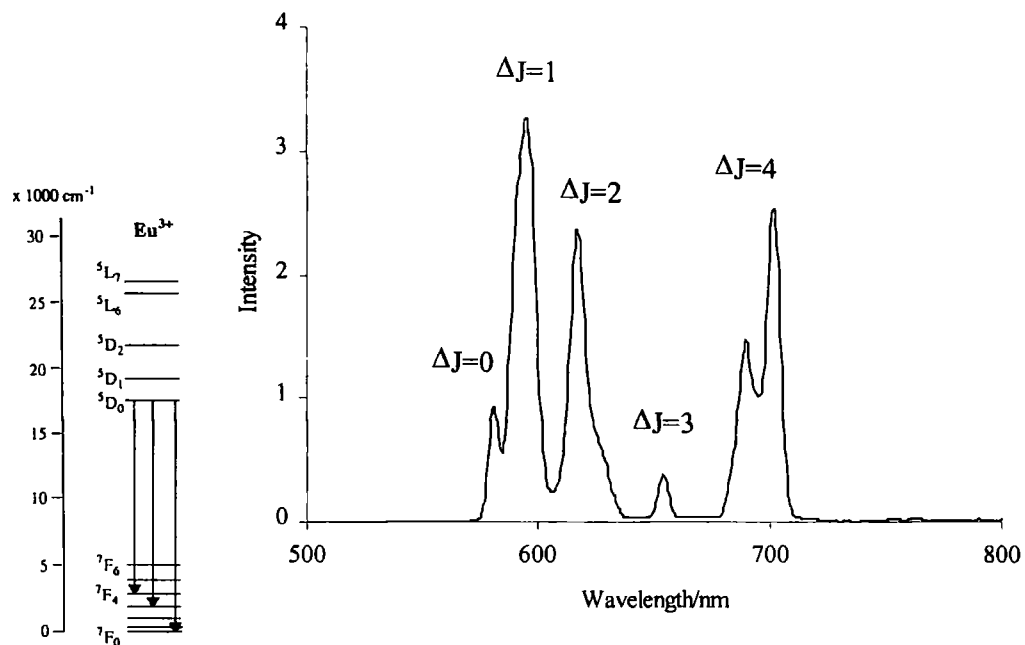


Figure 2.17 Phosphorescent emission from **[Eu.26]** and the energy transitions giving rise to the fine structure ($\lambda_{\text{ex}}=397$ nm, 293 K, H₂O).

Analysis of the phosphorescence spectra of the terbium monoamide complex **[Tb.26]** also showed characteristic phosphorescent emission arising from direct excitation ($\lambda_{\text{ex}}=355$ nm) or from excitation of the ligand-metal charge transfer band ($\lambda_{\text{ex}}<300$ nm). Emission from the ⁵D₄ to the different ground state ⁷F_n electronic levels gave rise to the corresponding bands (Figure 2.18).

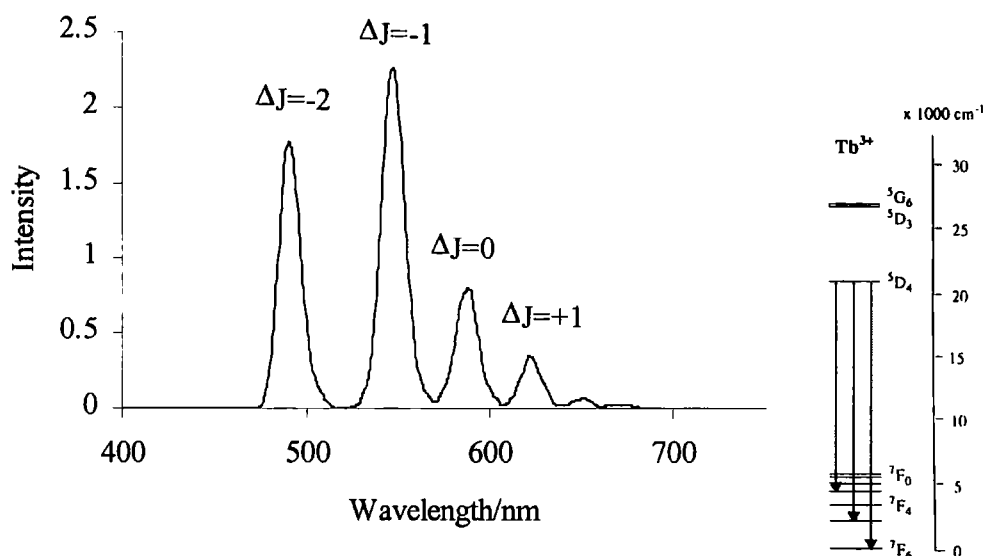


Figure 2.18 Phosphorescent emission from [Tb.26] and the energy transitions giving rise to the fine structure ($\lambda_{ex}=355\text{nm}$, 293 K, H_2O).

The europium [Eu.25] and terbium [Tb.25] complexes of the tetraamide ligand (25) also give rise to characteristic europium (Figure 2.19) and terbium emission by direct excitation at 397nm and 355nm respectively. Both complexes clearly showed the expected fine structure as previously observed for the monoamide complexes [Eu.26] and [Tb.26].

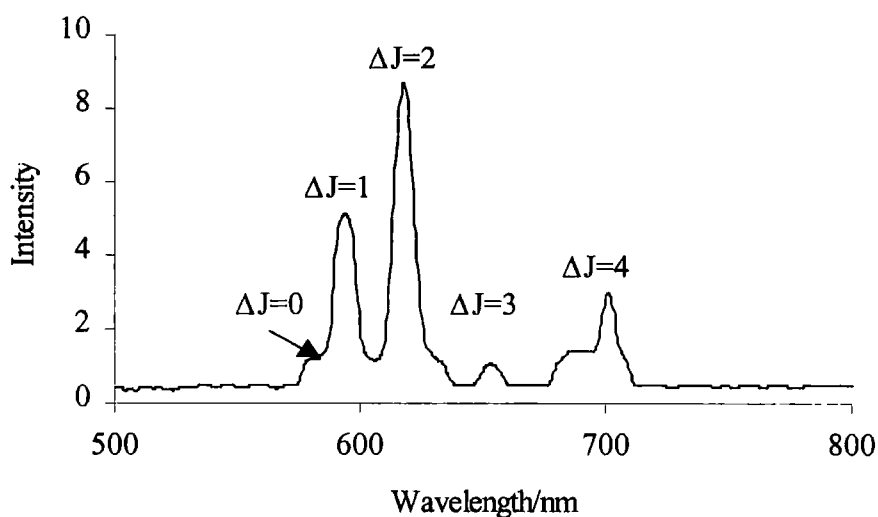


Figure 2.19 Phosphorescent emission from tetraamide [Eu.25] showing the relatively strong $\Delta J=2$ transition ($\lambda_{ex}=300\text{ nm}$, 293 K, H_2O).

Earlier research²² has also looked at the emission of complexes of 1, 4, 7, 10 tetraazacyclododecane tetraamide ligands. Here it was found that the emission intensity of the $\Delta J=2$ emission band of europium tetraamide complexes is sensitive to the coordination state of the metal centre. The emission of a europium complex in water, where the metal is 9-coordinate due to a single coordinated inner sphere water, shows a smaller $\Delta J=2/\Delta J=1$ ratio than the emission of the identical complex in anhydrous acetonitrile (Figure 2.20). The association constant for water (K_{assoc}) has been calculated as $33(\pm 4) \text{ M}^{-1}$, thus in anhydrous acetonitrile[§] the complex can be considered as being exclusively 8 coordinate, or possibly 9-coordinate with the ninth coordination site being occupied by acetonitrile

This implies that a relatively intense $\Delta J=2$ transition in such amide complexes is consistent with the absence of a direct Eu-water bond. Such behaviour is observed for the europium tetraamide complex [Eu.25] shown above (Figure 2.19). Here, in contrast to the monoamide complex [Eu.26] discussed previously (Figure 2.17), the intensity of emission from the $\Delta J=2$ band is surprisingly large relative to that of the $\Delta J=1$ manifold. This provides evidence for the absence of bound water in this complex, further evidence will be discussed below (pages 50-52).

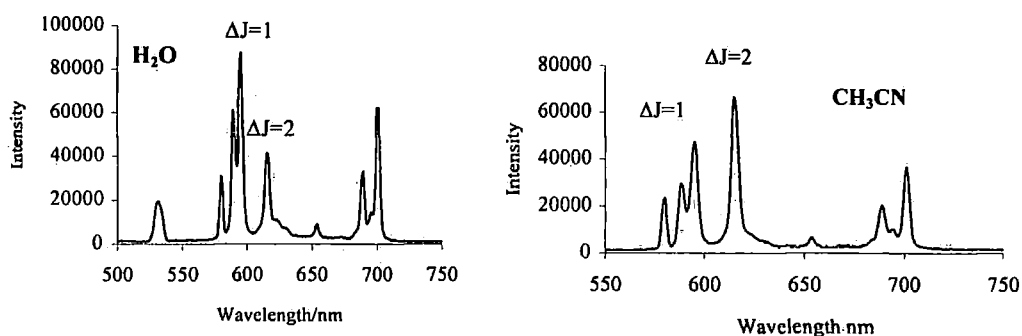
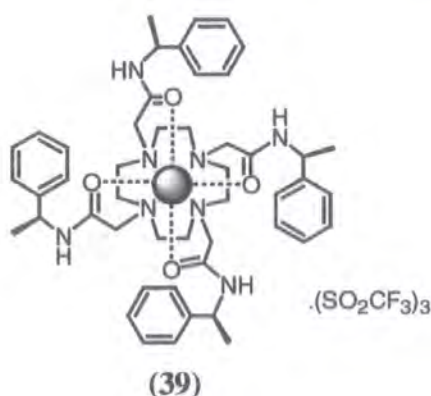


Figure 2.20 Emission from tetraamide europium complex [Eu.39] in H₂O and anhydrous CH₃CN.

[§] [Complex] = $1 \times 10^{-3} \text{ M}$, [H₂O] < $10 \times 10^{-3} \text{ M}$, 298 K.



2.4.4 Determination of Bound Water By Lifetime Measurement of the Monoamide Complexes.

The lifetime of emission ($\Delta J = -1$, 547nm) of the terbium complex [Tb.26] was measured in D₂O and H₂O solutions (Figure 2.21). The lifetime in H₂O (0.88 ms) was shorter than in D₂O (1.10 ms).[#] The change in observed lifetime between the complex in D₂O and H₂O solutions is due to the decreased vibrational deactivation of O-D oscillators over O-H oscillators. This has been discussed in detail previously (Chapter 1, pages 14-15).

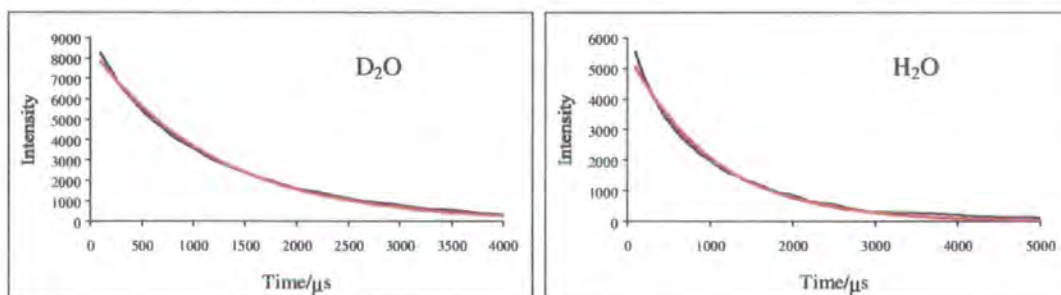


Figure 2.21 Phosphorescence decay curves for [Tb.26] in D₂O and H₂O, with a good correlation to a single exponential decay, allowing calculation of the rate constant for radiative decay.*

The calculated lifetimes allow determination of the *q* value of the complex, which corresponds to the number of water molecules bound to the metal centre. The *q* value is given by the equation below:

$$q = A' \Delta k_{\text{corr}}$$

[#] Concentration = 7.22×10^{-3} M, $\lambda_{\text{ex}} = 355$ nm

where A' is a proportionality constant specific to a given lanthanide ion (5.0 ms for terbium (III), 1.2 ms for europium (III)) and $k = \tau^{-1}$, where τ is the luminescent lifetime in milliseconds. Correction factors in Δk for the separate contribution to quenching from outer sphere water molecules are -0.25 ms^{-1} and -0.06 ms^{-1} for europium (III) and terbium (III) respectively. A further correction factor of -0.075 ms^{-1} is made for each exchangeable carbonyl-bound amide NH oscillator with europium (III).²³ Substitution of the values above into this equation gives the complex [Tb.26] a q value of 0.85.

The lifetime of emission ($\Delta J=1$, 595 nm) of the europium complex [Eu.26] was also measured in H_2O and D_2O solutions. The lifetime in H_2O (0.67 ms) was again shorter than in D_2O (2.38 ms).^{*} Substitution of the calculated lifetimes into the equation above gave the q value as 0.90.

The q values of 0.85 for the complex [Tb.26] and 0.90 for the complex [Eu.26] clearly show that the lanthanide ions are 9 coordinate with 8 coordination sites occupied by the ligand and a further site occupied by a single bound water.

2.4.5 Determination of Bound Water By Lifetime Measurement of the Tetraamide Complexes.

The lifetime of emission ($\Delta J=5$, 547nm) of the terbium tetraamide complex [Tb.25] was measured to be 1.54 ms in H_2O and 1.82 ms in D_2O .[†] These values allow the calculation of a q value of 0.20 for the tetraamide terbium complex [Tb.25].

The lifetime of emission ($\Delta J=2$, 619 nm) of the europium tetraamide complex [Eu.25] was also measured to be 0.52 ms in H_2O and 0.75 in D_2O .^{*} Substitution of these values into the equation given previously allows determination of the q value as

* Rate constants fitted by a least squares analysis to a model single exponential decay using Microsoft Excel.

‡ $\lambda_{\text{ex}}=397\text{nm}$, concentration = $1.74 \times 10^{-3}\text{M}$.

† $\lambda_{\text{ex}}=210\text{nm}$, concentration = $6.0 \times 10^{-6}\text{M}$.

* $\lambda_{\text{ex}}=210\text{nm}$, concentration = $6.0 \times 10^{-6}\text{M}$.

0.05. A summary of the lifetimes for the europium and terbium monoamide and tetraamide complexes is given in Table 2.1.

Complex	$k_{\text{H}_2\text{O}}/\text{ms}^{-1}$	$\tau_{\text{H}_2\text{O}}/\text{ms}$	$k_{\text{D}_2\text{O}}/\text{ms}^{-1}$	$\tau_{\text{D}_2\text{O}}/\text{ms}$	q
[Eu.25]	1.90	0.52	1.39	0.72	0.05
[Tb.25]	0.65	1.54	0.55	1.82	0.20
[Eu.26]	1.49	0.67	0.42	2.38	0.90
[Tb.26]	1.14	0.88	0.91	1.10	0.85

Table 2.1. Determination of q values for europium and terbium complexes of the tetraamide (25) and monoamide (26).

The q values of 0.20 for the complex [Tb.25] and 0.05 for the complex [Eu.25] surprisingly show that the lanthanide ions are only 8 coordinate with all 8 coordination sites occupied by the ligand and no sites occupied by bound water. Lanthanide complexes of tetraphosphinates of 1, 4, 7, 10 tetraazacyclododecane ((b2) and analogues) commonly exhibit zero hydration states ($q=0$) but this is unprecedented for tetraamide ligands. It is possible that the remaining (9th) coordination site is occupied by an oxygen from one of the methyl ethers on the primary face of one of the cyclodextrins, but without structural analysis this is not easily determined.

The lack of bound water in the tetraamide complexes is in direct contrast to the single bound water observed for the monoamide complexes [Tb.26] and [Eu.26]. This may be related to the greater rigidity of the tetraamide system shown earlier by ¹H NMR. Although the monoamide complexes interconvert slowly, they are able to interconvert between the two major (square antiprismatic) isomers, as shown by the presence of detectable amounts of the minor (twisted square antiprismatic) isomer in the case of the europium complex [Eu.26]. In contrast, the europium tetraamide complex [Eu.25] was shown to form only a single isomer in solution. The steric inhibition to the process of pendant arm rotation may also be associated with inhibition of water binding directly to the metal, hence the zero hydration state. The

lack of bound water serves to confirm the lack of available space around the metal centre and is consistent with the high rigidity of the complex.

2.5 Relaxivity and Paramagnetic Ions.

The relaxation of water by paramagnetic ions such as gadolinium has been exploited in the development of contrast agents for improving the sensitivity of MRI. The high toxicity of the aqua gadolinium (III) ion ($LD_{50}=1.4\text{mMkg}^{-1}$)²⁴ necessitates the use of thermodynamically and kinetically stable gadolinium complexes such as $[\text{Gd.DOTA}(\text{15})]^-$ ($\log K_a=24.7$,²⁵ where K_a is the stability constant), marketed under the tradename 'Dotarem'. Commercially available gadolinium contrast agents suffer the disadvantage of requiring high doses to be effective, this in turn leads to severe osmotic shock in patients due to the anionic nature of the complexes. Research towards improved contrast agents initially concentrated on developing charge neutral complexes, to reduce the osmotic shock to the patient, and on developing complexes which exhibit a higher relaxivity. More recently responsive (eg pH, pO_2) and targeted contrast agents are being sought.

The relaxivity, R_1 , of a complex is defined as the slope of the linear dependence between the relaxation rate and the concentration of the paramagnetic solute. It has also been described as "the increment of the water proton relaxation rate per unit concentration of contrast agent."²⁶ Two mechanisms have been found to be critical for the catalysis of water proton relaxation by a paramagnetic centre. The 'outer sphere' mechanism arises through the diffusion of the paramagnetic ion through the bulk solvent. and has been shown to depend on the electronic relaxation time (T_{1e}) and the spin state (S).²⁴ The 'inner sphere' mechanism arises from exchange of bound water molecules with the bulk solvent, hence leading to relaxation of the bulk solvent. The overall relaxivity is given by the sum of the inner sphere and outer sphere relaxivities plus the water relaxation rate.

$$R_1^{\text{obs}} = R_1^{\text{water}} + R_1^{\text{inner-sphere}} + R_1^{\text{outer-sphere}}$$

The longitudinal relaxivity (R_1) of a complex has been shown to be proportional to $[C]$, the concentration of the paramagnetic agent, and q , the number of coordinated water molecules, and inversely proportional to the sum of T_{1M} , the longitudinal or 'spin-lattice' proton relaxation time, and τ_m , the residence lifetime of a bound water molecule.

$$R_1 = \frac{[C]q}{55.6} \left(\frac{1}{T_{1M} + \tau_M} \right)$$

T_{1M} , the longitudinal proton relaxation time, is related to τ_R , the reorientational correlation time, and τ_S , the electron spin relaxation time. The correlation time, τ_R , is related to the rate of tumbling of the complex in solution, and hence is expected to increase linearly with increasing molecular mass; τ_S is dependent on the field strength.²⁷ Thus measurement of the relaxivity of a complex at a variety of field strengths gives a nuclear magnetic resonance dispersion (NMRD) profile which can be modelled to allow calculation of q , τ_M , τ_R and τ_S .

2.5.1 NMRD Profiles of the Monoamide Complex [Gd.26].

The NMRD profile of the monoamide complex [Gd.26] was obtained at 25°C and at 39°C (Figure 2.22). The profile was consistent with a monohydrated complex ($q=1$). The fitted profile was consistent with a τ_M value of 1.14 μ s at 25°C, typical τ_M values for monoamide derivatives of DO3A are generally *ca* 1 μ s.²⁸ The rotational correlation time, τ_R , was measured as 94 ps which is *ca.* half the expected value based on the molecular mass of the complex. This suggests that rotational freedom around the cyclodextrin unit results in ineffective coupling of the motion of the cyclodextrin with that of the bound lanthanide moiety. This allows the lanthanide, and its associated water molecule, to tumble more rapidly than an effectively coupled conjugate would, hence τ_R and the observed relaxivity are somewhat lower than expected.

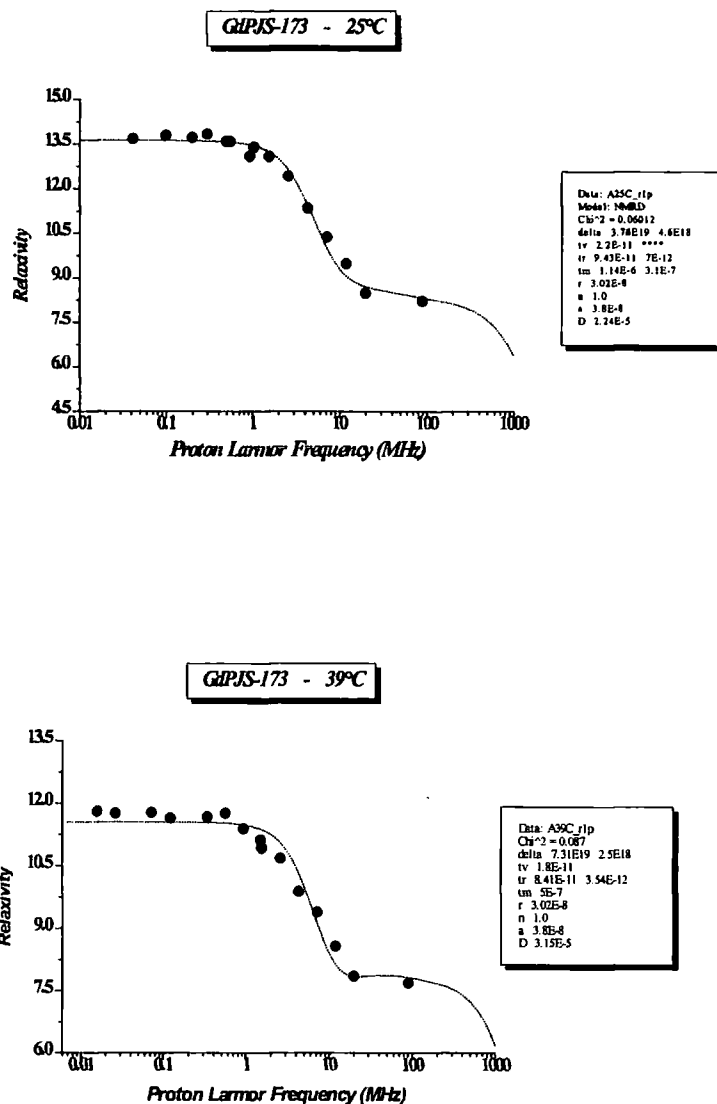
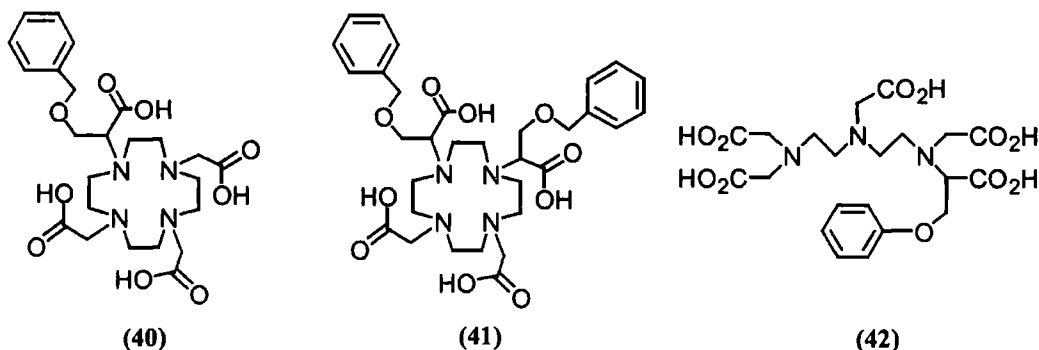


Figure 2.22 NMRD profiles of [Gd.26] at 25°C and at 39°C.

2.5.2 Interactions Of The Monoamide [Gd.26] With The Paramagnetic DOTAPh-Gd (III) Complex [Gd.40].

Previous work by Aime *et al.*²⁹ had demonstrated that the addition of β -cyclodextrin (1) to β -benzoyloxy- α -propionic derivatives of [Gd.DOTA], such as GdDOTAPh [Gd.40] and GdDOTAPh₂ [Gd.41], led to the formation of 1:1 and 2:1 inclusion compounds. The water proton relaxation rates (R_1) were observed to increase with the addition of β -cyclodextrin, consistent with an increased τ_R due to formation of

higher molecular mass inclusion complexes. The relaxivity profile with changing concentrations of β -cyclodextrin allowed calculation of K_f , the formation constant for the complex between β -cyclodextrin and GdDOTAPh₂ [**Gd.41**] as 286 M^{-1} , and between β -cyclodextrin and GdDPTAPh [**Gd.42**] as 217 M^{-1} . Although the results suggested significant formation of a 2:1 complex between β -cyclodextrin and GdDOTAPh₂ [**Gd.41**] the formation constants reported were not defined explicitly to correspond to formation of the 1:1 or 2:1 complexes.



Addition of the monoamide [**Gd.26**] to GdDOTAPh [**Gd.40**] was expected to lead to significant increases in relaxivity, due to both the presence of 2 gadolinium centres and the increase in τ_R , expected from formation of the higher molecular mass complex (Figure 2.23). The relaxivity measured upon addition of [**Gd.26**] to GdDOTAPh [**Gd.40**] was found to be significantly higher than the sum of the relaxivities of the complexes themselves (Figure 2.24). These results allowed calculation of K_{11} , the formation constant for the 1:1 complex, as 1742 M^{-1} , *ca* 7 times greater than the formation constant expected between β -cyclodextrin (**1**) and GdDOTAPh [**Gd.40**] (*ca* 200 M^{-1}).²⁹ The increase in stability of the inclusion complex is probably due to an increased rigidity of the complex [**Gd.26**] over the parent β -cyclodextrin (**1**), leading to a more favourable loss of translational entropy upon guest binding.

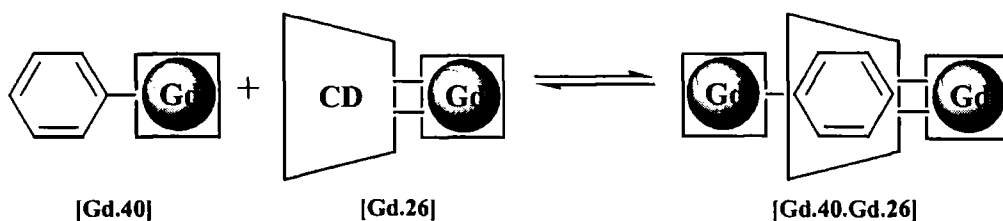


Figure 2.23 Formation of an inclusion complex between the monoamide complex [**Gd.26**] and GdDOTAPh [**Gd.40**].

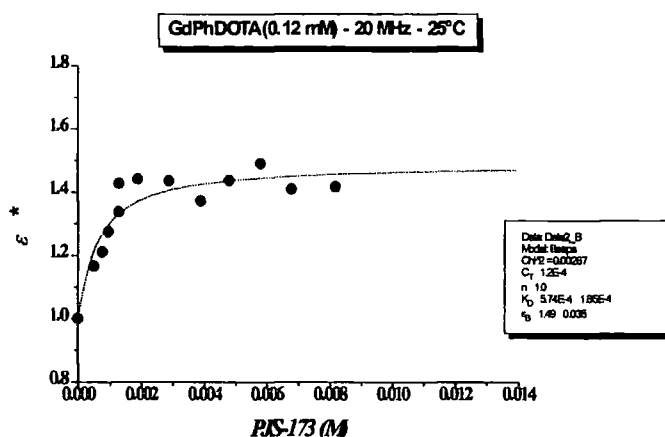


Figure 2.24. Increased relaxivity upon addition of [Gd.26] (labelled PJS173) to GdDOTAPh [Gd.40], where $\epsilon^* = (R_1^{\text{obs}} - R_{1W}) / (R_1^{\text{calc}})$ and R_1^{calc} is the sum of the relaxation rates of the two complexes as calculated from the known relaxivities (8.48 for [Gd.26] and 5.45 for GdDOTAPh [Gd.40])

2.6 Luminescence Properties.

2.6.1 Detection Properties of the Tetraamide Complexes [Eu.25] & [Tb.25].

Although luminescence from the lanthanides in these complexes is possible by direct excitation, or via excitation of the ligand-metal charge transfer band, the quantum yield is low and hence emission is weak. Sensitised emission, by energy transfer arising from the excitation of guests complexed within the cavity, has the potential to increase the efficiency of emission. Thus the effect of adding aromatic guests capable of binding within the cyclodextrin cavities to the europium and terbium complexes [Eu.25] and [Tb.25] was investigated.

As previously discussed, the tetraamide host contains 4 possible binding sites suitable for the inclusion of size specific guests. Successful intramolecular energy transfer can be considered as being dependent on two factors. Firstly, the guest must bind within the cavity in a manner which allows it to approach close enough to the metal centre for energy transfer to be effective. The rate of energy transfer is

assumed to be proportional to r^{-6} , where r is the distance between the two centres. Secondly the triplet energy level of the donor, in this case the guest, must be suitable for energy transfer to the given lanthanide. In the case of europium (III) and terbium (III), the triplet energy must be greater than 210 kJmol^{-1} and 244 kJmol^{-1} respectively.

Previous work^{30,31,32} had shown that tryptophan can act as a fairly efficient substrate for energy transfer to terbium ions. However addition of aliquots of L-tryptophan to an aqueous solution of the terbium tetraamide complex **[Tb.25]** resulted in a reduction in the intensity of emission from the metal centre. Addition of 2-acetylnaphthalene also resulted in an identical reduction of luminescence.

The lack of energy transfer to the metal centre may either be a consequence of poor guest binding into the cyclodextrin cavity, or result from deactivation of the excited states of either the metal or the aromatic guest. As both guest species were expected to exhibit strong binding affinities to cyclodextrin ($K_{11} = 324$ & 513 M^{-1} for 2-acetylnaphthalene^{10,33} & L-tryptophan^{10,34} respectively[§]), and both species were also expected to exhibit energy transfer to terbium ions, it was anticipated that the lack of energy transfer was due to a combination of both factors.

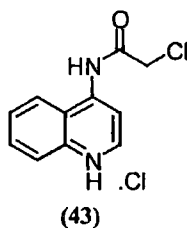
To investigate the possible problems in more detail, the addition of 2-*p*-toluidino-6-naphthalenesulfonate (2,6-TNS, **4**) to the europium tetraamide complex **[Eu.25]** was investigated. 2,6-TNS (**4**) has been shown to exhibit stronger binding to β -cyclodextrin (**1**) ($K_{11} = 1980 \text{ M}^{-1}$),^{35,*} approximately 3 times greater than that for naphthalene. It has also been shown to exhibit enhanced fluorescence upon binding into β -cyclodextrin (**1**).³⁶ Upon addition of 2,6-TNS (**4**) to the europium tetraamide complex **[Eu.25]** luminescence from the lanthanide was again reduced, although to a lesser extent than observed previously. Analysis of the fluorescence of the guest relative to a solution of equivalent concentration without the host showed significant fluorescent enhancement, suggesting that binding to the cyclodextrin was occurring.[#]

[§] 293K, H₂O.

^{*} 293K, H₂O.

[#] Assuming $K_{11} \approx 2000 \text{ M}^{-1}$, 3% of the host and 3% of the guest are expected to be bound at the concentrations used in the luminescence experiment, where $[\text{host}] = [\text{guest}] = 1.5 \times 10^{-5} \text{ M}$.

Addition of per-O-methyl- β -cyclodextrin (**5**) to a solution of 2,6-TNS (**4**) also showed a similar fluorescence enhancement. This confirmed the observation that binding of the guests into the cyclodextrin cavity was occurring. The experiment was also repeated with addition of a substituted quinoline (**43**) with an identical set of observations.



From these results it was still unclear if the lack of sensitised binding was due simply to a lack of efficient energy transfer or a combination of this and a lack of guest binding into the cyclodextrin cavities. It was anticipated that although inefficient energy transfer may be critical to inhibiting sensitised emission, the competitive binding of 3 triflate counterions to the 3^+ electronic charge of the complex could prove counterproductive. It was also felt that the charge density of the complex may also reduce binding of guests into the cyclodextrins. This concluded investigations into the tetraamide complexes and attention was shifted onto the analogous monoamide complexes.

2.6.2 Detection Properties of the Monoamide Complexes [Eu.26], [Tb.26] & [Yb.26].

Previous work by Nocera *et al.*³ had demonstrated energy transfer from naphthalene to terbium (III) for a cyclodextrin-lanthanide conjugate as discussed previously (pages 24-26). Addition of naphthalene to an aerated solution of the terbium monoamide complex [Tb.26] however resulted in a reduction in the luminescent emission observed. This suggested that a slow rate of energy transfer was inhibiting successful sensitisation of the lanthanide. A slow energy transfer rate would result from a relatively long distance (r) between the donor and acceptor, the rate of energy transfer is accepted as being proportional to r^{-6} . It was anticipated that removal of oxygen from the system would remove a significant deactivation pathway for the excited triplet naphthalene and lead to an enhancement in the emission intensity from

the lanthanide. Indeed in a degassed solution,^Φ addition of naphthalene to the terbium complex [Tb.26] did result in energy transfer to the metal centre, observable by an increase in the intensity of metal emission (Figure 2.25).

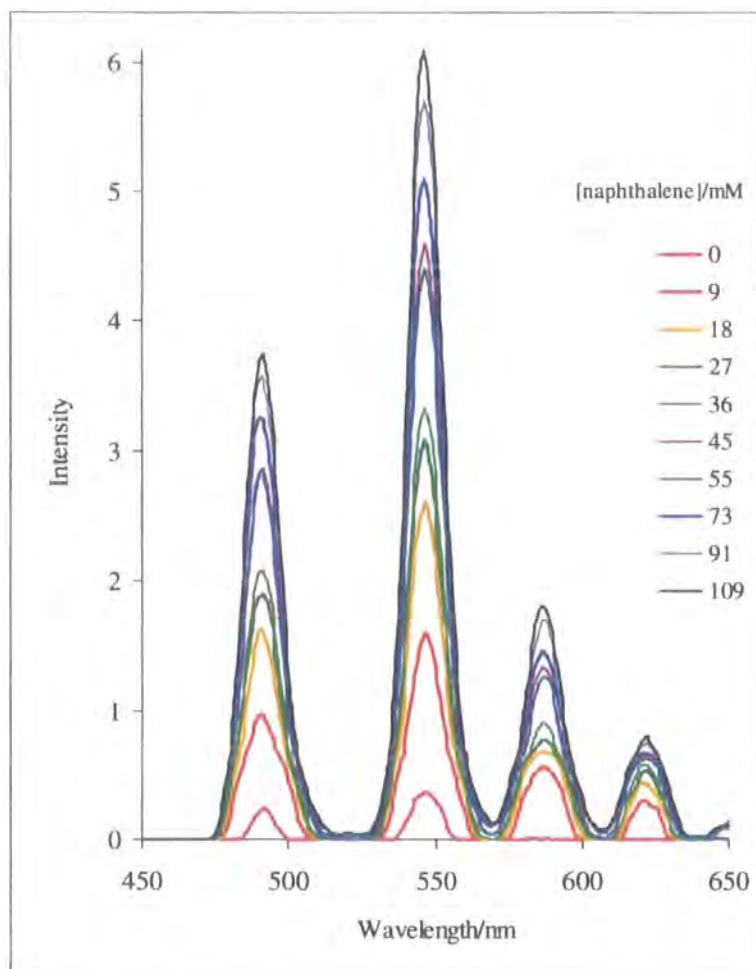


Figure 2.25 Increased emission from [Tb.26] upon addition of naphthalene ($\lambda_{\text{ex}}=275\text{nm}$, [Tb.26] $=1.4\times 10^{-4}\text{M}$, 50%MeOH/H₂O, 293 K).

Analysis of the excitation spectrum of the lanthanide emission peaks also showed a band increasing in intensity as a function of naphthalene concentration. The excitation spectrum corresponded to naphthalene absorption between 270 and 310nm (Figure 2.26). This confirms that the increasing intensity of lanthanide emission is due to energy transfer from the naphthalene.

^Φ 293K, H₂O.

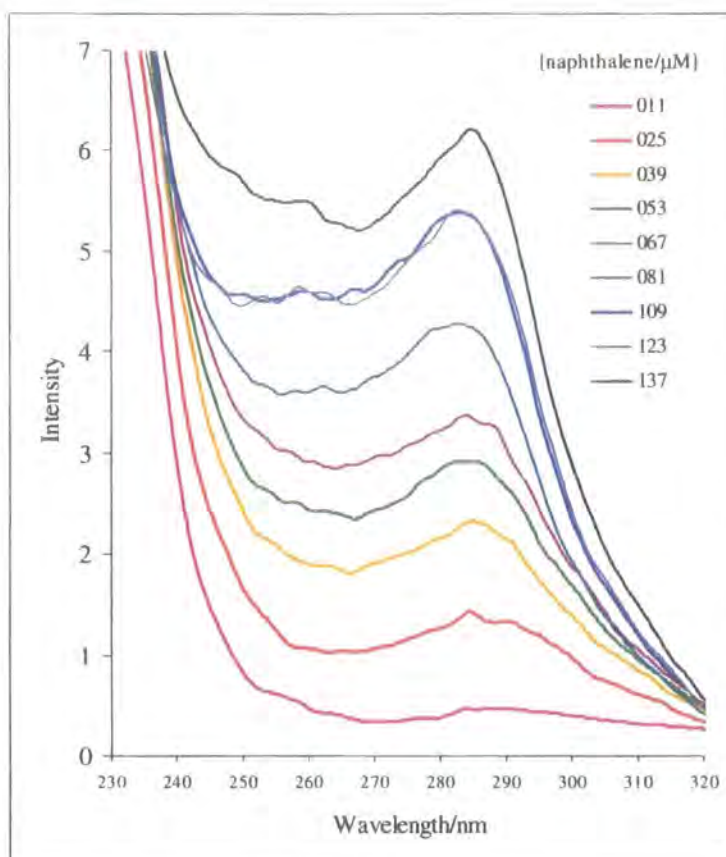


Figure 2.26 Excitation spectrum of [Tb.26] at increasing concentrations of naphthalene ($\lambda_{em}=547\text{nm}$, [Tb.26]= $1.4\times 10^{-4}\text{M}$, 50% MeOH/H₂O, 293 K).

The association constant between naphthalene and [Tb.26] was calculated to be $10,200\text{ M}^{-1}\ast \pm 10\%\dagger$ using a modified Benesi-Hildebrand analysis (Appendix A)^{37,38} (Figure 2.27). This is *circa* 14 times greater than that reported between naphthalene and β -cyclodextrin in water where $K_{11}=685\text{M}^{-1}$.^{39,\psi} The difference cannot simply be attributed to the change in solvent. Indeed the solvent change may be likely to cause a minor reduction to the binding affinity. The reduction in hydrogen bonding and increased cavity size which occurs on O-methylation of the hydroxyl groups also is unlikely to account for such a large increase in binding affinity. The increased binding affinity however may be due to the increased rigidity of the system, entropically favouring inclusion of guests into the cavity. Such an increase is

\ast 293 K, 50% MeOH/H₂O.

\dagger Calculated by linear regression.

ψ H₂O, 293K.

consistent with that observed for the binding of GdDOTAPh [Gd.40] with [Gd.26] observed by NMRD (pages 55-56).

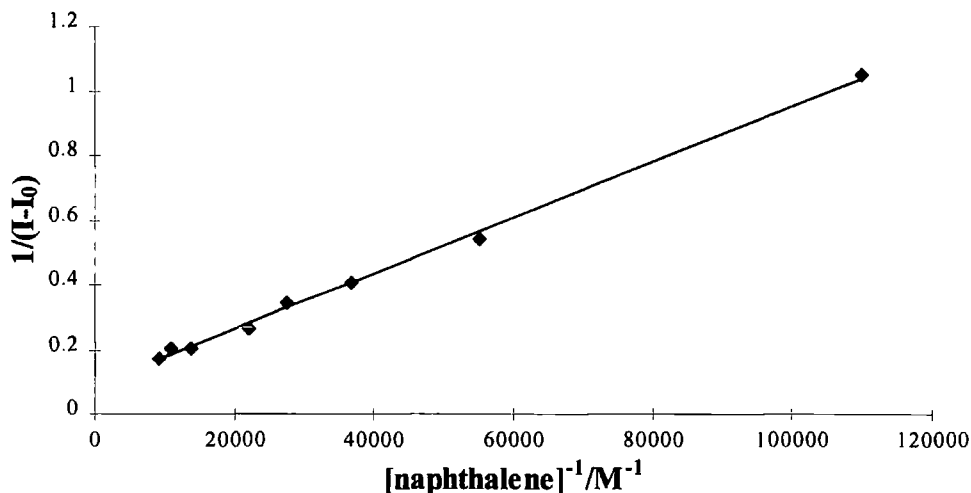


Figure 2.27 Benesi-Hildebrand analysis of the complexation of naphthalene with [Tb.26] (Intensity of excitation at 285nm, $\lambda_{em}=547nm$, [Tb.26]= $1.4 \times 10^{-4}M$, 50%MeOH/H₂O, 293 K).

Sensitised lanthanide emission was also observed upon addition of 1- and 2-methylnaphthalene, 2-bromonaphthalene and *p-t*-butyl benzoic acid methyl ester to the terbium complex [Tb.26] in degassed solutions.* In each of these cases the increases in metal luminescent emission intensity were too small to allow a meaningful Benesi-Hildebrand analysis to determine binding affinities. In contrast the addition of 1-bromonaphthalene, naphthaldehyde, quinoline, D-tryptophan and (S)-(-)-1-(1-naphthyl)ethylamine to the terbium complex [Tb.26] all showed a reduction of metal emission upon addition of the guests. Analysis of the fluorescence spectra in each of these cases clearly showed fluorescent enhancement thus demonstrating that binding is occurring. The reduction of long lived luminescent emission in these cases is therefore probably due to a combination of factors. Such factors could include an inefficient energy transfer step, presumably associated with a larger than optimal energy gap between the aryl triplet and the terbium ⁵D₄ level and a larger than optimal intramolecular distance. Deactivation of the excited metal

* 293 K, 50% MeOH/H₂O.

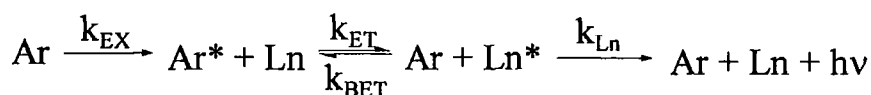
or triplet states would also inhibit sensitised emission, as could low triplet quantum yields (Φ_{ISC}) for the aromatic moieties.

The electron transfer mechanism attributed to sensitisation of ytterbium(III) can potentially reduce problems associated with inefficient energy transfer. The rate of electron transfer has been shown to be proportional to $e^{(-r\beta/2)}$, where r is the distance between the donor and acceptor, and β is the rate of decay of coupling with distance, and generally approximates to 1\AA^{-1} .⁴⁰ The lower distance dependence of electron transfer compared to the energy transfer mechanism operating for europium (III) and terbium (III) has allowed electron transfer to occur between proteins with a separation greater than 10\AA .

Addition of naphthalene ($8.6 \times 10^{-5}\text{ M}$) or phenanthridine ($3.0 \times 10^{-5}\text{ M}$) to **[Yb.26]** ($1.07 \times 10^{-4}\text{ M}$) in degassed aqueous methanol (50% v/v) however resulted in no sensitised ytterbium emission. It is possible that electron transfer is inefficient due to a large intermolecular distance between the metal and the chromophore, however insulation of the chromophore by the cyclodextrin moiety, inhibiting electron transfer, is a more likely explanation for the lack of sensitised emission.

2.7 Photokinetic Studies.

The time-resolved emission profile of sensitised luminescent lanthanide systems such as those described above is controlled by the rates of energy transfer (k_{ET}) and emission (k_{Ln}). In the case of terbium systems, the situation can be further complicated as the energy levels of the excited states of the donor and metal centre may allow a temperature dependent back energy transfer process to occur (Scheme 2.7).



Scheme 2.7 Rates of excitation and emission of a lanthanide centre.

Other competitive deactivation pathways can occur, such as O₂ quenching of the donor excited state and vibrational -OH and -NH deactivation of the excited lanthanide. Oxygen quenching can be limited by degassing the solution, -OH deactivation is reduced by protecting the lanthanide in a protective 'cage' such as that provided by the DOTA type ligands or by using deuteriated solvent.

The time resolved profile of lanthanide emission typically consists of two distinct components (Figure 2.28): a decay, usually mono or bi-exponential in character (k_2), and a 'grow-in', or rise, with its own characteristic rate constant (k_1). The 'grow in' generally becomes more discernible with decreasing temperature. It has previously been determined⁴¹ that if the rate of energy transfer (k_{ET}) is much faster than the rate of emission (k_{Ln}), then k_1 is equivalent to k_{ET} and k_2 to k_{Ln} . Similarly if k_{ET} is much less than k_{Ln} then k_2 is equivalent to k_{ET} .

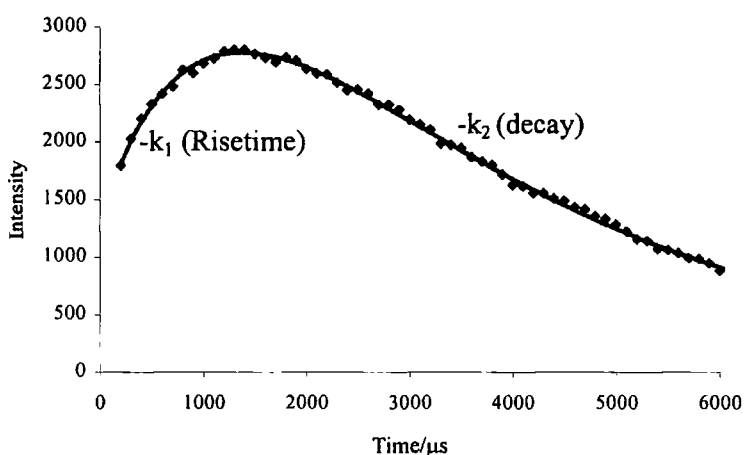
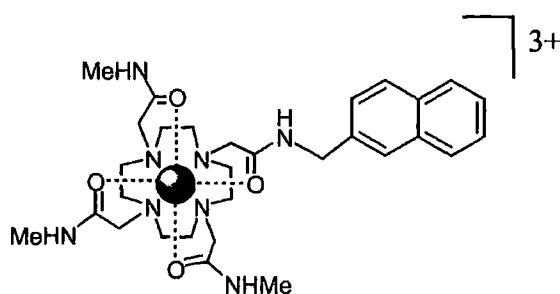


Figure 2.28 Luminescent emission profile of [Tb.26] + naphthalene showing separate 'rise' (k_1) and decay (k_2) components ($[Complex]=9.0 \times 10^{-5} M$, $[naphthalene]=3.0 \times 10^{-3} M$, 50% MeOH/H₂O, degassed, 240K.).

The rate of decay of the sensitising aromatic triplet state has also been shown to correlate to the 'rise-time' (k_1) and decay (k_2) of the lanthanide for a terbium complex appended to naphthalene (44).⁴² In this case the rapid rise-time of the lanthanide emission (k_1 , where $k_1=(\tau_1)^{-1}$) was associated with a lifetime of 8.1 μs, and the slow decay (k_2 , where $k_2=(\tau_2)^{-1}$) with a lifetime of 2.0ms at 150K. Study of the naphthyl triplet absorption spectrum by flash photolysis showed a fast component, with a lifetime of 8.4 μs and a slow component with a lifetime of 2.0ms.



(44)

The close correlation between the two triplet lifetimes and the rise and decay lifetimes of the lanthanide showed that back energy transfer allowed an equilibrium to be rapidly established between the lanthanide and the triplet state of the naphthyl group. This equilibrium resulted from the small energy gap between the triplet naphthyl (259 kJmol^{-1}) and emissive terbium 5D_4 (255 kJmol^{-1}) states which allowed competitive back energy transfer from the metal to the naphthalene. This competitive process inhibited sensitised luminescence from the metal. It was a combination of these observations which led us to examine the luminescence temperature dependence and triplet behaviour of naphthalenes included into the cavity of the cyclodextrin-terbium conjugate [Tb.26].

2.7.1 Variable Temperature Luminescence.

The emission and excitation spectra of the terbium monoamide complex [Tb.26] sensitised by the addition of naphthalene was investigated as a function of temperature. As expected, sensitised metal emission was observed to increase in intensity as the temperature was reduced from 295 K to 240 K. This can be attributed to a reduction in the rate of competitive back energy transfer from the excited metal to the naphthalene, and a reduction in the rate of other temperature dependent deactivation pathways of the metal or the triplet naphthalene. The lifetime of metal emission was also observed to increase by 400% with the reduction in temperature. A large enhancement of 280% was also observed for the analogous system sensitised with 1-methylnaphthalene. 1-Methylnaphthalene also enhanced emission from the europium monoamide complex [Eu.26] by 180% (Figure 2.29).

No significant increase in lifetime was observed for the terbium complex [Tb.26] in the absence of the naphthyl sensitiser (*circa* 10%) over the temperature range 295 K

to 240 K. This shows that lower temperatures can increase the efficiency of energy transfer for sensitised emission, such as the sensitisation of [Tb.26] and [Eu.26] with naphthalene and 1-methylnaphthalene. Systems showing weak sensitisation or where direct excitation of the metal occurs, such as the direct excitation of [Tb.26] show little significant variation in lifetime with temperature.

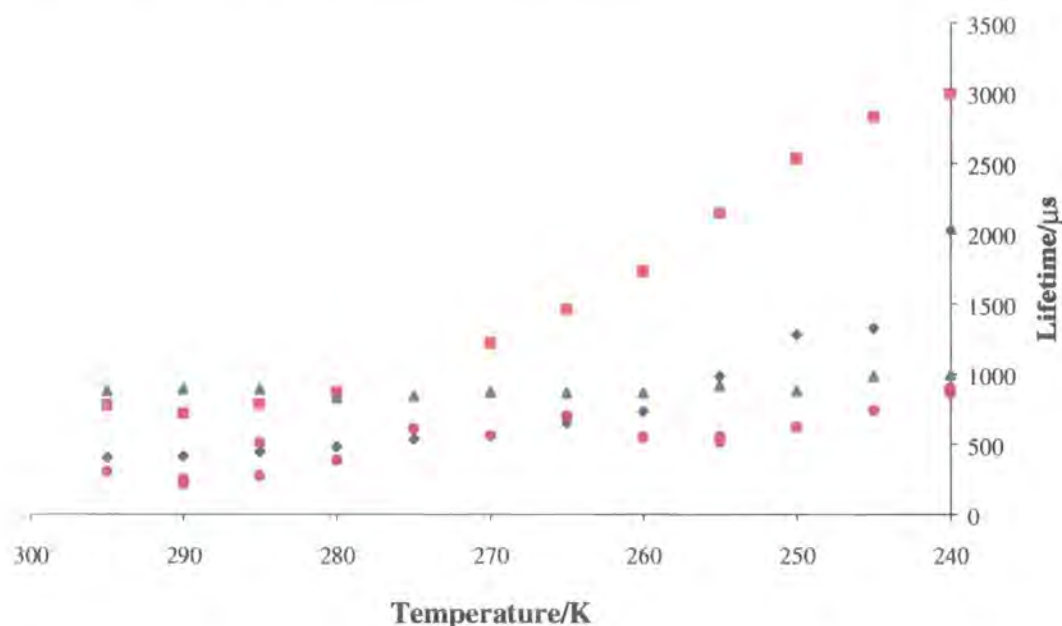


Figure 2.29 Increase in luminescent lifetime with decreasing temperature for [Tb.26] (▲), [Tb.26] + naphthalene (◆), [Tb.26] + 1-methylnaphthalene (■) and [Eu.26] + 1-methylnaphthalene (●) ([Complex]= 9.0×10^{-5} M, [aromatic]= 3.0×10^{-3} M, 50% MeOH/H₂O, degassed).

The emission profile of the systems described above show two components, a single exponential decay of the metal and a faster 'grow-in' or rise-time (Figure 2.28). The rise-time was also observed to increase with decreasing temperature, growing rapidly below 260K (Figure 2.30). The observation of a 'grow-in' component to the metal emission profile shows that energy transfer to the metal is inefficient. This may be either due to a slow rate of energy transfer or to significant back energy transfer leading to the establishment of an equilibrium between the excited metal and triplet naphthalene states.

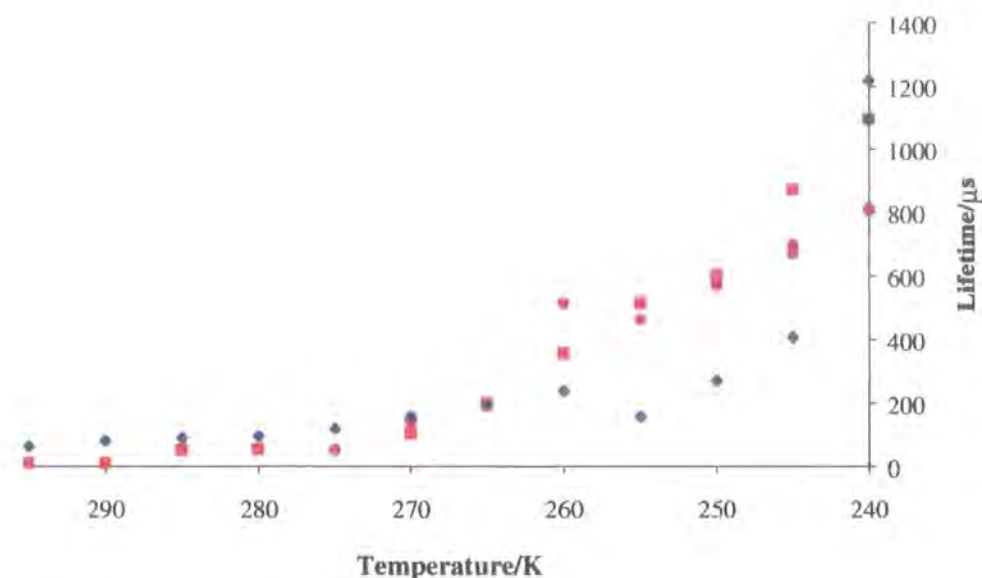


Figure 2.30 Increase in luminescent 'grow in' lifetime with decreasing temperature for [Tb.26] + naphthalene (♦), [Tb.26] + 1-methylnaphthalene (■) and [Eu.26] + 1-methylnaphthalene (●).*

2.7.2 Flash Photolysis Of Naphthalene-cyclodextrin-lanthanide Conjugates.

The triplet-triplet absorption lifetime and lanthanide emission were observed in degassed 50% aqueous methanol at 295 and 240K.[§] Decay of the triplet excited state fitted to a single exponential with good residuals and was associated with a lifetime of 43μs at 295K and 180μs at 240K.* Interestingly unbound 1-methylnaphthalene showed a triplet lifetime of 92μs at 295K and 915μs at 240K in this solvent system. This shows that the naphthyl triplet state is slightly deactivated by inclusion into the cavity of these cyclodextrin-lanthanide systems. The reduction in triplet lifetime is likely to be a result of competitive energy transfer to the lanthanide centre.

The lanthanide emission was fitted to a double exponential decay, with one exponential describing the grow-in and the other the decay. The emission showed a 'grow-in' lifetime of 55 μs and a decay of 1.1 ms at 240K. These lifetimes were significantly different to those observed under the conditions for variable

* [Complex]= 9.0×10^{-5} M, [aromatic]= 3.0×10^{-3} M, 50% MeOH/H₂O, degassed.

§ Concentration of [Tb.26]= 3.2×10^{-4} M. [1-Methylnaphthalene]= 1.7×10^{-4} M. Assuming $K_{11} \sim 10,000\text{M}^{-1}$ then ~70% of 1-methylnaphthalene is bound within cyclodextrin.

temperature luminescence, where the terbium showed a 'grow-in' lifetime of 1.1 ms and *circa* 10 μ s, and a decay lifetime of 3.0 ms and 780 μ s at 240K and 295K respectively. This difference may be attributed to increased triplet-triplet annihilation due to a higher overall aromatic concentration in the case of the flash photolysis experiment. These results are summarised in table 4.2.

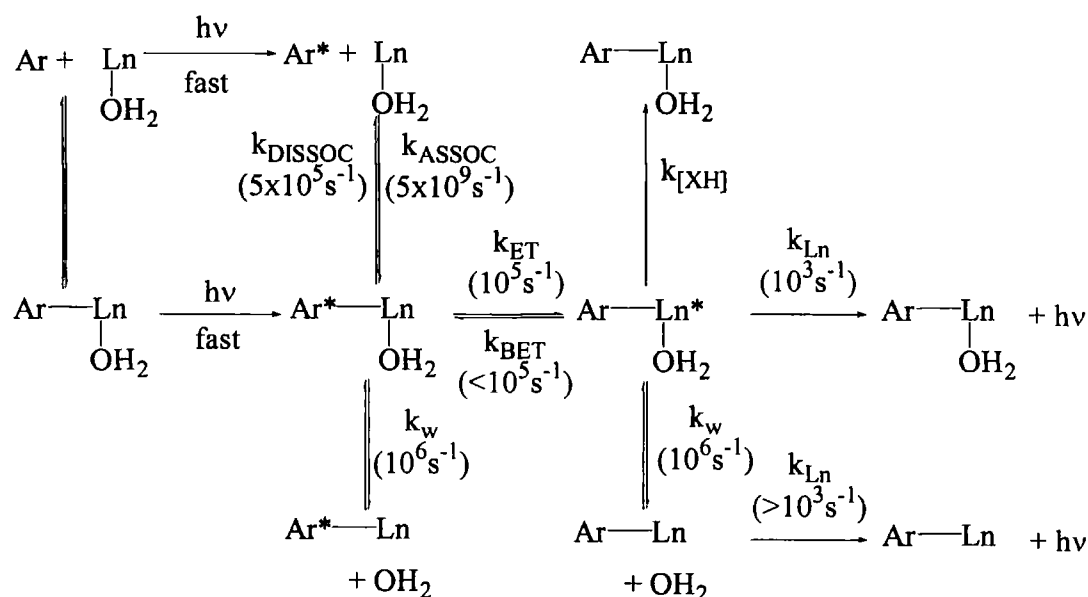
		τ_{240K}/μ S	τ_{295K}/μ S
Flash photolysis	T ₁ decay	180	43
	Ln decay	1100	-
	Ln 'grow-in'	55	-
Tb emission	Ln decay	3000	780
	Ln 'grow-in'	10	1100

Table 4.2. Lanthanide 'grow-in' and decay lifetimes, and triplet decay lifetimes, for [Tb.26] and 1-methylnaphthalene at 240 and 295K.

It can clearly be seen that neither the 'grow-in' nor decay lifetimes of the lanthanide emission correspond to the triplet lifetime measured by flash photolysis. This would suggest that the situation is more complicated than that described by Scheme 2.7. Two distinct possibilities would explain this behaviour. Firstly, if the rates of energy transfer and lanthanide emission are similar, they would not be expected to match those of either the 'grow-in' or the decay. The rate of energy transfer is generally accepted to be proportional to r^{-6} , where r is the distance between donor and acceptor. Thus an increase in this distance from 5Å to 7Å would reduce the rate of energy transfer by *circa* 90%. Such a decrease in k_{ET} is predicted given that the naphthyl moiety, by nature of its complexation within the cyclodextrin, is further removed from the metal centre than the appended system described by Parker *et al.*⁴² The rate of energy transfer can thus be estimated to be *ca* 10^5 s⁻¹.

Further, a number of other deactivation pathways, of similar rates to that of the lanthanide decay rate, could exist to deactivate the triplet naphthalene, competing with the pathways of energy transfer and lanthanide emission (Scheme 2.8).

* Experimental error in lifetime measurements was estimated as $\pm 10\%$.



Scheme 2.8. Possible activation and deactivation pathways for sensitised lanthanide emission. Estimates of relevant rate constants are given.

Back energy transfer from the excited lanthanide to the triplet state of the naphthalene is expected to occur at a slightly slower rate than that of energy transfer (10^5 s^{-1}) and hence to act as a competitive deactivation pathway. Dissociation of excited naphthalene from the cavity would also prevent energy transfer to the metal, opening up the possibility of collisional deactivation by the solvent environment. The rate of dissociation, given a binding affinity (K_{11}) of *ca* $10,000 \text{ M}^{-1}$ (measured experimentally, see pages 60-61) and assuming a diffusion controlled association rate of *ca* $5 \times 10^9 \text{ s}^{-1}$, can be estimated at *ca* $5 \times 10^5 \text{ s}^{-1}$. Dissociation of water from the excited lanthanide is expected to occur at a rate of *ca* 10^6 s^{-1} ²¹ and lead to formation of an alternative emitting lanthanide with its own characteristic rate of emission. Oxygen quenching of the lanthanide or naphthalene should not be a significant deactivation pathway in this case, oxygen having been removed by degassing of the sample. Deactivation of the lanthanide excited state by other energy matched vibrational oscillators (NH and CH) however could also be significant. It is clear that too many competing processes are occurring to allow a rigorous kinetic analysis.

2.8 References.

- ¹ D. Parker, P. K. Senanayake, J. A. G. Williams, *J. Chem. Soc., Perkin Trans. 2*, 1998, 2129.
- ² Z. Pikramenou, D. G. Nocera, *Inorg. Chem.*, 1992, **31**, 532.
- ³ Z. Pikramenou, K. M. Johnson, D. G. Nocera, *Tetrahedron Lett.*, 1993, **34**, 3531.
- ⁴ M. A. Mortellaro, D. G. Nocera, *J. Am. Chem. Soc.*, 1996, **118**, 7414.
- ⁵ I. Sanemasa, T. Takuma, T. Deguchi, *Bull. Chem. Soc. Jpn.*, 1989, **62**, 3098.
- ⁶ T. J. Wenzel, M. S. Boygo, E. L. Lebeau, *J. Am. Chem. Soc.*, 1994, **116**, 4858.
- ⁷ F. Charbonnier, T. Humbert, A. Marsura, *Tetrahedron Lett.*, 1998, **39**, 3481.
- ⁸ D. Parker, J. A. G. Williams, *J. Chem. Soc., Dalton Trans.*, 1996, 3613.
- ⁹ J. Szejtli, *J. Incl. Phenom. Mol. Recogn.*, 1992, **14**, 25.
- ¹⁰ M. V. Rekharsky, Y. Inoue, *Chem. Rev.*, 1998, **98**, 1875.
- ¹¹ G. C. Catana, F. V. Bright, *Anal. Chem.*, 1989, **61**, 905.
- ¹² A. Nakamura, K. Saitoh, F. Toda, *Chem. Lett.*, 1989, 2209.
- ¹³ S. E. Brown, J. H. Coates, D. R. Coghlan, C. J. Easton, S. J. van Eyk, W. Janowski, A. Lepore, S. F. Lincoln, Y. Luo, B. L. May, D. S. Schiesser, P. Wang, M. L. Williams, *Aust. J. Chem.*, 1993, **46**, 953.
- ¹⁴ G. Nelles, M. Weisser, R. Back, P. Wohlfart, G. Wenz, S. Mittler-Neher, *J. Am. Chem. Soc.*, 1996, **118**, 5039.
- ¹⁵ N. Zhong, H. S. Byun, R. Bittman, *Tetrahedron Lett.*, 1998, **39**, 2919.
- ¹⁶ H. Parrot-Lopez, F. Djedaani, B. Perly, A.W. Coleman, H. Galons, M. Miocque, *Tetrahedron Lett.*, 1990, **31**, 1999.
- ¹⁷ Z. Chen, J. S. Bradshaw, M. L. Lee, *Tetrahedron Lett.*, 1996, **37**, 6831.
- ¹⁸ G. Yi, W. Li, J. S. Bradshaw, A. Malik, M. L. Lee, *J. Heterocyclic Chem.*, 1995, **32**, 1715.
- ¹⁹ M. Woods, Ph. D. Thesis, University of Durham, 1998.
- ²⁰ Shift Reagents in NMR Spectroscopy, A. D. Sherry, C. F. G. C. Geraldès, Chapter 4, in *Lanthanide Probes in Life, Chemical and Earth Sciences: Theory and Practice*, J. -C. G. Bünzli, G. R. Choppin, Elsevier, 1989.
- ²¹ S. Aime, A. Barge, J. I. Bruce, M. Botta, J. A. K. Howard, J. M. Moloney, D. Parker, A. S. de Sousa, M. Woods, *J. Am. Chem. Soc.*, 1999, **121**, 5762.

- ²² S. Aime, A. Barge, M. Botta, J. A. K. Howard, R. Katakya, M. P. Lowe, J. Molony, D. Parker, A. S. de Sousa, *Chem. Commun.*, 1999, 1047.
- ²³ A. Beeby, I. M. Clarkson, R. S. Dickens, S. Faulkner, D. Parker, L. Royle, A. S. de Sousa, J. A. G. Williams, M. Woods, *J. Chem. Soc., Perkin Trans. 2*, 1999, 493.
- ²⁴ R. B. Lauffer, *Chem. Rev.*, 1987, **87**, 901.
- ²⁵ W. P. Cacheris, S. K. Nickle, A. D. Sherry, *Inorg. Chem.*, 1987, **26**, 958.
- ²⁶ S. Aime, A. S. Batsanov, M. Botta, J. A. K. Howard, D. Parker, K. Senanayake, J. A. G. Williams, *Inorg. Chem.*, 1994, **33**, 4696.
- ²⁷ N. Bloembergen, L. O. Morgan, *J. Phys. Chem.*, 1961, **34**, 842.
- ²⁸ Personal communication from M. Botta.
- ²⁹ S. Aime, M. Botta, M. Panero, M. Grandi, F. Uggeri, *Magn. Reson. Chem.*, 1991, **29**, 923.
- ³⁰ C. K. Luk, *Biochemistry*, 1971, **10**, 2838.
- ³¹ H. G. Brittain, F. S. Richardson, R. B. Martin, *J. Am. Chem. Soc.*, 1976, **98**, 8255.
- ³² W. de W. Horrocks, Jr., W. E. Collier, *J. Am. Chem. Soc.*, 1981, **103**, 2856.
- ³³ Q.-X. Guo, X.-Q. Zheng, X.-Q. Ruan, S. H. Luo, Y. C. Liu, *J. Incl. Phenom. Mol. Recogn.*, 1996, **26**, 175.
- ³⁴ K. Matsuyama, S. El-Gizawy, J. H. Perrin, *Drug Dev. Ind. Pharm.*, 1987, **13**, 2687.
- ³⁵ A. Nakamura, K. Saitoh, F. Toda, *Chem. Lett.*, 1989, 2209.
- ³⁶ N. Sarkar, K. Das, D. Nath, K. Bhattacharyya, *Chem. Phys. Lett.*, 1992, **196**, 491.
- ³⁷ H. A. Benesi, J. H. Hildebrand, *J. Am. Chem. Soc.*, 1949, **71**, 2703.
- ³⁸ K. A. Connors, *Binding Constants, The Measurement of Molecular Complex Stability*, John Wiley & Sons, New York, 1987.
- ³⁹ I. Sanemasa, T. Takuma, T. Deguchi, *Bull. Chem. Soc. Jpn.*, 1989, **62**, 3098.
- ⁴⁰ *Electron Transfer*, H. B. Gray, W. R. Ellis Jr., Chapter 6, in *Bioinorganic Chemistry*, I. Bertini, H. B. Gray, S. J. Lippard, J. S. Valentine, University Science Books, 1994.
- ⁴¹ A. Beeby, S. Faulkner, D. Parker, J. A. G. Williams, *Phys. Chem. Chem. Phys.*, submitted.
- ⁴² A. Beeby, D. Parker, J. A. G. Williams, *J. Chem. Soc., Perkin Trans. 2*, 1996, 1565.

Chapter 3

Bromonaphthalene- appended Cyclodextrin Systems.

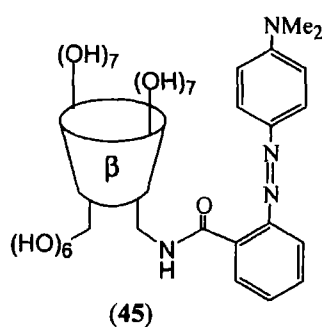
3. Bromonaphthalene-appended Cyclodextrin Systems.

3.1. Introduction.

3.1.1. Chromogenic Indicators.

The use of chemical indicators which change colour in response to variations in their ionic or molecular environment has been widely used in diagnostic and sensory systems, the most common example being the development of chromogenic pH indicators. Recently the development of related indicators involving cyclodextrin conjugates has been investigated.

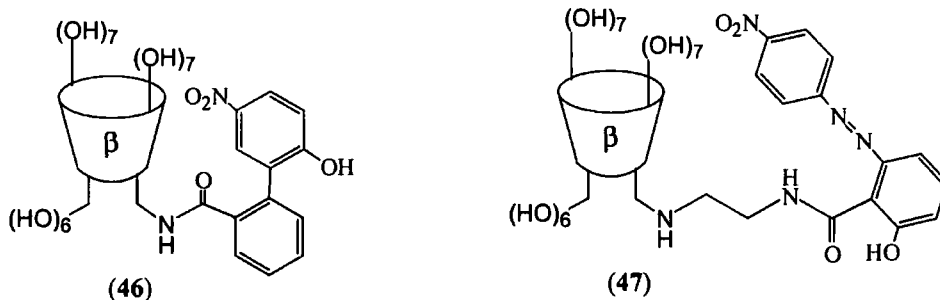
The properties of a β -cyclodextrin derivative modified at the primary face with methyl red (**45**) have been reported by Ueno *et al.*¹ Methyl red is known to change colour from yellow to red in aqueous solution with decreasing pH ($pK_a=5.0$, 293K). The colour change results first from a change in absorbance as the methyl red is protonated to an ammonium species, then subsequent proton transfer to the related azonium ion. Protonation of the methyl red modified cyclodextrin (**45**) in acidic media (pH 1.6) was observed to occur readily. However proton transfer to the azonium ion was inhibited by the 'self-inclusion' of the methyl red moiety into the appended cyclodextrin cavity.



Addition of species such as 1-adamantanecarboxylic acid as competitive guests resulted in the displacement of the methyl red from the cyclodextrin cavity. Proton transfer was thus able to readily occur resulting in a characteristic colour change from yellow to red. The change in absorption with increasing guest concentration

was related to the strength of binding between the cyclodextrin and the added guest. Modest chiral discrimination for L-camphor, L-fenchone and L-menthol over their respective D-enantiomers (1.48, 3.20 and 1.18-fold respectively) was also reported.¹

Two related systems in which β -cyclodextrin was appended with *p*-nitrophenol (**46**)² and alizarin yellow (**47**)³ were also investigated by Ueno *et al.* Nitrophenol changes from yellow to colourless in aqueous solution upon decreasing pH. A similar change was observed for the cyclodextrin-*p*-nitrophenol conjugate (**46**) with a pK_a of 6.40.² Addition of the guest molecule 1-adamantanol, which was expected to competitively bind within the cyclodextrin, increased the apparent pK_a to 6.73. Thus the addition of a competitive guest promoted the colour change from yellow to colourless at pH 6.50. The initial inclusion, and subsequent competitive exclusion of the *p*-nitrophenolic moiety from the cyclodextrin cavity was also observed by circular dichroism. Analysis of the absorbance at varying concentrations confirmed that the intramolecular 'self-complex', rather than intermolecular complexes, was the dominant species prior to competitive guest binding.



β -Cyclodextrin modified with alizarin yellow (**47**) was found to exhibit a markedly different pH dependency than alizarin yellow itself.³ Alizarin yellow changes colour from yellow to red upon increasing pH with a pK_a of 10.98. This colour change is brought about by deprotonation of the phenolic hydroxyl group to form the phenolate anion. In contrast, the alizarin yellow cyclodextrin conjugate (**47**) was found to display two pK_a values: a pK_{a1} of 4.88 corresponding to deprotonation of the phenolic hydroxyl group on the alizarin yellow moiety, and a pK_{a2} of 8.89 corresponding to the secondary amine on the tether. A change of colour with decreasing pH was similarly observed for the conjugate (**47**) as for alizarin yellow, although the pH range over which this spectral variation occurs was markedly different. Upon competitive guest binding the pK_a values changed to 5.11 (pK_{a1}) and

7.56 (pK_{a2}) reflecting the exclusion of the alizarin yellow moiety from the cyclodextrin cavity. Binding constants for various guests were calculated, including 1- and 2-adamantanol. Slight chiral discrimination of (+)-menthol, camphor and borneol over their respective (-) enantiomers (1.02, 1.09 and 1.02-fold respectively) was also observed.

3.1.2. Fluorescence Change Indicators.

The hydrophobic cavity of cyclodextrins provides a binding site for 'size-matched' guests. Species within the cavity are protected from interactions with solvent, dissolved molecular oxygen and interactions with other potentially deactivating molecules. This typically reduces the degree of collisional quenching of the excited state of bound aromatic species, resulting in increased fluorescent lifetimes and emission intensities. Such an enhancement is commonly used as a tool for determining binding affinities of aromatic species into cyclodextrin cavities; the change in fluorescence intensity, or lifetime, with changing guest concentration can be directly correlated to the strength of binding of the aromatic guest within the cyclodextrin cavity.

The binding of species which do not display fluorescence enhancement can be monitored by competitive displacement of a complexed species which does. This technique has been utilised by Bhattacharyya *et al.*⁴ whereby a reduction in fluorescence enhancement of 2,6-toluidino-naphthalenesulfonate (2,6-TNS, **4**) in α - (**2**) and β -cyclodextrin (**1**) was observed due to the competitive binding of urea. Interestingly, the fluorescence lifetime of 2,6-TNS (**4**) in β -cyclodextrin (**1**) was shown to consist of two components corresponding to a 1:1 and a 2:1 host:guest complex. Competitive binding of urea was found to reduce the lifetime of the 1:1, but not the 2:1 complex. This showed that although urea was able to displace 2,6-TNS (**4**) from the 1:1 complex, in the 2:1 complex the greater degree of encapsulation of the aromatic species strongly inhibited its displacement.

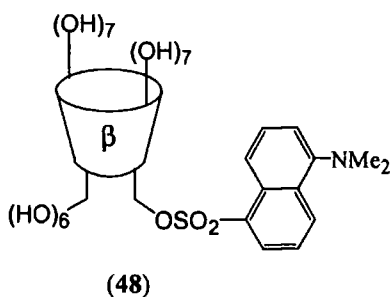
The fluorescence enhancement of 2,6-TNS (**4**) in its complexes with α - (**2**), β - (**1**) and γ -cyclodextrin (**3**) was also used to monitor the rate of cyclodextrin hydrolysis

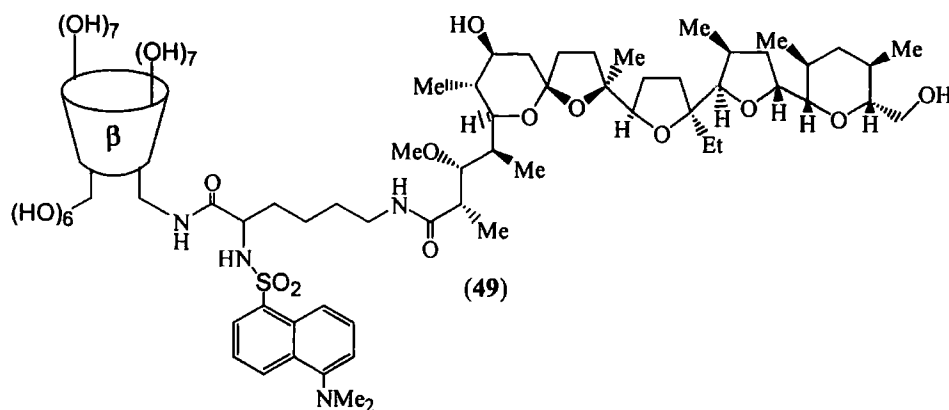
by the enzyme Taka-amylase A.⁵ Although acyclic dextrans are also reported to show fluorescence enhancement, the effect is small relative to that of cyclodextrins.

Enzymatic hydrolysis of cyclodextrin could thus be monitored by the reduction in fluorescence emission intensity from the 2,6-TNS (4), reflecting the reduction in available binding cavities.

A number of species in which the potential fluorophore is directly appended to the cyclodextrin have also been investigated. For example significant research has been directed toward dansyl-modified cyclodextrins. The dansyl group exhibits strong fluorescence in hydrophobic environments but fluorescence is weak in water. Thus the complexation and decomplexation of dansyl into the hydrophobic cyclodextrin cavity can be monitored in water by changes in the fluorescence intensity.

Ueno *et al.* have reported the synthesis of a dansyl modified β -cyclodextrin which is modified at the primary (C(6)) face (48).⁶ The analogous C(2) and C(3) modified systems were also synthesised. The three systems displayed a fluorescence component with an enhanced lifetime consistent with emission from a complexed dansyl moiety. Addition of a competitive guest, such as adamantanol, led to a decreased fluorescence emission intensity of the C(6) (48) and C(2)-modified β -cyclodextrins, signalling exclusion of the dansyl from the cyclodextrin cavity. This exclusion was confirmed by changes to the circular dichroism spectra of the dansyl-cyclodextrin systems. A reduction in fluorescent emission intensity was also observed for the C(3) modified dansyl- β -cyclodextrin, however the process was unusually slow (occurring over several minutes). This suggests that the dansyl moiety may be complexed more deeply within the cyclodextrin cavity for the C(3) analogue and significant deformation of the cyclodextrin is required before decomplexation can occur.





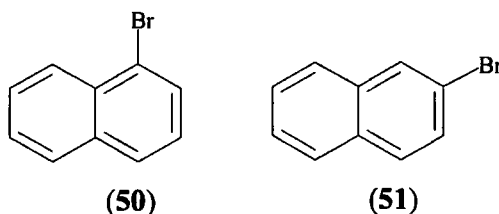
Ueno *et al.* also reported the synthesis of β -cyclodextrin modified with both dansyl and monensin moieties (49).⁷ This species also showed enhanced fluorescence due to the self-inclusion of dansyl into the cyclodextrin; the fluorescence decay exhibited two components with distinct lifetimes. The longer lived component, with a lifetime of 18.2 ns, compared to *ca* 17 ns for similar dansyl modified cyclodextrins, was attributed to emission from the intramolecular self-complex. The shorter lived component exhibited a lifetime of 10.9 ns, attributed to emission from the species with the dansyl unit excluded from the cavity into the bulk water. Other dansyl modified cyclodextrins have typically shown shorter lifetimes, of *ca* 6 ns, for the shorter lived component. The lifetime enhancement in this case was attributed to an increased hydrophobicity of the environment surrounding the excluded dansyl moiety due to the appended monensin unit.

The fluorescence enhancement displayed by the dansyl-monensin-cyclodextrin conjugate (49) decreased upon addition of competitive guests such as 1-adamantanol, L-borneol and ursodeoxycholic acid.⁷ The chiral resolution of various enantiomeric terpenes was also reported, a four-fold greater fluorescence reduction was observed for L-camphor than for D-camphor. A greater fluorescence reduction was also reported upon addition of alkali metal ions such as Na^+ , K^+ , Li^+ and Cs^+ . This effect was attributed to the formation of a hydrophobic 'end-cap' by the metal ion binding monensin unit which causes deepening of the cyclodextrin cavity and a corresponding increase in the binding strength of guest species. The sensitivity enhancement was in the order $Na^+ > K^+ > Li^+ > Cs^+$ which mirrors the strength of metal ion binding to monensin.

3.1.3. Phosphorescent Enhancement of Bromonaphthalenes in Cyclodextrin.

The phosphorescent properties of bromonaphthalenes are well established. Facile quenching by dissolved molecular oxygen or solvent in the solution state, however, has inhibited their application as useful probes. Recently, attempts to shield the naphthalenes from dissolved oxygen have utilised cyclodextrins as ready-made micropolar environments.

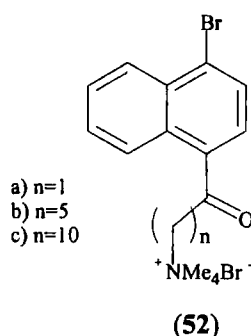
The work was pioneered by Turro *et al.* who demonstrated that the phosphorescent lifetime of 1-bromonaphthalene (**50**) in nitrogen purged systems* could be increased from *ca* 0.1 ms to *ca* 1.6 ms by the addition of β -cyclodextrin (**1**).⁸ Conversely little lifetime enhancement was observed upon addition of β -cyclodextrin (**1**) to 2-bromonaphthalene (**51**). It was proposed that the bromine group was complexed more deeply into the cyclodextrin cavity for 1-bromo than for 2-bromonaphthalene so that in the latter case the bromine atom was more readily available for non-radiative de-excitation pathways. Little phosphorescence was observed in all cases when the solvent was water however, τ_p for the cyclodextrin/1-bromonaphthalene (**50**) system increased with increasing acetonitrile concentration, indicating that acetonitrile was also involved in the shielding process.



Turro also investigated the phosphorescent properties of amine-appended 1-bromonaphthalenes (**52**) with cyclodextrins.⁹ It was found that inclusion of the naphthyl unit into γ -cyclodextrin (**3**) led to a red shift and a reduction in intensity of the UV absorbance of the naphthyl moiety. A slight increase in the intensity of phosphorescent emission and the phosphorescence lifetimes was also observed upon addition of β - (**1**) and γ -cyclodextrin (**3**) to the naphthalene. Addition of $\text{Co}(\text{NH}_3)_6^{3+}$ as an aqueous phase phosphorescence quencher led to a reduction in the lifetime and intensity of phosphorescent emission but to a lesser degree than a system containing no cyclodextrin. As expected, no change in luminescent properties was observed

* 10% MeCN in H₂O.

after addition of α -cyclodextrin (**2**) to the guest, the naphthyl unit being too large to insert into the cavity.

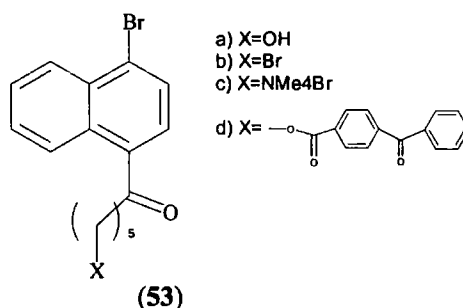


Comparison of naphthyl analogues with varying amine-tether lengths (**52 a-c**) showed that an increase in lifetime was observed as the tether length was increased. Turro showed that the triplet lifetimes were dependent upon the rate of dissociation of the host-guest complex, increasing tether lengths were shown to lead to increases in the host-guest association constant.⁹ In the case of the complex between γ -cyclodextrin and (**52c**), two decay pathways seem to exist, one considerably longer in lifetime. Turro has proposed the formation of a complex where the naphthyl unit is inserted sideways with the alkyl chain also coiled within the cavity. As this would leave the bromine atom exposed, dissociation of the complex was shown to be necessary for efficient quenching to occur.

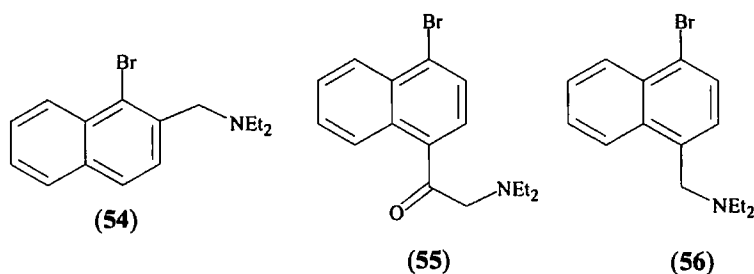
In later work Turro showed that complexes of γ -cyclodextrin (**3**) and 5-appended-1-bromonaphthalenes (**53**) were able to phosphoresce in solutions containing dissolved molecular oxygen.¹⁰ Expanding on his theory of the importance of dissociation for efficient quenching, he investigated the proposal that slowing the rate of dissociation to below that of phosphorescence should effectively avoid effects from aqueous quenchers. It was reported that only minor quenching of luminescent emission was observed for various appended systems (**53 a-d**) in oxygen saturated solutions.[§] In the absence of the cyclodextrin, phosphorescent emission of the naphthyl moieties was only observable in nitrogen purged solutions, the emission being completely quenched by oxygen. Analysis of the emission decay again suggested that the naphthyl moieties could exist in two different environments: corresponding to either two different complexation geometries, or the presence of both 1:1 and 2:1 host:guest

[§] MeCN or H₂O solutions.

complexes. The hydroxyl- (**53a**), bromo- (**53b**) and biphenyl- (**53d**) appended systems displayed both fast and slow relaxation pathways, the amine-appended system (**53c**) showed only a fast decay. The observed increase in phosphorescent intensity and lifetime upon addition of γ -cyclodextrin (**3**) to the naphthyl guest showed that the fast decay was from an associated complex rather than from a dissociated guest. The slow decay was shown to be limited by diffusion from the cyclodextrin, suggesting that quenching occurs on the dissociated complex.



Recently de Silva *et al.* have investigated the quenching of 1-bromonaphthalene (**50**) by appended tertiary amines.¹¹ Earlier work by Davidson *et al.*^{12,13} had demonstrated that tertiary amines were able to quench the triplet excited state of 1-chloronaphthalene in polar solvents. De Silva expanded on this by appending 1-bromonaphthalene with tertiary amines (**54**, **55** and **56**) and complexing them into β -cyclodextrin (**1**). The ortho-substituted bromonaphthalene (**54**) showed weak phosphorescence in alkaline solution (pH8).[†] Protonation of the amine at pH3 led to significant phosphorescence enhancement. Comparison with the phosphorescence of the guest in the absence of cyclodextrin (**1**) revealed a fourfold enhancement due to binding to the host. The para-substituted bromonaphthalenes (**55**, **56**) showed no phosphorescence enhancement in the presence of the cyclodextrin (**1**). De Silva argues that a combination of hydrophobic (**55**) and steric (**55** and **56**) factors inhibited their complexation into the cavity.



[†] Degassed H₂O, [CD]=5mM, [Nap]=0.05mM, λ_{ex} =283nm, gate=4ms, delay=0.1ms.

Nocera *et al.* have conducted the first studies using a modified cyclodextrin.¹⁴ in which the interaction of 1-bromonaphthalene (**50**) with a β -cyclodextrin derivatised with a glucosyl unit attached to the primary face[#] was studied. The glucosyl unit served to increase the water solubility of the host 40 fold with only a slight reduction in the strength of guest binding. In aerated aqueous solution the host-guest complex exhibited characteristic fluorescence* but no phosphorescence. Addition of a bulky alcohol such as *t*-butanol (3% v/v) caused an enhancement of the fluorescence and switching on of phosphorescence[§] from the naphthalene. Although the binding strength of guests is increased upon addition of most alcohols this was not the case for cyclohexanol (CycOH). This result shows that the effect cannot be explained simply by an increase in binding.

Nocera proposed formation of a cyclodextrin-naphthyl-alcohol ternary complex which protected the phosphor from oxygen quenching. Studies demonstrated that the oxygen quenching rate was reduced as the bulkiness of the alcohol was increased, showing a trend of decreasing quenching rates (and hence increasing relative emission) for the series 1-BuOH>1-PrOH>2-PrOH>2-BuOH>*t*-BuOH>CycOH.

3.2. Aims.

This project aimed to develop cyclodextrin based detection systems reporting via long lived phosphorescent emission. It was envisaged that 1-bromo and 2-bromonaphthalenes appended to β -cyclodextrin might exhibit enhanced phosphorescent lifetimes compared to 1-bromo and 2-bromonaphthalene alone, (**50** & **51**), due to formation of intramolecular self-inclusion complexes. Addition of suitable guests optically transparent at *ca* 290 nm, was expected to lead to competitive complexation of the guest and exclusion of the bromonaphthalene into the bulk solvent. Solvent or oxygen quenching of the naphthalene triplet state should

[#] The exact structure of the cyclodextrin derivative was not discussed.

* λ_{em} =340nm.

§ λ_{em} =493nm, 510nm, λ_{ex} =313nm, [CD]=1mM, delay=0.1ms, gate=1.0ms.

be observable by a decrease in the phosphorescent lifetime and emission intensity. The bromonaphthalene appended cyclodextrin could thus operate as an off/on sensor for important optically transparent species such as steroids, terpenes and adamantane derivatives (Figure 3.1).

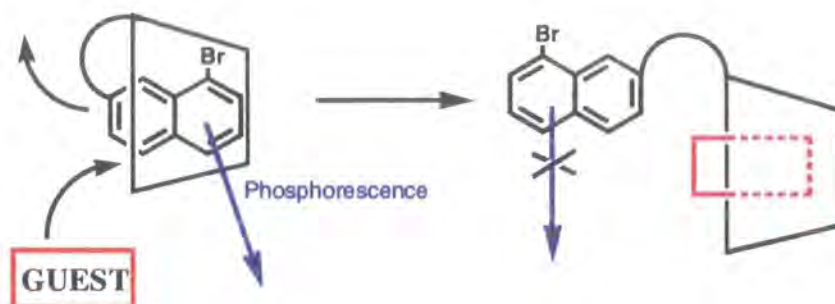


Figure 3.1. Bromonaphthalene cyclodextrin conjugates as phosphorescent off/on sensors.

Four target bromonaphthalene appended cyclodextrin systems (Figure 3.2) have been designed. Each system is appended once at the primary face of cyclodextrin with a bromonaphthalene derivative, the remaining cyclodextrin hydroxyl groups are O-methylated for increased water solubility. O-Methylation of the hydroxyls was also expected to deepen the cyclodextrin cavity and possibly lead to increased binding of guests (see Chapter 2, pages 30-31). The four systems differ by the substitution pattern on the naphthalene and by the tether length, in the hope that this would allow the optimal geometry for the system to be determined. One system, {1'',3''-bis-[2'-(1'-bromonaphthyl)]-2''-butylcarbamoyl}-per-O-methyl- β -cyclodextrin (**60**) also has two bromonaphthalene units appended onto cyclodextrin. It was expected that this may allow simultaneous observation of the luminescence behaviour of both complexed and uncomplexed bromonaphthalenes.

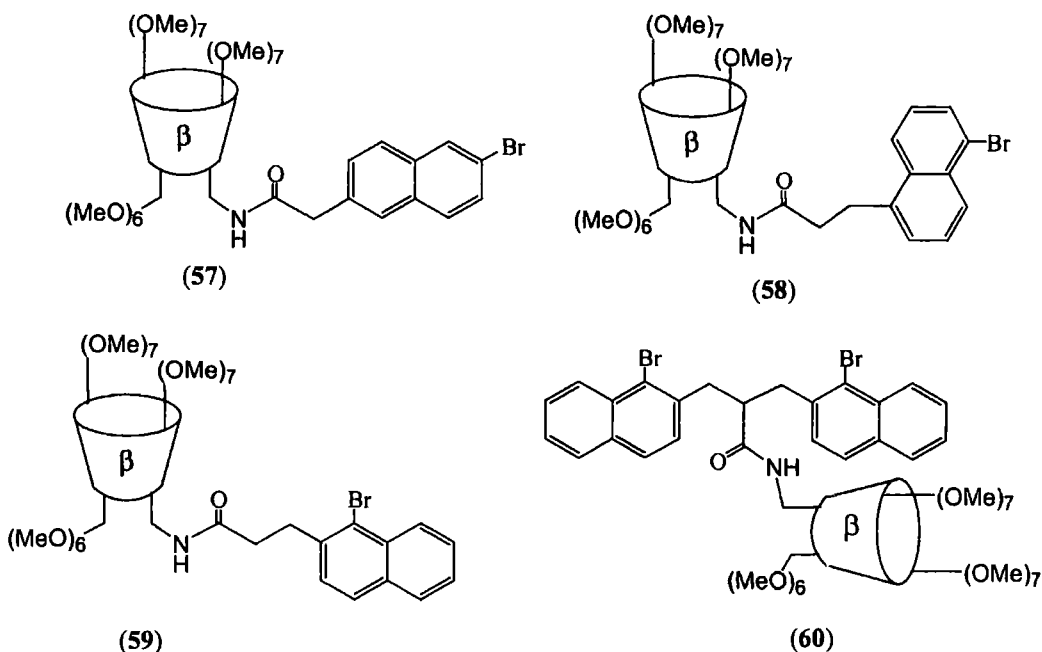


Figure 3.2. Target bromonaphthalene sensor systems (57-60).

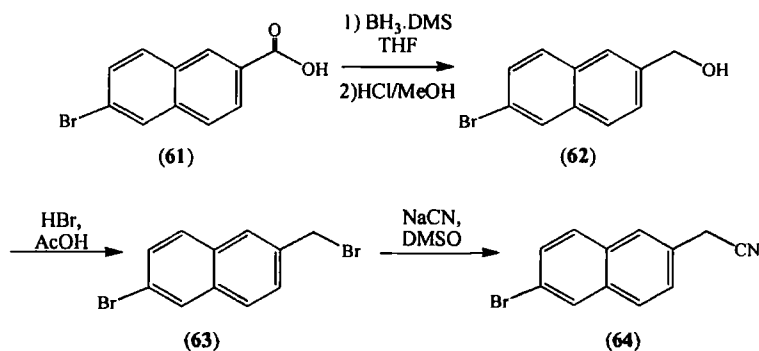
3.3. Synthetic Methodology.

3.3.1. Synthesis of [6'-(2'-Bromonaphthyl)methylcarbamoyl]-per-O-methyl- β -cyclodextrin (57).

The synthesis of mono-[6'-(2'-bromonaphthyl)methylcarbamoyl]-per-O-methyl- β -cyclodextrin (57) was achieved via chain extension of the commercially available 2-bromo-6-naphthoic acid (61) followed by peptide coupling to mono-amino-per-O-methyl- β -cyclodextrin (31).

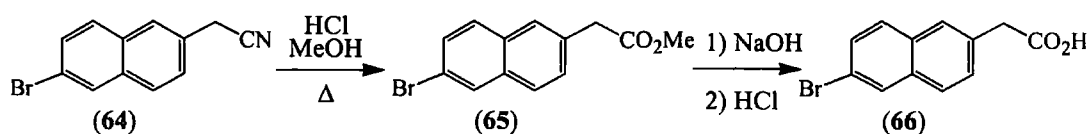
Reduction of 2-bromo-6-naphthoic acid (61) occurred readily with borane-dimethylsulfide complex (Scheme 3.1), hydrolysis of the resulting borane complex occurred in refluxing HCl solution (1M in methanol) giving 6-(2-bromonaphthyl)methanol (62) in good yield (85%). Conversion to 2-bromo-6-bromomethylnaphthalene (63) occurred readily in refluxing HBr in acetic acid in excellent yield (96%).¹⁵ Selective substitution of the naphthyl bromide over the aryl bromide occurred over 18 hours at 60°C in anhydrous DMSO with sodium

cyanide. Purification by chromatatron chromatography gave 6-(2-bromonaphthyl)acetonitrile (**64**) in good yield (79%).



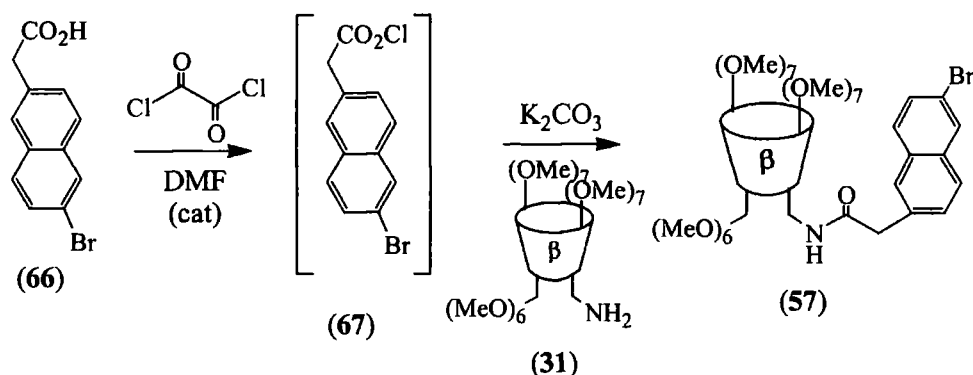
Scheme 3.1. Preparation of 6-(2-bromonaphthyl)acetonitrile (**64**).

Oxidation of 6-(2-bromonaphthyl)acetonitrile (**64**) occurred under reflux in anhydrous methanolic hydrochloric acid to give 6-(2-bromonaphthyl)acetic acid methyl ester (**65**) in an 89% yield (Scheme 3.2).¹⁵ Subsequent base hydrolysis of the methyl ester gave 6-(2-bromonaphthyl)acetic acid (**66**) in a good yield (92%; 53% from 2-bromo-6-naphthoic acid (**61**)).¹⁵



Scheme 3.2. Preparation of 6-(2-bromonaphthyl)acetic acid (**66**).

Coupling of 6-(2-bromonaphthyl)acetic acid (**66**) with mono-amino-per-O-methyl- β -cyclodextrin (**31**) occurred via *in situ* formation of the intermediate acid chloride (**67**) from 6-(2-bromonaphthyl)acetic acid (**66**) and oxalyl chloride. Addition of mono-amino-per-O-methyl- β -cyclodextrin (**31**) and potassium carbonate in dichloromethane resulted in elimination of hydrogen chloride and formation of the amide. Purification by column chromatography gave the desired mono-[6'-(2'-bromonaphthyl)methylcarbamoyl]-per-O-methyl- β -cyclodextrin (**57**) in modest yield (18%).

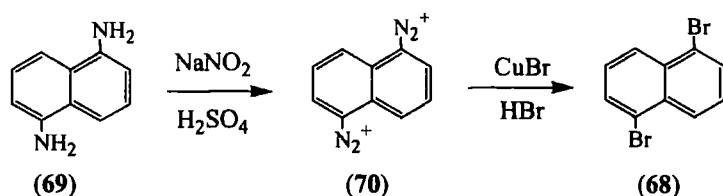


Scheme 3.3. Preparation of mono-[6'-(2'-bromonaphthyl)methylcarbamoyl]-per-O-methyl- β -cyclodextrin (57).

3.3.2. Synthesis of [5'-(1'-Bromonaphthyl)ethylcarbamoyl]-per-O-methyl- β -cyclodextrin (58).

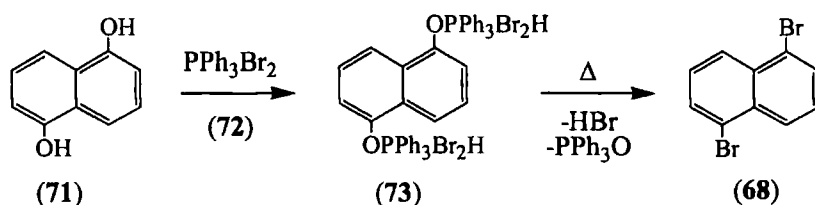
The synthetic approach described for the preparation of mono-6'-[2'-bromonaphthyl)methylcarbamoyl]-per-O-methyl- β -cyclodextrin (57) could not be replicated for synthesis of mono-[5'-(1'-bromonaphthyl)ethylcarbamoyl]-per-O-methyl- β -cyclodextrin (58). The lack of appropriate commercially available starting materials, and the longer tether length between the cyclodextrin and the naphthalene required an alternative synthetic approach. This approach relied on the synthesis of 1,5-dibromonaphthalene (68) as a versatile building unit.

1,5-Dibromonaphthalene (68) was initially prepared as described by Hodgson and Whitehurst.¹⁶ Using a Sandmeyer reaction 1,5-diamino naphthalene (69) in chilled sulfuric acid was converted to its di-diazonium ion (70) *in situ* by the addition of sodium nitrite. The addition of copper(I) bromide in hydrobromic acid promoted a double substitution on both the C(1) and C(5) positions to yield 1,5-dibromonaphthalene (68) (Scheme 3.4). Although this is an established approach to 1,5-dibromonaphthalene (68), certain problems were encountered. The reaction is capricious and larger scale synthesis was inhibited by the difficulties of extracting the product from the large volumes of copper salts generated during the reaction. Chloride ion contamination of the product, leading to competitive formation of 1-bromo-5-chloronaphthalene and 1,5-dichloronaphthalene also occurred.



Scheme 3.4. Preparation of 1,5-dibromonaphthalene (68).

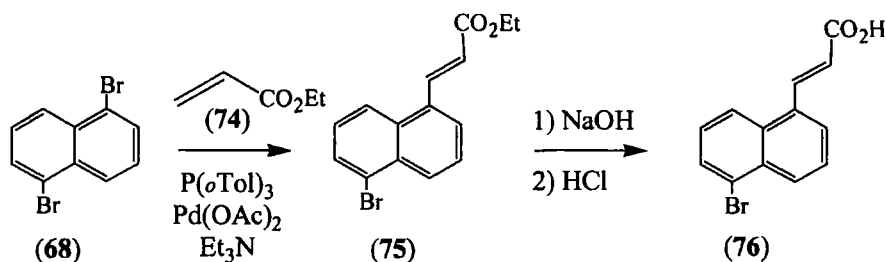
Schaefer and Higgins¹⁷ described a route to benzyl halides from the related phenols by reaction with triphenylphosphine dihalide generated *in situ* from the dihalide and triphenylphosphine. This approach was adapted to generate 1,5-dibromonaphthalene (68) from 1,5-dinaphthol (71) (Scheme 3.5). Here addition of commercially available dibromotriphenyl phosphorane (72) to 1,5-dinaphthol (71) generated the disubstituted intermediate complex (73) after heating for 1 hour at 80°C in acetonitrile. Removal of the solvent and subsequent heating in a Woods metal bath for *ca* 30 minutes resulted in a rearrangement to give hydrogen bromide, triphenylphosphine oxide and 1,5-dibromonaphthalene (68). The desired 1,5-dibromonaphthalene (68) was isolated as a white crystalline solid by Soxhlet extraction into *n*-hexane followed by column chromatography and recrystallisation from boiling ethanol. Although yields were modest (28%), the reaction conditions for this approach were less awkward than for the classical Sandmeyer reaction and the work up procedure was less time-consuming. The reaction was also found to be more reliable and gave product of a higher purity.



Scheme 3.5. Alternative preparation of 1,5-dibromonaphthalene (68).

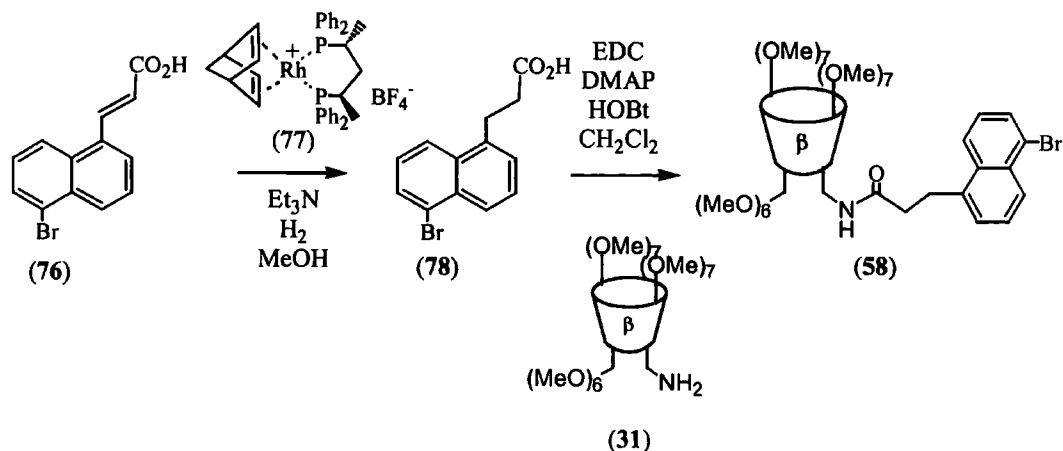
Stoichiometric reaction of 1,5-dibromonaphthalene (68) with a single equivalent of ethyl acrylate (74) occurred readily to give *trans*-3'-[5-(1-bromonaphthyl)]propenoate (75) (Scheme 3.6). This variation on the vinylic hydrogen substitution reaction proposed by Dieck and Heck¹⁸ utilised a catalyst

generated *in situ* from palladium acetate and tri-*o*-tolylphosphine as described by Ziegler Jr. and Heck.¹⁹ Although yields were modest (46%), recovered 1,5-dibromonaphthalene (**68**) (47%) accounted for most of the remaining material. Hydrolysis of the ethyl ester occurred in near quantitative yield (95%) in a solution of methanol, THF and sodium hydroxide (2M) over 18 hours at room temperature. Addition of aqueous hydrochloric acid (5M) precipitated trans-3'-[5-(1-bromonaphthyl)]propenoic acid (**76**) as a white crystalline solid.



Scheme 3.6. Preparation of trans-3'-[5-(1-bromonaphthyl)]propenoic acid (**76**).

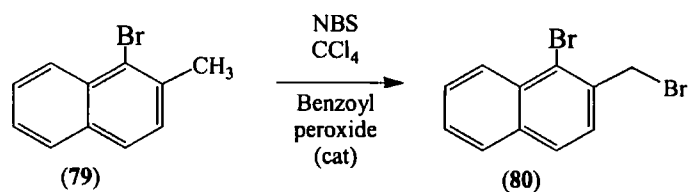
Selective hydrogenation of the unsaturated vinylic bond in trans-3'-[5-(1-bromonaphthyl)]propenoic acid (**76**) proved to be less than straightforward. Common palladium and platinum hydrogenation catalysts were found to mediate catalytic dehalogenation of the aryl bromide in competition with hydrogenation of the double bond. However use of a sterically hindered rhodium catalyst, (2*S*, 4*S*)-(-)-2,4-bis(diphenylphosphino)pentanenorbomadiene) rhodium (I) hexafluorophosphate (**77**), under a hydrogen atmosphere (40 psi) exclusively generated the desired 3'-[5-(1-bromonaphthyl)]propanoic acid (**78**) in 24 hours (Scheme 3.7). Purification by column chromatography gave the desired acid in good yield (59%). Observation by GC-MS showed that dehalogenation occurred for reaction times significantly over 24 hours. Condensation of 3'-[5-(1-bromonaphthyl)]propanoic acid (**78**) with mono-amino-per-O-methyl- β -cyclodextrin (**31**) occurred readily using standard amide coupling conditions. Purification by column chromatography gave the desired mono-[5'-(1'-bromonaphthyl)ethylcarbamoyl]-per-O-methyl- β -cyclodextrin (**58**) in good yield (79%).



Scheme 3.7. Preparation of mono-[5'-(1'-bromonaphthyl)ethylcarbamoyl]-per-O-methyl- β -cyclodextrin (**58**).

3.3.3. Synthesis of Mono-[2'-(1'-Bromonaphthyl)ethylcarbamoyl]-per-O-methyl- β -cyclodextrin (**59**).

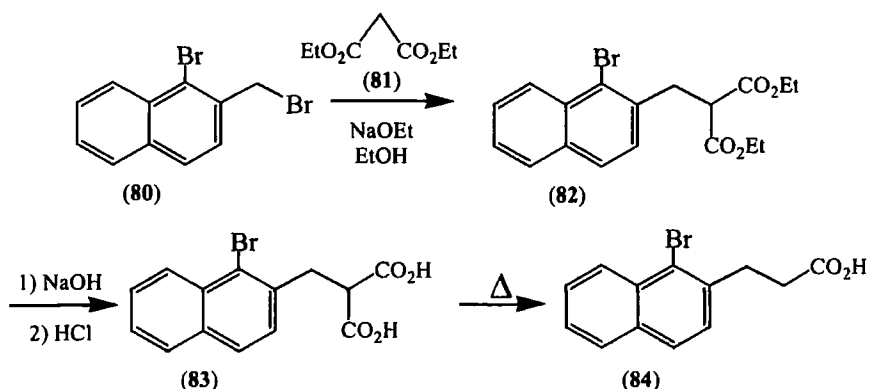
Successful synthesis of mono-[2'-(1'-bromonaphthyl)ethylcarbamoyl]-per-O-methyl- β -cyclodextrin (**59**) was dependent upon the synthesis of 1-bromonaphthalene with a linking arm at the 2' position. Free radical substitution of 1-bromo-2-methylnaphthalene (**79**) using N-bromosuccinimide in carbon tetrachloride (Scheme 3.8) afforded 1-bromo-2-bromomethylnaphthalene (**80**) after purification by recrystallisation (50% $\text{CH}_2\text{Cl}_2/n$ -hexane) in 56% yield.²⁰



Scheme 3.8. Preparation of 1-bromo-2-bromomethylnaphthalene (**80**).

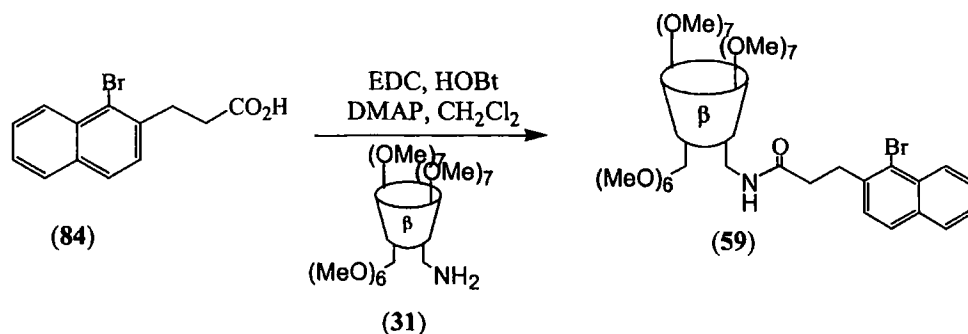
Addition of diethyl malonate (**81**) to 1-bromo-2-bromomethylnaphthalene (**80**) occurred readily upon reaction with sodium ethoxide generated *in situ* from sodium and ethanol (Scheme 3.9). The resulting diester (**82**) was obtained in good yield (56%) after purification by column chromatography. The diester (**82**) was readily

hydrolysed in a refluxing solution of ethanol and sodium hydroxide (2M) and addition of aqueous hydrobromic acid led to precipitation of the diacid (**83**) as a white solid. Decarboxylation of the diacid (**83**) was achieved upon heating in a Woods metal bath for 15 minutes. The resulting melt was extracted into THF, then into aqueous sodium hydroxide. 3'-[2-(1-Bromonaphthyl)]propanoic acid (**84**) was then precipitated as a yellow solid by the addition of aqueous hydrobromic acid in an overall yield of 35% from 1-bromo-2-bromomethyl naphthalene (**80**).²¹



Scheme 3.9. Preparation of 3'-[2-(1-bromonaphthyl)]propanoic acid (**84**).

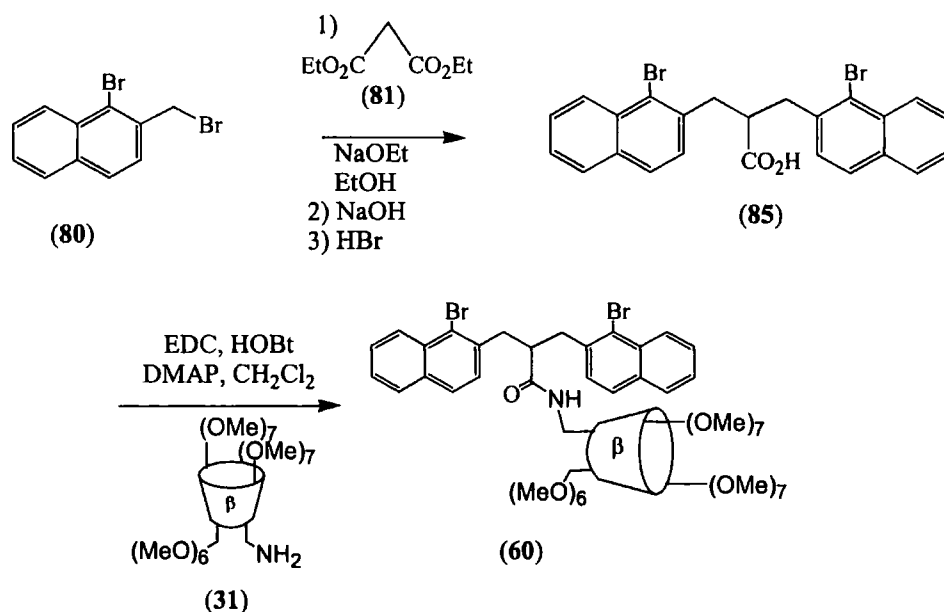
Condensation of 3'-[2-(1-bromonaphthyl)]propanoic acid (**84**) with mono-amino-per-O-methyl- β -cyclodextrin (**31**) occurred readily using standard peptide coupling methods (Scheme 3.10). Purification by column chromatography and dialysis gave the desired mono-[2'-(1'-bromonaphthyl)ethylcarbamoyl]-per-O-methyl- β -cyclodextrin (**59**) in 54% yield.



Scheme 3.10. Preparation of mono-[2'-(1'-bromonaphthyl)ethylcarbamoyl]-per-O-methyl- β -cyclodextrin (**59**).

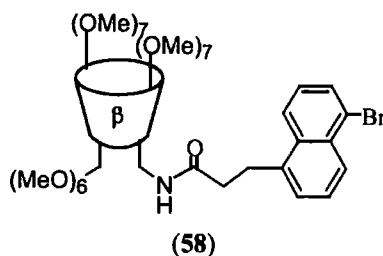
3.3.4 Synthesis of Mono-{1'',3''-bis-[2'-(1'-bromonaphthyl)]-2''-butylcarbamoyl}-per-O-methyl- β -cyclodextrin (**60**).

Synthesis of mono-{1'',3''-bis-[2'-(1'-bromonaphthyl)]-2''-butylcarbamoyl}-per-O-methyl- β -cyclodextrin (**60**) was achieved from 1-bromo-2-bromomethylnaphthalene (**80**). The addition of diethyl malonate (**81**) to two equivalents of 1-bromo-2-bromomethylnaphthalene (**80**) occurred with sodium ethoxide generated *in situ* from sodium and ethanol (Scheme 3.11). After base hydrolysis of the resulting diester, decarboxylation was achieved by the addition of hydrobromic acid. The resulting acid was extracted into dichloromethane and recrystallised from boiling toluene to give 2'-[2-(1-bromonaphthyl)methyl]-3'-[2-(1-bromonaphthyl)]-1'-propanoic acid (**85**) in 35% yield. Condensation of 2'-[2-(1-bromonaphthyl)methyl]-3'-[2-(1-bromonaphthyl)]-1'-propanoic acid (**85**) with mono-amino-per-O-methyl- β -cyclodextrin (**31**) was again achieved using standard amide coupling procedures to give the desired mono-{1'',3''-bis-[2'-(1'-bromonaphthyl)]-2''-butylcarbamoyl}-per-O-methyl- β -cyclodextrin (**60**) in good yield (81%).



Scheme 3.11. Preparation of mono-{1'',3''-bis-[2'-(1'-bromonaphthyl)]-2''-butylcarbamoyl}-per-O-methyl- β -cyclodextrin (**60**).

3.4. Luminescence Studies.



The luminescent properties of the bromonaphthalene-cyclodextrin conjugate (58) were examined in degassed methanol. The total emission spectrum (TES)* showed a fluorescent band centred at 360 nm, and a broad phosphorescent emissive band with maxima at 505 nm and 546 nm. A phosphorescence emission spectra (PES)[§] showed the phosphorescent emission in the absence of fluorescent emission (Figure 3.3). The lifetime of phosphorescent emission[§] was measured to be 0.12 ms \pm 2%[#]. Neither addition of *ca* 40 mole equivalents of cholesterol[®] nor β -cyclodextrin[®] (1) as potential competitive guests or hosts respectively resulted in any significant change in the phosphorescent emission intensity or the phosphorescent lifetime. However phosphorescence was readily quenched by aeration or by changing the solvent to degassed 10% MeCN/H₂O.

* [58]=1.0 x 10⁻⁴M, gate=5 ms, λ_{ex} =291 nm.

[§] Delay = 0.05 ms, gate = 5 ms, λ_{ex} = 291 nm.

[§] [58]=1.0 x 10⁻⁴M, λ_{ex} = 291 nm, λ_{em} = 546 nm.

[#] Statistical error calculated from deviation from a single exponential decay model.

[®] Degassed, MeOH. [58]=1x10⁻⁴M, [cholesterol]=4x10⁻³M. Assuming K_{11} for the intermolecular complex (58.cholesterol) \approx 600M⁻¹, then \approx 70% of the conjugate (58) contains bound cholesterol.

[®] Degassed, 10% MeOH/H₂O. [58]=1x10⁻⁴M, [1]=4x10⁻³M. Assuming K_{11} for the intermolecular complex (58.1) \approx 600M⁻¹, then \approx 70% of the conjugate (58) is bound to β -cyclodextrin (1).

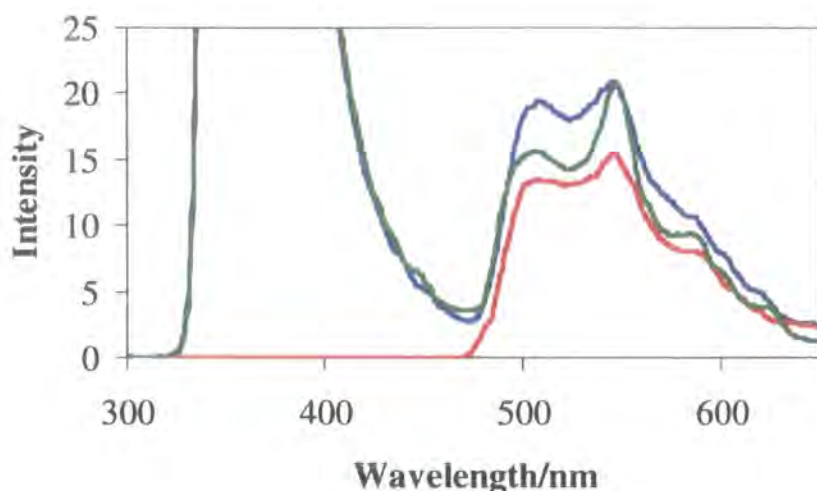
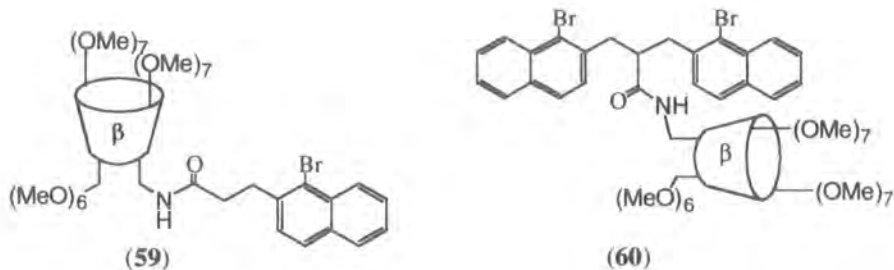


Figure 3.3. Total emission spectrum (—), phosphorescent emission spectrum (—), and total emission spectrum after addition of 40 equivalents of cholesterol (—) for (58).



Similar observations were made for the bromonaphthalene-cyclodextrin conjugates (59 & 60). Both showed a fluorescent emissive band centred at 360 nm and a broad phosphorescent emissive band with maxima at 500 nm and 534 nm[†] (Figure 3.4). The lifetime of phosphorescent emission in both cases was measured to be 0.08 ms \pm 5%[‡]. Addition of cholesterol again led to virtually no change in the intensity or lifetime of emission. Aeration of the samples resulted in total quenching of all phosphorescence.

[†] Concentration = 1.0×10^{-4} M, delay = 0 ms (TES), 0.05 ms (PES), gate = 5 ms, λ_{ex} = 291 nm.

[‡] Concentration = 1.0×10^{-4} M, λ_{ex} = 277 nm, λ_{em} = 543 nm, statistical error.

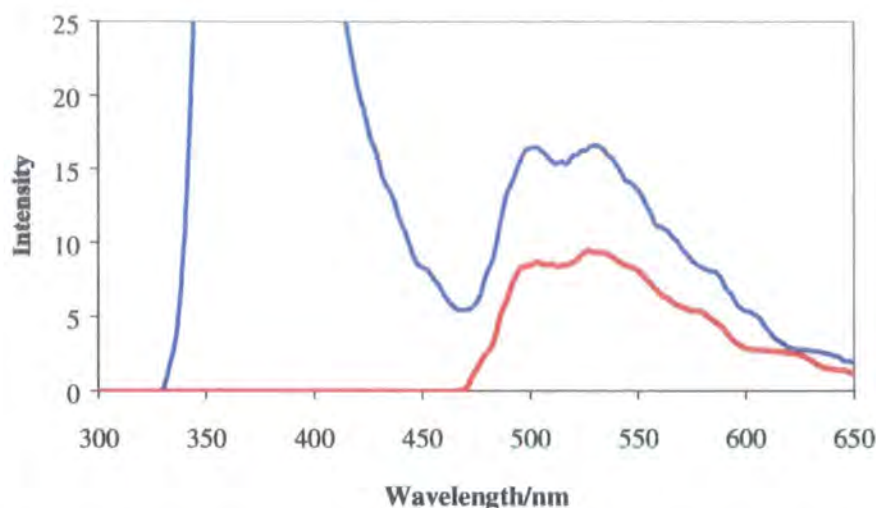
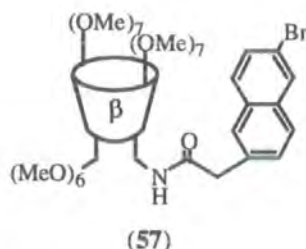


Figure 3.4. Total emission spectrum (—) and phosphorescent emission spectrum (—) for (59).

Surprisingly, of all the bromonaphthalene cyclodextrin conjugates, the 2-bromo conjugate (57) exhibited the greatest phosphorescent emission lifetime, which was estimated to be $0.17 \text{ ms} \pm 2\%$ ^{*}. Lifetimes for all of the reported systems (57-60) however, are of a similar magnitude to that of 1-bromonaphthalene (50) itself, which has been measured under similar conditions to be 0.17 ms [†].



It can clearly be seen that for the bromonaphthalene-cyclodextrin systems described above (57-60) no enhancement of the phosphorescent lifetime had occurred relative to 1-bromonaphthalene (50) itself. A significant enhancement had been predicted on the basis of the work described earlier (pages 77-80), where phosphorescent lifetimes of bromonaphthalenes were increased from *ca* 0.1 ms to 1.6 ms by the addition of cyclodextrin.

^{*} [57] = $1.0 \times 10^{-4} \text{ M}$, $\lambda_{\text{ex}} = 287 \text{ nm}$, $\lambda_{\text{em}} = 526 \text{ nm}$; statistical error.

[†] [50] = $1.29 \times 10^{-4} \text{ M}$, $\lambda_{\text{em}} = 525 \text{ nm}$, $\lambda_{\text{ex}} = 300 \text{ nm}$.

A possible explanation for the lack of phosphorescent enhancement for the conjugates (57-60) is that complexation of the bromonaphthalene moiety into the cavity of β -cyclodextrin derivatives is sterically inhibited by the further functionalisation around the naphthyl ring. The absence of self-complexation would result in a permanent exclusion of the bromonaphthalene into the bulk solvent, hence its behaviour would mimic that of bromonaphthalene alone.

Insufficient flexibility in the linking unit between the naphthalene and the cyclodextrin, which would inhibit the formation of an intramolecular 'self-inclusion' complex, could also inhibit complexation. This second proposal however is inconsistent with the fluorescence and colour change detectors developed by Ueno *et al.* and described earlier (pages 72-76) which were apparently able to form intramolecular self-complexes with similar or even shorter linking units. The lack of change in lifetime upon addition of β -cyclodextrin to the conjugate (58) (page 90) is also inconsistent with this proposal as it suggests that the bromonaphthalene moiety is unable to form either inter- or intra-molecular complexes.

3.5. Further Work.

The development of analogous naphthyl linkers with longer chain lengths may allow sufficient flexibility to allow insertion of the naphthalene through the primary face. Another approach, which may work well in combination with an increased tether length, would be to append the bromonaphthalene to the secondary face of the cyclodextrin. The wider rim at the secondary face may then favour self-inclusion of the naphthalene. However the most promising approach would be to append the naphthalenes to a γ -cyclodextrin derivative, allowing less constrained insertion into the larger cavity.

3.6. References.

- ¹ A. Ueno, T. Kuwabara, A. Nakamura, F. Toda, *Nature*, 1992, **356**, 136.
- ² T. Kuwabara, A. Matsushita, A. Nakamura, A. Ueno, F. Toda, *Chem. Lett.*, 1993, 2081.
- ³ T. Aoyagi, A. Nakamura, H. Ikeda, H. Mihara, A. Ueno, *Anal. Chem.*, 1997, **69**, 659.
- ⁴ N. Sarkar, K. Das, D. Nath, K. Bhattacharyya, *Chem. Phys. Lett.*, 1992, **196**, 491.
- ⁵ H. Kondo, H. Nakatani, K. Hiromi, *J. Biochem.*, 1976, **79**, 393.
- ⁶ Y. Wang, T. Ikeda, H. Ikeda, A. Ueno, F. Toda, *Bull. Chem. Soc. Jpn.*, 1994, **67**, 1598.
- ⁷ A. Ueno, A. Ikeda, H. Ikeda, T. Ikeda, F. Toda, *J. Org. Chem.*, 1999, **64**, 382.
- ⁸ N. J. Turro, J. D. Bolt, Y. Kuroda, I. Tabushi, *Photochem., Photobiol.*, 1982, **35**, 69.
- ⁹ N. J. Turro, T. Okubo, C.-J. Chung, *J. Am. Chem. Soc.*, 1982, **104**, 1789.
- ¹⁰ N. J. Turro, S. Cox, X. Li, *Photochem., Photobiol.*, 1983, **37**, 149.
- ¹¹ R. A. Bissell, A. P. de Silva, Q. N. Gunaratne, P. L. M. Lynch, C. P. McCoy, G. E. M. Maguire, K. R. A. S. Sandanayake, *Fluorescent Chemosensors For Ions And Molecule Recognition*, American Chemical Society, 1993, p53-57.
- ¹² R. A. Beechcroft, R. S. Davidson, D. Goodwin, *Tet. Lett.*, 1983, **24**, 5673.
- ¹³ R. A. Beechcroft, R. S. Davidson, D. Goodwin, J. E. Pratt, X. J. Luo, *J. Chem. Soc. Faraday Trans. 2*, 1986, **82**, 2393.
- ¹⁴ A. Ponce, P. A. Wong, J. J. Way, D. G. Nocera, *J. Phys. Chem.*, 1993, **97**, 11137.
- ¹⁵ R. G. Jones, Q. F. Soper, O. K. Behrens, J. W. Corse, *J. Am. Chem. Soc.*, 1948, **70**, 2843.
- ¹⁶ H. H. Hodgson, J. S. Whitehurst, *J. Chem. Soc.*, 1947, 80.
- ¹⁷ J. P. Schaefer, J. Higgins, *J. Org. Chem.*, 1967, **32**, 1607.
- ¹⁸ H. A. Dieck, R. F. Heck, *J. Am. Chem. Soc.*, 1974, **96**, 1133.
- ¹⁹ C. B. Ziegler, Jr., R. F. Heck, *J. Org. Chem.*, 1978, **43**, 2941.
- ²⁰ R. Adams, L. O. Binder, *J. Am. Chem. Soc.*, 1941, **63**, 2771.
- ²¹ L. A. Carpino, Y. -Z. Lin, *J. Org. Chem.*, 1990, **55**, 247.

Chapter 4

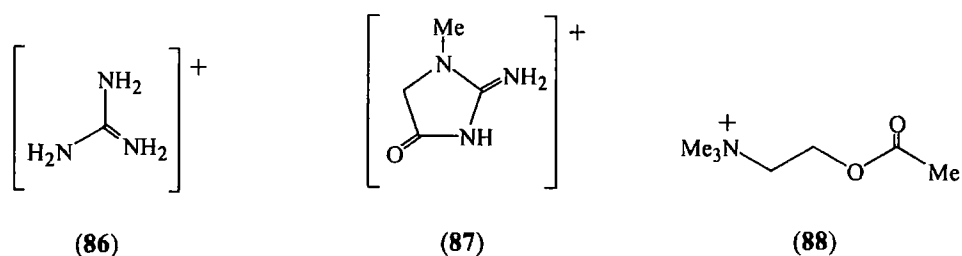
Detectors for Flow and Membrane Inclusion.

4. Detectors for Flow and Membrane Inclusion.

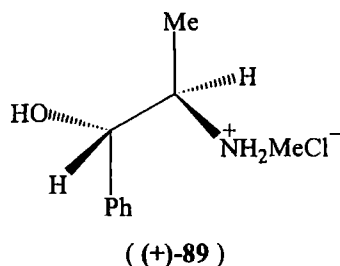
4.1 Introduction.

4.1.1 Cyclodextrins in Ion Selective Electrodes.

The use of alkylated cyclodextrins as ionophores in ion selective electrodes has been explored by Parker *et al.*¹ The lipophilic cyclodextrins 2,6-didodecyl- α - and β -cyclodextrin, as well as per-O-ethyl- β -cyclodextrin were examined for the detection of guanidine, creatinine and a selection of alkylated tetraalkylammonium ions. Guanidinium ions (**86**) were detected at concentrations of *ca* 10^{-6} M, as was the metabolite creatinine (**87**). The neurotransmitter acetylcholine (**88**) was detected at sub micromolar concentrations.



Chiral selectivity has also been exhibited by the lipophilic per-O-octyl- α -cyclodextrin incorporated into an ion selective electrode.² The electrode displayed a selectivity for (+)-ephedrinium hydrochloride (**89**) over the (-) enantiomer corresponding to an energy difference of $2.4 (\pm 0.05) \text{ kJmol}^{-1}$ for formation of the diastereomeric complexes. After standardisation against solutions of predetermined enantiomeric purity the electrode was calibrated to directly measure the enantiomeric purity of ephedrinium and related chiral salts.

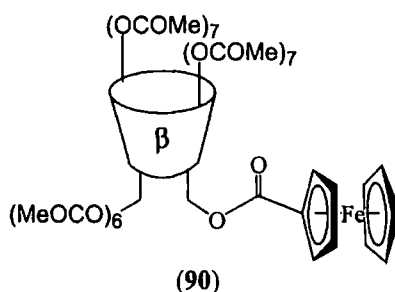


Addition of 1,1'-bis(methoxymethyl)ferrocene to ion selective electrodes has been shown to improve selectivity and sensitivity.³ The ferrocenyl moiety acted as a charge shuttle in a membrane which incorporated the lipophilic per-O-ethyl- β -

cyclodextrin as an artificial receptor for charge diffuse ions such as acetylcholine (88). It was reported that sub picomolar concentrations of acetylcholine (88) were detectable by this membrane.

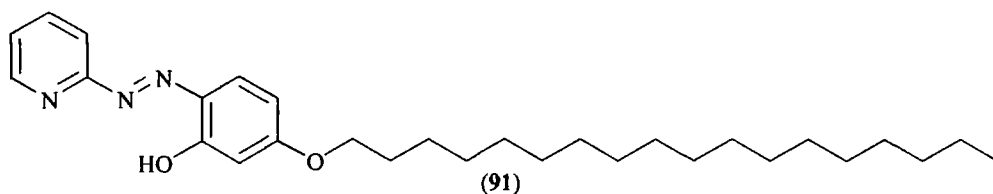
4.1.2 Ferrocene-cyclodextrin Conjugates.

The intermolecular complex formed between ferrocene and β -cyclodextrin has been shown to act as a strong oxidant and an efficient electron-transfer mediator for oxidising NADH.⁴ This occurs despite the low concentration of the complex in solution caused by its relatively low stability constant ($K_{11}=50M^{-1}$ (DMSO, 298K)).⁵ Other ferrocene derivatives have also displayed equally low stability constants, K_{11} for the complex between the lipophilic cyclodextrin derivative per-O-ethyl- β -cyclodextrin and 1,1'-bis(hydroxymethylmethylether)ferrocene ($CDCl_3$, 298K) has been calculated as $20M^{-1}$ by PGSE NMR.⁶ To overcome the problems of low complex concentration, Osa *et al.*⁷ prepared the mono-ferrocene-per-acetyl-cyclodextrin conjugate (90) which displayed quasi-irreversible redox properties in acetonitrile. Addition of benzyl alcohol or 1-naphthalene methanol promoted a catalytic current, observed by cyclic voltammetry, and resulted in complete oxidation to benzaldehyde and 1-naphthaldehyde, respectively. No such observation was made for the analogous methyl ferrocencarboxylate in the presence of per-O-acetyl- β -cyclodextrin. The catalytic activity was attributed to oxidation of the ferrocene moiety followed by complexation of the guest alcohol. It was suggested that the enforced proximity of the cyclodextrin-bound alcohol and the cyclodextrin-appended ferrocene allowed facile electron transfer before decomplexation of the oxidised guest.



4.1.4 Optodes.

The use of ionophores appended to chromophoric reporters in chemosensing optodes has been explored by Wang *et al.*⁸ in the development of an optode membrane for Zn(II) ions. Use of the lipophilic metal ion indicator dye [1-octadecyloxy-4-(2-pyridylazo)resorcinol (91) allowed detection of Zn(II) ions between 1×10^{-6} M - 3×10^{-3} M concentrations by an absorbance enhancement at 523 nm. In contrast to the surface responsive ion selective membranes discussed above, optodes rely on diffusion through the bulk membrane to signal a response, response times therefore tend to be significantly slower than for ISE's. Response times for the optode system above were good, taking 5 minutes to reach 95% of the final signal (t_{95}).



More comprehensive reviews of optode and ion selective membrane technology are given by Bakker *et al.*^{9,10} and Seiler and Simon.¹¹ No examples of cyclodextrin based optodes could be found by the author by a BIDS search using the keywords "cyclodextrin" and "optode".

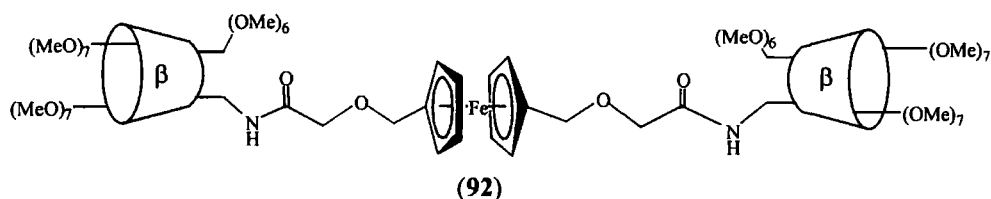
4.1.4 Cyclodextrins in Capillary Electrophoresis.

The use of cyclodextrins as chiral resolution agents in capillary electrophoresis has been investigated by Lurie *et al.*¹² Chiral resolution of a number of cationic drugs of forensic interest, such as amphetamine, methamphetamine, cocaine, cathinone and propoxyphene, was reported for capillary electrophoresis with added cyclodextrins. Resolution and migration speed could be adjusted by varying the ratio of the two most effective cyclodextrins used, namely the charge neutral hydrophilic 2,6-di-O-methyl- β -cyclodextrin and the anionic β -cyclodextrin sulfobutyl ether. Chiral resolution occurs on the basis of differences in stability constants between the cyclodextrin and the analyte, the more stable complex being retained longer on the capillary column. The use of anionic cyclodextrins can improve resolution further for

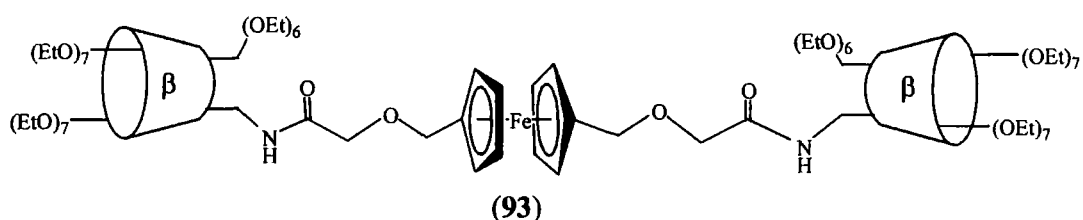
cationic analytes as a result of the large difference in retention between the neutral host guest complex and the ionic host and guest components.

4.2 Aims.

The hydrophilic ferrocene-per-O-methyl- β -cyclodextrin conjugate (**92**) was designed for use in capillary flow electrophoresis. The system provided two binding sites for the inclusion of suitable analytes in the hope that this would allow a greater sensitivity. The catalytic oxidation properties of the ferrocene-cyclodextrin conjugate (**92**) were also to be investigated.

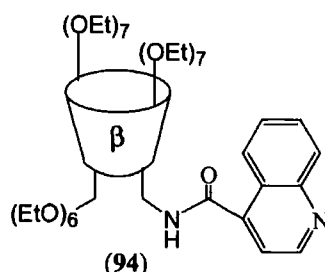


The analogous lipophilic ferrocene-cyclodextrin conjugate (**93**) was designed for inclusion in ion selective electrode membranes. It was hoped that directly appending the charge shuttle ferrocenyl moiety to the ionophoric binding site would improve the response time of the system.



The quinoline-appended cyclodextrin (**94**) has been designed for use in a membrane optode for the detection of charged diffuse species, for example acetylcholine (**88**). The cyclodextrin fulfils two roles in this system: Firstly, O-ethylation of the hydroxyl groups should render the conjugate lipophilic, and therefore appropriate for inclusion into the PVC based membrane. Furthermore, the cavity of the cyclodextrin is expected to act as a host site for inclusion of analytes such as acetylcholine (**88**). The

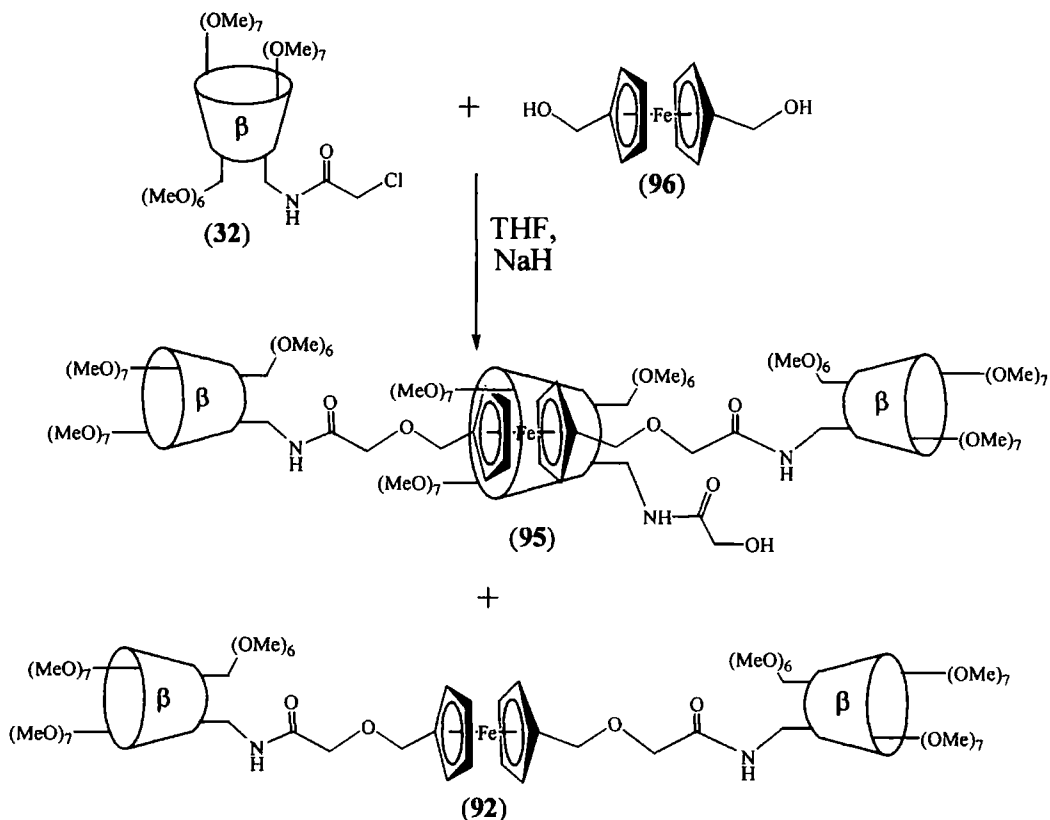
quinoline (**94**) was expected to display a pK_a of *ca* 4-5, which is expected to be increased by *ca* 2 when incorporated into a polymer membrane¹³ and to show perturbations in the fluorescence spectra upon protonation. Inclusion of a charged species such as acetylcholine (**88**) in buffered media should inhibit protonation of the quinoline by electrostatic repulsion, therefore giving rise to a characteristic change in fluorescence.



4.3. Synthetic Methodology.

4.3.1. Synthesis of Hydrophilic Ferrocene-cyclodextrin Conjugates (**92** & **95**).

The coupling of mono-(chloromethylcarbamoyl)-per-O-methyl- β -cyclodextrin (**32**) with 1,1'-bis(hydroxymethyl)ferrocene (**96**) was achieved with sodium hydride in anhydrous THF (Scheme 4.1). Analysis by HPLC showed the presence of two species with weak chromophores which were subsequently separated by preparative HPLC. MALDI-TOF mass spectrometry (Figure 4.1) and ¹H NMR spectroscopy showed that the two species corresponded to 2:1 (**92**) and 3:1 (**95**) adducts of the cyclodextrin and the ferrocene moieties. These were assigned as the thread (2:1) and rotaxane (3:1) of a cyclodextrin-ferrocene conjugate, and were isolated in 19% and 11% yield respectively. Formation of the rotaxane (**95**) was attributed to formation of a 1:1 complex between the cyclodextrin and the ferrocene prior to addition of a further two cyclodextrin molecules onto the ferrocene hydroxyl anions.



Scheme 4.1. Preparation of hydrophilic ferrocene-cyclodextrin conjugates (**92** & **95**).

P. J. Skinner
 (DHB) PJS12712
 Data: 2a0001.7 25 Mar 98 13:15 Cal: TEST 15 May 97 12:04
 Kratos Kompact MALDI 4 V5.1.2 + Linear High Power: 96
 %Int. 100% =24 mV[sum= 4827 mV] Profiles 0-200 Smooth Av 20 -Baseline 80

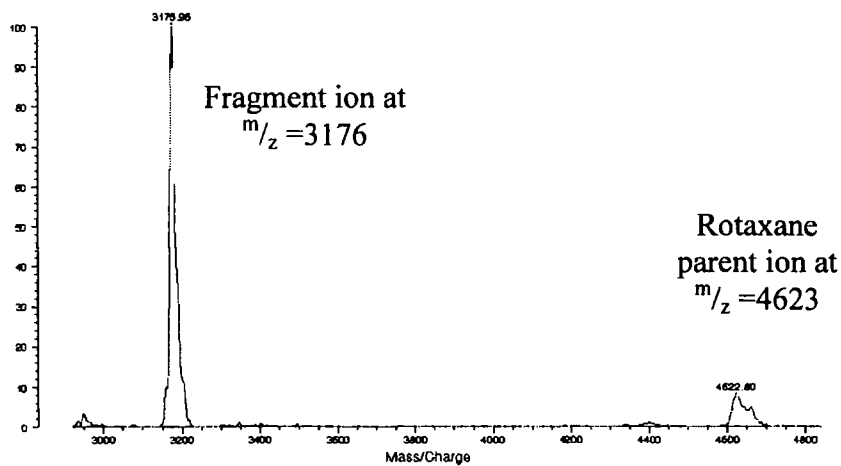


Figure 4.1 MALDI-TOF MS of rotaxane (**95**) showing parent ion ($m/z=4623$) and fragmentation ion ($m/z=3176$). The thread (**92**) showed only the parent ion ($m/z=3173$).



Chromophoric species within chiral environments can display selective absorption of left or right handed light. This has commonly been used to detect aromatic species complexed within the chiral cyclodextrin cavity.^{14,15,16} The circular dichroism spectra of the rotaxane (**95**) showed a weak negative induced CD band at 460 nm at a 2.0 mM concentration (Figure 4.2). This corresponds to absorbance by the ferrocene chromophore and confirms that the ferrocene is in the chiral environment of the cyclodextrin. The magnitude of the induced CD remained more or less unchanged with decreasing sample concentration, albeit with a greater noise to signal ratio. This suggests that the effect is intramolecular in nature with the ferrocene bound within the cavity of the cyclodextrin, consistent with the structure of the rotaxane (**95**). No induced CD band was observed for neither the thread (**92**) at an equivalent concentration, nor the intermolecular complex between per-O-methyl- β -cyclodextrin (**5**) and 1,1'-bis(hydroxymethyl)ferrocene (**96**) over the concentration range 0.5-10 mM.

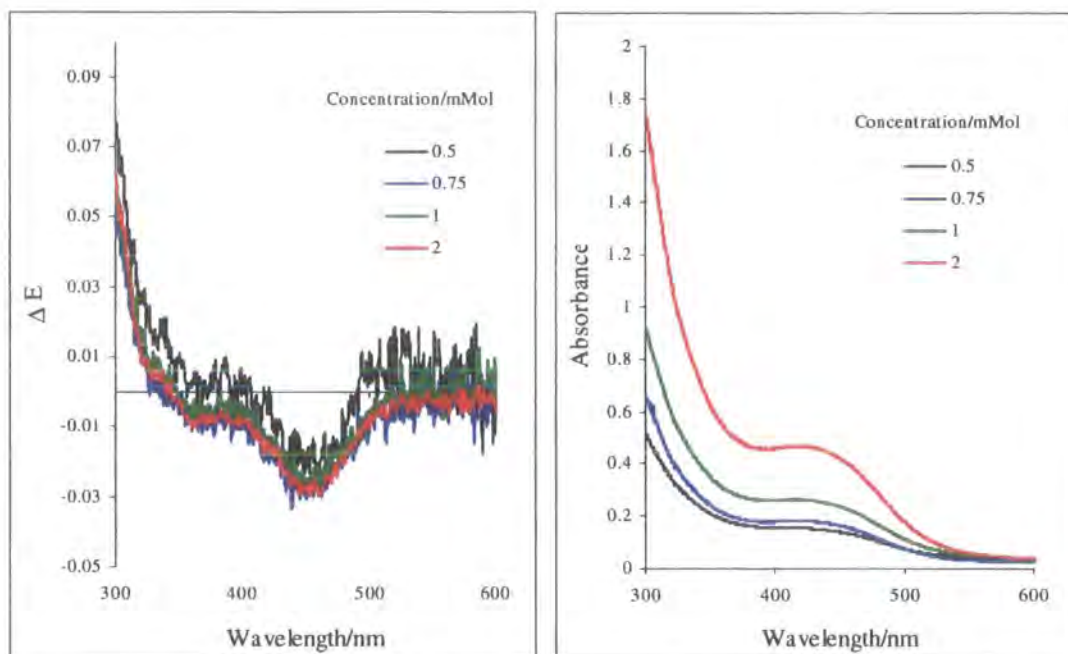
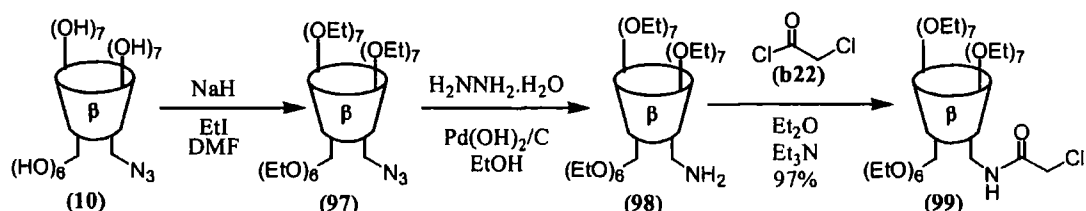


Figure 4.2 CD spectra and UV absorbance spectra of the rotaxane (**95**).

4.3.2 Synthesis of Monofunctionalised Lipophilic Cyclodextrins.

A mono-functionalised lipophilic cyclodextrin was successfully synthesised by O-ethylation of mono-azido- β -cyclodextrin (**10**) (Scheme 4.2), the synthesis of which was described earlier (Chapter 2, pages 32-33). Reaction of mono-azido- β -cyclodextrin (**10**) with sodium hydride and ethyl iodide was carried out in DMF over 4 days (Scheme 4.2). The resulting mono-azido-per-O-ethyl- β -cyclodextrin (**97**) was readily separable from inorganic residues by extraction into hexane, however separation of residual per-O-ethyl- β -cyclodextrin was anticipated to be more problematic due to its similar solubility and polarity. Therefore, reduction of mono-azido-per-O-ethyl- β -cyclodextrin (**97**) to mono-amino-per-O-ethyl- β -cyclodextrin (**98**) was performed prior to further purification.

The reduction of mono-azido-per-O-ethyl- β -cyclodextrin (**97**) to mono-amino-per-O-ethyl- β -cyclodextrin (**98**) was achieved by a different procedure than that described previously for the O-methylated analogue (Chapter 2, pages 35). Reduction was achieved using hydrazine hydrate in ethanol in the presence of catalytic palladium hydroxide (1% on carbon) (Scheme 4.2). This procedure had certain advantages over that described for reduction of mono-azido-per-O-methyl- β -cyclodextrin (**27**). The time taken for complete reaction to occur was significantly shorter (36 hours, *cf* 4 days) and the resulting product also was less coloured due to the decolourising effect of carbon. The significantly different polarities of mono-amino-per-O-ethyl- β -cyclodextrin (**98**) and per-O-ethyl- β -cyclodextrin allowed facile purification by column chromatography to give the desired mono-amino-per-O-ethyl- β -cyclodextrin (**98**) in good yield (63% from mono-azido- β -cyclodextrin (**10**)).

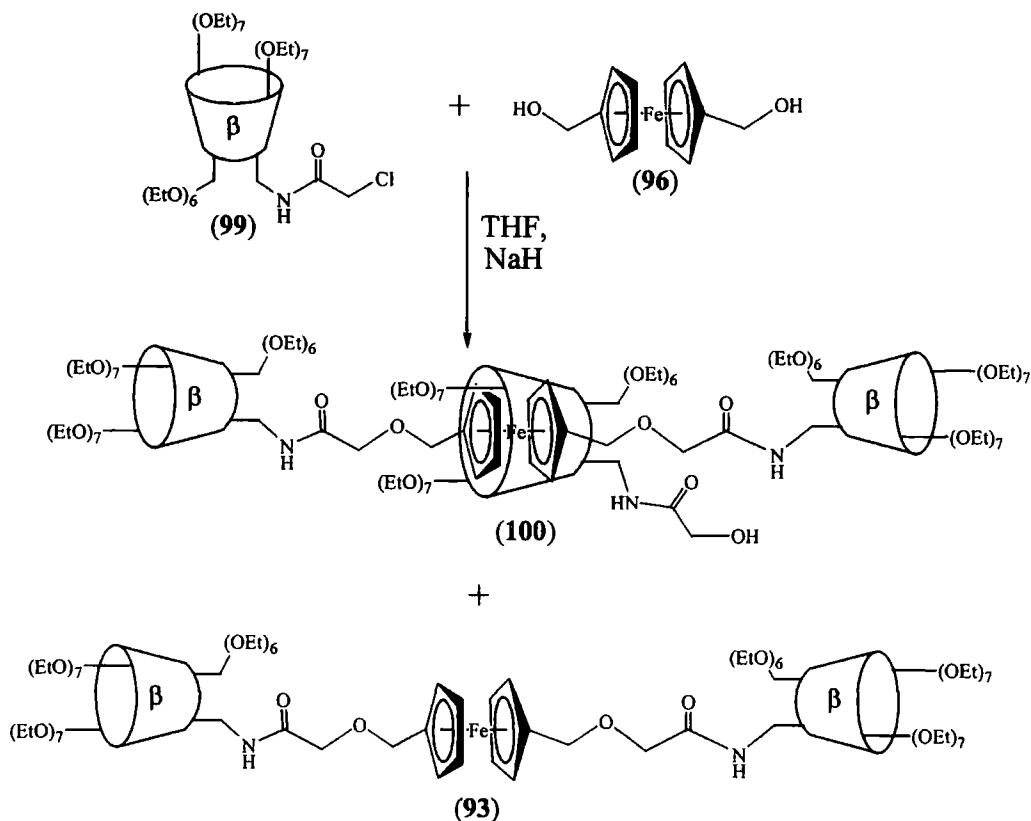


Scheme 4.2. Preparation of mono-amino-per-O-ethyl- β -cyclodextrin (**98**) and mono-chloromethylcarbamoyl-per-O-ethyl- β -cyclodextrin (**99**).

Mono-chloromethylcarbamoyl-per-O-ethyl- β -cyclodextrin (**99**) was readily synthesised by nucleophilic substitution of mono-amino-per-O-ethyl- β -cyclodextrin (**98**) with chloroacetylchloride (**33**) (Scheme 4.2). Purification through a silica plug gave the desired mono-chloromethylcarbamoyl-per-O-ethyl- β -cyclodextrin (**99**) in excellent yield (97%, 22% from β -cyclodextrin (**1**)).

4.3.3. Synthesis of Lipophilic Ferrocene-cyclodextrin Conjugates (93** & **100**).**

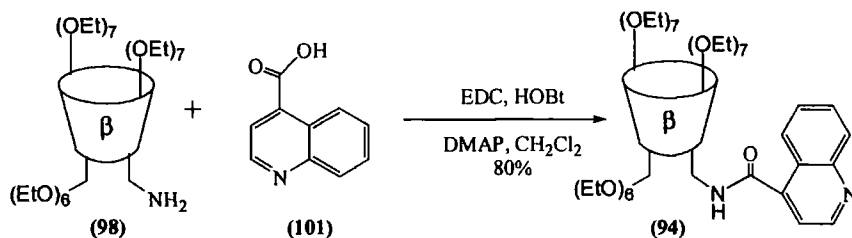
Coupling of mono-(chloromethylcarbamoyl)-per-O-ethyl- β -cyclodextrin (**99**) with 1,1'-bis(hydroxymethyl)ferrocene (**96**) was carried out using sodium hydride in anhydrous THF (Scheme 4.3). In contrast to the O-methyl analogue described earlier (pages 100-101), the cyclodextrin and ferrocenyl moieties were allowed to equilibrate for 30 minutes before addition of sodium hydride in order to favour formation of the intramolecular complex necessary for formation of the rotaxane. Analysis by MALDI-TOF mass spectrometry suggested that the resulting solid contained a mixture of the rotaxane (**100**) and thread (**93**). The chromophores of the two species, however, proved too weakly absorbing to allow purification by preparative HPLC. The identical polarities of the two species also prevented purification by column chromatography.



Scheme 4.3. Preparation of lipophilic ferrocene-cyclodextrin conjugates (**93** & **100**).

4.3.4. Synthesis of a Lipophilic Cyclodextrin For Optometry (**94**).

Coupling of quinoline-4-carboxylic acid (**101**) and mono-amino-per-O-ethyl- β -cyclodextrin (**98**) occurred readily using a standard peptide coupling procedure (Scheme 4.4). Purification by column chromatography gave (4'-quinolylylcarbamoyl)-per-O-ethyl- β -cyclodextrin (**94**) in 80% yield.



Scheme 4.4. Preparation of (4'-quinolylylcarbamoyl)-per-O-ethyl- β -cyclodextrin (**94**).

The fluorescence emission of (4'-quinolylcarbamoyl)-per-O-ethyl- β -cyclodextrin (**94**) showed 4 distinct maxima at 311 nm, 333 nm, 349 nm and 367 nm. The intensity of emission at these maxima increased with decreasing pH (Figure 4.3). This allowed calculation of the pK_a of (4'-quinolylcarbamoyl)-per-O-ethyl- β -cyclodextrin (**94**) as 5.2 in 90% MeOH/H₂O. This corresponds to a pK_a of 4.7 in H₂O (Figure 4.4).¹⁷

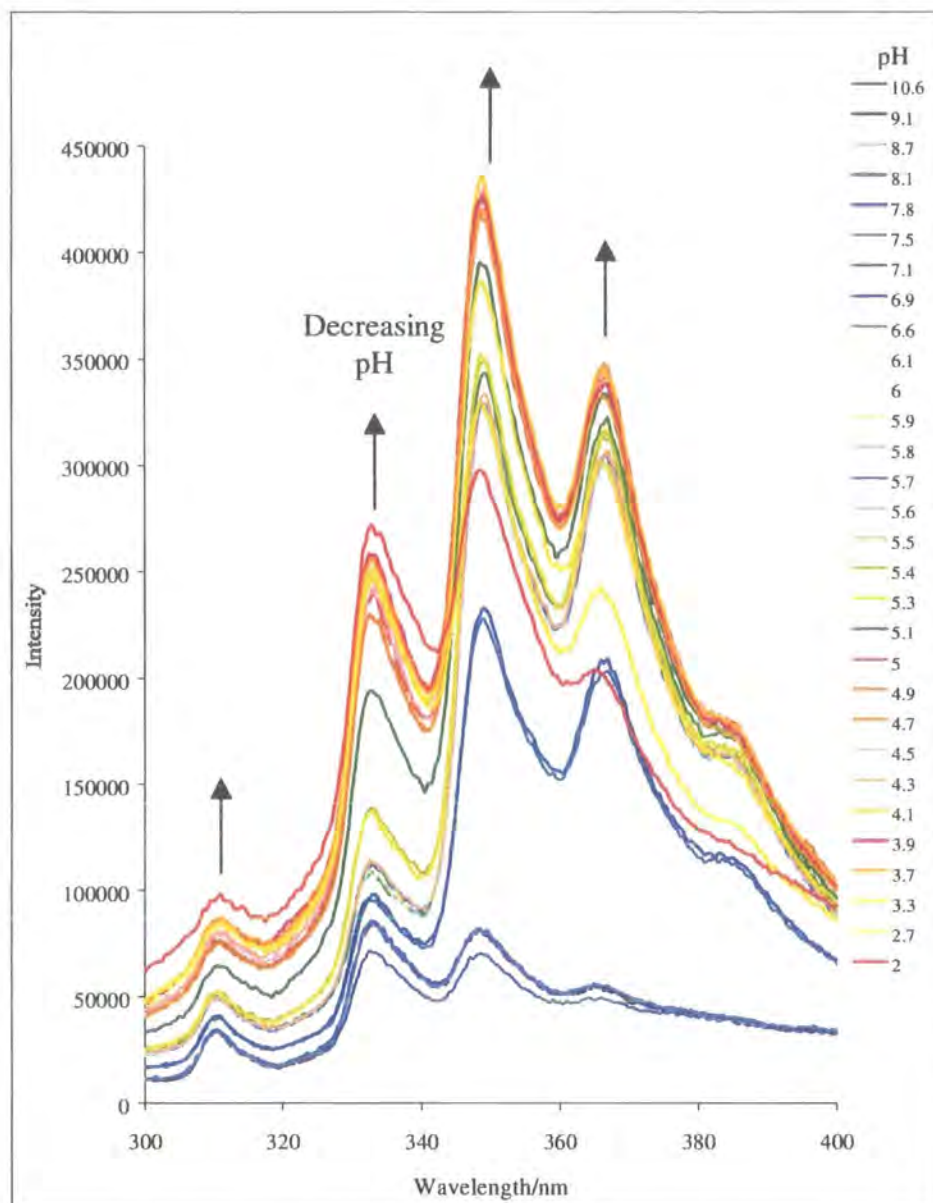


Figure 4.3 Increasing fluorescence emission from (4'-quinolylcarbamoyl)-per-O-ethyl- β -cyclodextrin (**94**) with decreasing pH (concentration= 4.9×10^{-5} M, 90% MeOH/H₂O, 0.1 M NMe₄Cl, pH varied by addition of TFA, λ_{ex} =284 nm, 298K).

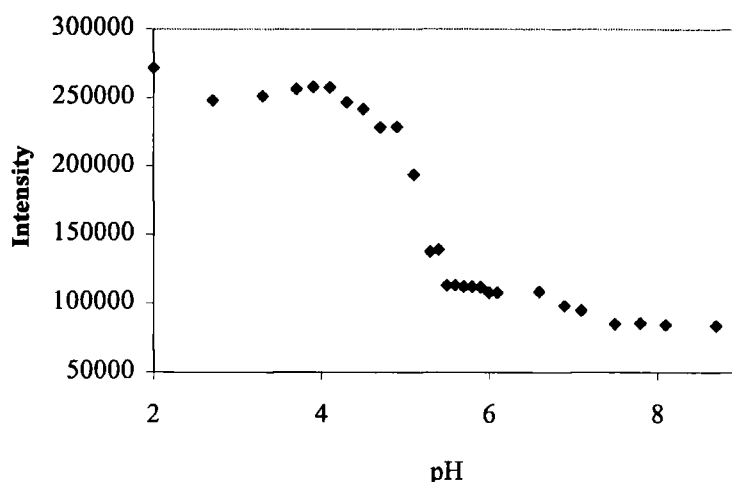


Figure 4.4 Intensity of emission of (4'-quinolylylcarbamoyle)-per-O-ethyl- β -cyclodextrin (**94**) with decreasing pH allowing calculation of pK_a (concentration= 4.9×10^{-5} M, 90% MeOH/H₂O, 0.1M NMe₄Cl, acidified by addition of TFA, λ_{ex} =284 nm, λ_{em} =333 nm, 298K).

4.4. Detection Properties.

4.4.1 Detection Properties of the Quinoline-appended Cyclodextrin (**94**).

The following work was carried out by Stephanie Blair and Dr Ritu Katakya at the University of Durham. Preliminary results are shown below.

The quinoline-appended cyclodextrin was included into a membrane containing 2.5% of the cyclodextrin (**94**), 32.5% PVC and 65% of the plasticiser DOS. The optode membrane was used to examine the response to the presence of acetylcholine (**88**) at concentrations between 1×10^{-4} M and 1×10^{-8} M in a buffered medium (pH=7.14) (Figure 4.5). This detection range compares favourably to that of the cyclodextrin-based ion selective electrodes developed by Parker *et al.*¹ and described earlier (page 96).

Surprisingly, fluorescent emission from the membrane incorporated quinoline-conjugate (**94**) was observed to increase upon addition of acetylcholine (**88**). Given that fluorescent emission from the conjugate (**94**) in solution increased with

increasing pH (Figure 4.3), it was expected that binding of the cationic acetylcholine (**88**) to the cyclodextrin (**94**) in acidic media would result in deprotonation of the quinoline moiety and hence a reduction in the intensity of fluorescent emission. The deviation from the expected observation is likely to be due to a change in the fluorescence properties of the conjugate (**94**) due to incorporation into the polymer membrane.

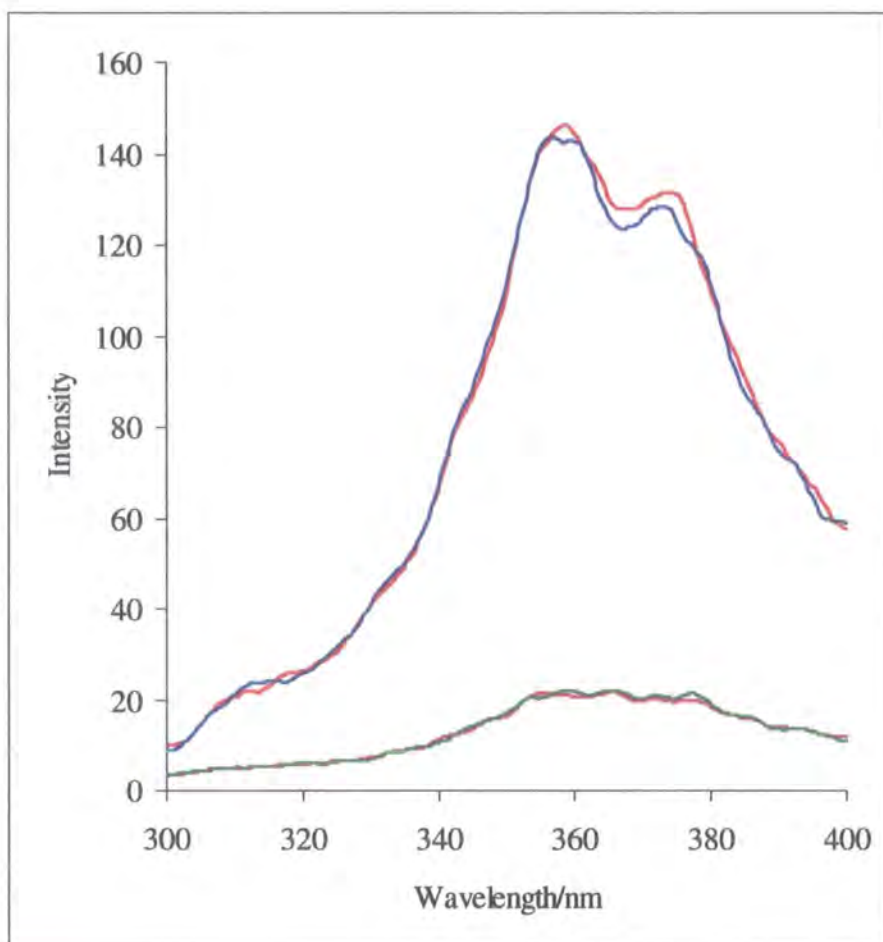


Figure 4.5 Detection properties of optode incorporated (**94**). Graph shows fluorescent emission intensity from the membrane held within a flow cell with tris (tris(hydroxymethyl)amino methane.maleic acid) buffer (pH=7.14) and (—) no acetylcholine (**88**), (---) 1×10^{-8} M acetylcholine (**88**), (—) 1×10^{-6} M acetylcholine (**88**), (—) 1×10^{-4} M acetylcholine (**88**), H_2O , 298K, $\lambda_{ex}=253nm$.

The fluorescence behaviour of the membrane incorporated quinoline-conjugate (**94**) was also observed whilst contained within a flow-cell. This allowed observation of

the time response of the changes in fluorescence due to the presence of acetylcholine (**88**) (Figure 4.6). Alternately exposing the membrane to varying concentrations of acetylcholine (**88**) confirmed that that the membrane incorporated quinoline-cyclodextrin conjugate (**96**) was suitable for detection of acetylcholine (**88**) at a concentration of *ca* 10^{-6} M. The membrane showed a reasonable time response; t_{95} , the time taken for the signal to reach 95% of its final value, was measured as *ca* 13 minutes, which is consistent with related literature response times.

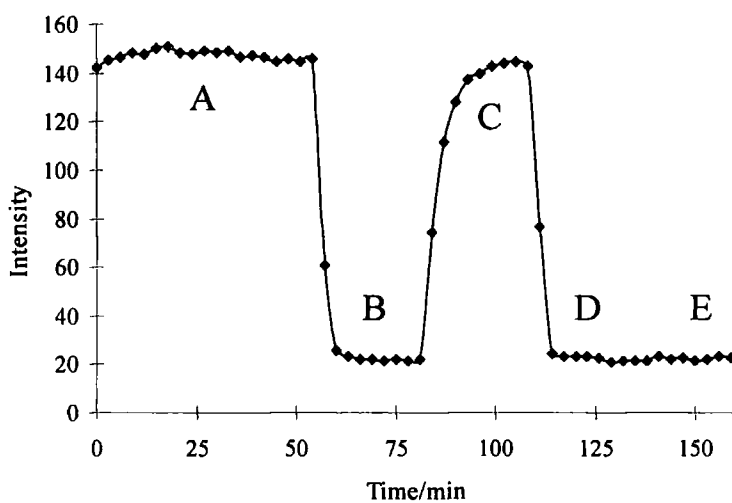


Figure 4.6 Time response for optode incorporated (**94**). Graph shows intensity from the membrane held within a flow cell with A: 1×10^{-4} M acetylcholine (**88**), B: tris buffer (pH=7.14), C: 1×10^{-6} M acetylcholine (**88**), D: tris buffer (pH=7.14), E: 1×10^{-8} M acetylcholine (**88**), H_2O , 298K, $\lambda_{ex}=253nm$, $\lambda_{em}=350nm$.

Further fluorometric analysis of the optode incorporated quinoline-cyclodextrin conjugate (**94**), capillary flow electrophoresis and catalytic oxidation studies on the hydrophilic ferrocene-cyclodextrin conjugates (**92 & 95**) and ion selective electrode studies on the membrane incorporated lipophilic ferrocene-cyclodextrin conjugates (**93 & 100**) are ongoing and awaiting completion by persons other than the author.

4.5 References.

- ¹ P. M. Kelly, R. Katakya, D. Parker, A. F. Patti, *J. Chem. Soc., Perkin Trans. 2*, 1995, 1955.
- ² P. S. Bates, R. Katakya, D. Parker, *J. Chem. Soc., Chem. Comm*, 1992, 153.
- ³ R. Katakya, D. Parker, *Analyst*, 1996, **121**, 1829.
- ⁴ T. Matsue, D. H. Evans, T. Osa, N. Kobayashi, *J. Am. Chem. Soc.*, 1985, **107**, 3411.
- ⁵ B. Siegel, R. Breslow, *J. Am. Chem. Soc.*, 1975, **97**, 6869.
- ⁶ Personal communication from Y. Cohen.
- ⁷ I. Suzuki, Q. Chen, Y. Kashiwagi, T. Osa, A. Ueno, *Chem. Lett.*, 1993, 1719.
- ⁸ K. Wang, K. Seiler, B. Rusterholz, W. Simon, *Analyst*, 1992, **117**, 57.
- ⁹ U. Spichiger, W. Simon, E. Bakker, M. Lerchi, P. Bühlmann, J. -P. Haug, M. Kuratli, S. Ozawa, S. West, *Sensors and Actuators B*, 1993, **11**, 1.
- ¹⁰ E. Bakker, P. Bühlmann, E. Pretsch, *Chem. Rev.*, 1997, **97**, 3083.
- ¹¹ K. Seiler, W. Simon, *Anal. Chim. Acta*, 1992, **266**, 73.
- ¹² I. S. Lurie, R. F. X. Klein, T. A. D. Cason, M. J. LeBelle, R. Brenneisen, R. E. Weinberger, *Anal. Chem.*, 1994, **66**, 4019.
- ¹³ E. Bakker, M. Lerchi, T. Rosatzin, B. Rusterholz, W. Simon, *Anal. Chim. Acta*, 1993, **278**, 211.
- ¹⁴ S. Monti, G. Köhler, G. Grabner, *J. Phys. Chem.*, 1993, **97**, 13011.
- ¹⁵ M. Kodaka, *J. Phys. Chem.*, 1998, **102**, 8101.
- ¹⁶ T. Matsue, D. H. Evans, T. Osa, N. Kobayashi, *J. Am. Chem. Soc.*, 1985, **107**, 3411.
- ¹⁷ R. G. Bates, *Determination of pH; Theory and Practice*, J. Wiley & Sons Inc., 1964, p224.

Chapter 5

Experimental Methods

5 Experimental Methods.

5.1 Methods.

Reaction Conditions.

For all reactions performed, temperatures are quoted in degrees Celsius. All reactions were carried out in apparatus which had been oven dried, and cooled under argon. Reactions requiring an inert atmosphere or anhydrous condition were carried out under a dynamic atmosphere of dry, oxygen-free argon using standard Schlenk-line techniques. Solvents were dried by distillation from the appropriate drying agent where required with the exception of N, N-dimethylformamide and dimethylsulfoxide which were used directly from "sure-seal" bottles. Water was purified by the PURITE_{STILL} plus system.

Purification Procedures.

Thin layer chromatography was carried out using aluminium backed silica plates with (Merck Art 5554) or without (Merck Art 5554) a fluorescent indicator. Plates containing non-fluorescent species were developed by immersion in aqueous sulfuric acid solution (50% v/v) and heating (400°C), the compound(s) appearing at charred black spot(s). Preparative column chromatography was carried out using silica (Merck silica gel 60, 230-400 mesh). Preparative HPLC was carried out using a 'Hypersil semiprep' column. Benzoylated dialysis tubing (Sigma, D-2272 or D-7884) with a molecular weight cut off of 1200-2000 amu was used in water as supplied and sealed by tying at both ends. Dialysis was also carried out using a Spectrum Spectra/Por® MacroDialyzer using CEA (Cellulose Ester Asymmetric) membranes with a MWCO of 1000, 2000 or 5000 amu. Membranes were washed with water before use, and the chamber operated in a flow dialysis mode using water as a reservoir solvent.

Characterisation.

¹H NMR spectra were recorded at 65.26 MHz on a 1.53T magnet connected to a Varian VXR400 console, at 199.99 MHz on Varian Mercury-200, Gemini-200, and VXR200 spectrometers, at 299.91 MHz on a Varian Unity-300, at 399.96 MHz on a Varian VXR400 and at 499.79 MHz on a Varian Unity Inova-500 spectrometer. ¹³C NMR spectra were recorded on the Varian Gemini-200 and Mercury-200 spectrometers operating at 50.29 MHz, the Varian Unity-300 operating at 75.41 MHz, the Varian VXR400 operating at 100.58 MHz and the Varian Unity Inova-500 operating at 125.67 MHz. Chemical shifts are given in ppm to higher frequency of TMS and are reported consecutively as position (δ_{H} and δ_{C}), relative integral, multiplicity (abbreviated as singlet (s), doublet (d), triplet (t), doublet of doublets (dd), doublet of triplets (dt), doublet of doublet of doublets (ddd) or multiplet (m)) with coupling constants (J) reported in Hz.

Infra-red spectra were recorded on a Perkin-Elmer 1600 FT-IR spectrometer using a 'Golden Gate' accessory and absorbance maxima are quoted in wavenumbers.

Ultraviolet spectra were recorded on a Unicam UV2 spectrometer.

Electrospray ionisation mass spectra were obtained on a VG II platform (Fisons Instruments) with methanol, except where stated as water, as carrier solvent. VG 7070E and Micromass Autospec spectrometers were also used, operating in EI ionisation mode. MALDI-TOF spectra were recorded on a Kratos Kompact 4 spectrometer, operated in linear or reflectron detection mode to generate positively charged ions. 2,5-Dihydroxybenzoic acid was applied as a matrix. Accurate mass were obtained from the EPSRC National mass Spectrometry Service Centre, University of Wales, Swansea.

Elemental analyses were determined on an Exeter Analytical CE440 Elemental Analyser. Metal and halogen concentrations were determined on a Dionex DX500 Ion Chromatograph. Melting points were determined on a Reichert Köfler block melting point apparatus and are uncorrected.

NMRD profiles were obtained by S. Aime and M. Botta at the Università di Torino, Torino, Italy. The profiles were acquired between 0.01-10 MHz on a Stelar Field Cycling Relaxometer, at 20 MHz on a Stelar Spinmaster and at 90 MHz on a Jeol EX 90.

Optical Spectroscopy.

Fluorescence and phosphorescence spectra were acquired using a Perkin-Elmer LS 50B Luminescence Spectrometer controlled through Perkin-Elmer Fluorescence Data Manager Instrument Control Version 3.00 on a PC, or using an Instruments SA Fluorolog controlled through DataMax for Windows Version 2.1 on a PC. Samples were held in a degassing cell equipped with a 10mm pathlength square cuvette and a degassing bulb. Degassing was achieved using the 'freeze-pump-thaw' method.

Lifetime measurements were acquired on the same spectrometer using a program designed and written by Dr. Andrew Beeby (University of Durham) on a PC. Decays were fitted using Microsoft excel to single or double exponential functions of the form $I(t) = A_0 + A_1 e^{-k_1 t} + A_2 e^{-k_2 t}$.

Low temperature data were acquired using cells held in an optical cryostat (Oxford Instruments DN-704). Temperatures could be maintained at 77-330±0.1K using an Oxford Instruments ITC-6 temperature controller. The sample was contained in a degassing cell equipped with degassing bulb and a cell made from square section fused silica tubing with a 10mm nominal pathlength.

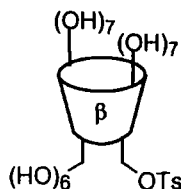
Laser flash photolysis was carried out with a 90° geometry for pump and probe beams. Excitation was carried out using the 4th harmonic of a Q-switched Nd-YAG laser (Spectra Physics GCR-150-10) emitting at a wavelength of 266nm. The pulse energy delivered was less than 1mJ per pulse at the sample. The probe beam was supplied by a continuous wave W lamp. Transmitted light was passed through a monochromator (Spex Triax 320) and the intensity recorded using a photomultiplier (Hamamatsu R928) operating in DC-mode. The signal was recorded and averaged using a digital oscilloscope (Tektronix TDS-320) and the transient transferred to a PC for analysis.

Ytterbium complexes were excited at 266nm in an identical manner as for flash photolysis experiments. Ytterbium emission was detected in the range 980-1000nm using a liquid nitrogen cooled germanium diode (North Coast EO817P).

Circular dichroism spectra were acquired by the EPSRC Chiroptical and ULIRS Optical Spectroscopy Centres, Kings College, London.

5.2 Experimental for Chapter 2.

Mono-(6^A-O-toluenesulfonyl-6^A-deoxy)- β -cyclodextrin (**9**).



Method 1.

Mono-6-O-toluenesulfonyl-6-deoxy- β -cyclodextrin (**9**) was prepared following the procedure described by Easton *et al.*¹ β -Cyclodextrin (**1**) (6.05 g, 5.3 mmol) was dried under vacuum for 18 hours then dissolved in pyridine (50 cm³, freshly distilled over KOH). *p*-Toluenesulfonyl chloride (1.15 g, 6.0 mmol, recrystallised from petroleum ether) was added as a solid in portions over one hour. The solution was stirred at room temperature for a further 24 hours. The solvent was then removed under reduced pressure and the residue was washed successively with dichloromethane (3 x 50 cm³) and acetone (3 x 50 cm³). The solid was recrystallised from boiling water (70 cm³) to afford a colourless solid (1.18 g, 0.9 mmol, 17 %).

Method 2.

Mono-6-O-toluenesulfonyl-6-deoxy- β -cyclodextrin (**9**) was also prepared following an adaptation of the procedure described by Zhong *et al.*² β -Cyclodextrin (**1**) (11 g, 10.4 mmol) and *p*-toluenesulfonyl chloride (5.2 g, 27.3 mmol, recrystallised from

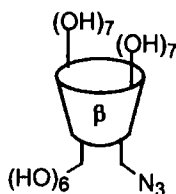
petroleum ether) were stirred as a suspension in water (250 cm³). After 3 hours, aqueous sodium hydroxide (60 cm³, 2M) was added and the solution stirred for a further 30 minutes. Ammonium chloride (20 g) was added until the pH of the solution reached 8. The solution was chilled for 18 hours and the resulting precipitate collected by vacuum filtration to afford a white solid. (5.19 g, 4.03 mmol, 39 %).

$R_f=0.53$ (5:4:3 t-BuOH:EtOH:H₂O, silica).

m/e (ES⁺): 1306 [M+NH₄]⁺, 1312 [M+Na]⁺.

mp: 168-170°C dec. (lit. 168-170°C dec.).³

Mono-(6^A-azido-6^A-deoxy)- β -cyclodextrin (10).



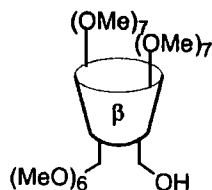
Mono-6-azido-6-deoxy- β -cyclodextrin (**10**) was prepared following the procedure described by Perly et al.⁴ Mono-6-O-toluenesulfonyl-6-deoxy- β -cyclodextrin (**9**) (1.94 g, 1.5 mmol) was dried under vacuum for 18 hours (overnight) then dissolved in dry DMF (30 cm³). Lithium azide (0.82 g, 15 mmol) was added and the solution was stirred at 100°C for 5 hours. The solvent was removed under reduced pressure (20 mmHg, 40°C), the residual solid was dissolved in warm water (40 cm³) and added to chilled acetone (250 cm³). The resulting precipitate was collected by vacuum filtration to afford a cream solid (1.62 g, 1.4 mmol, 93 %).

$R_f=0.48$ (5:4:3 t-BuOH:EtOH:H₂O, silica).

m/e (ES⁺): 1177 [M+NH₄]⁺.

mp: 215-220°C dec. (lit. 210-220°C dec.).⁴

6^A-Hydroxy-heptakis-(2,3-di-O-methyl)-6^B,6^C,6^D,6^E,6^F,6^G-hexa-O-methyl- β -cyclodextrin (12).



Mono-6-hydroxy-per-O-methyl- β -cyclodextrin (**12**) was prepared following the procedure described by Bradshaw et al.⁵ β -Cyclodextrin (**1**) (4.54 g, 4.0 mmol) and imidazole (0.61 g, 9.0 mmol) were dried under vacuum for 18 hours, then dissolved in dry DMF (100 cm³) under argon. *tert*-Butyldimethylsilylchloride (1.24 g, 8.2 mmol) dissolved in dry DMF (20 cm³) was added dropwise over 2 hours.

After 2 hours the solution was cooled to 0°C and sodium hydride (6.4 g, 260 mmol) added slowly over 5 minutes. The solution was then stirred at 0°C for 30 minutes and at room temperature for a further hour. The solution was then cooled to 0°C and methyl iodide (77 g, 545 mmol) added dropwise over 1 hour and the mixture stirred at room temperature for 3 days. The solution was then cooled to 0°C, excess hydride quenched by the addition of methanol (15 cm³) and the mixture added to chilled water (400 cm³). The solution was extracted into chloroform (4 x 100 cm³), the combined organic extracts were washed successively with aqueous sodium thiosulphate solution (75 cm³, 3% w/v) and water (3 x 75 cm³), and dried (K₂CO₃), filtered and solvent removed under reduced pressure to yield a cream solid (6.35 g).

The cream solid was dissolved in methanol (300 cm³) and ammonium fluoride (2.15 g, 58.1 mmol) added. The solution was boiled under reflux for 30 hours then solvents removed under reduced pressure. The residual solid was redissolved in ethyl acetate (100 cm³), filtered and solvent removed under reduced pressure to yield a yellow solid (6.06 g).

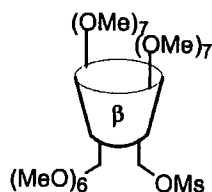
Purification by column chromatography (1% MeOH/CHCl₃, silica) gave a yellow solid (1.15 g, 0.81 mmol, 20 %).

$R_f=0.52$ (10:1 CHCl_3 :MeOH, silica).⁵

m/e (ES+): 1432 $[\text{M}+\text{NH}_4]^+$.

$\delta_{\text{H}}(\text{CDCl}_3)$: 5.30-4.95 (m, 7H, C(1)-H), 3.95-2.95 (m, 103H), of which 3.38 (s), 3.50 (s) and 3.64 (s) are for OCH_3 groups.⁵

6^A-O-Methanesulfonyl-6^A-deoxy-heptakis-(2,3-di-O-methyl)- 6^B,6^C,6^D,6^E,6^F,6^G-hexa-O-methyl- β -cyclodextrin (30).



Mono-6-hydroxy-per-O-methyl- β -cyclodextrin (**12**) (1.015 g, 0.72 mmol) and triethylamine (0.100 g, 0.99 mmol) were dissolved in dry THF (10 cm^3) and chilled to -15°C . Methanesulfonyl chloride (0.250 g, 2.2 mmol) was added dropwise and the solution stirred at -15°C for 1 hour, and at room temperature for a further 2 hours. The solvent was removed under reduced pressure and the resulting solid dissolved in water (30 cm^3) and extracted into chloroform (4 x 50 cm^3). The combined organic extracts were dried (K_2CO_3), filtered and solvent removed under reduced pressure to yield mono-6-O-methanesulfonyl-6-deoxy-per-O-methyl- β -cyclodextrin (**30**) as a colourless glassy solid (1.07 g, 0.72 mmol, 100 %).

$R_f=0.70$ (10:1 CHCl_3 :MeOH, silica).

m/e (ES+): 1510 $[\text{M}+\text{NH}_4]^+$.

mp: 74-76 $^\circ\text{C}$.

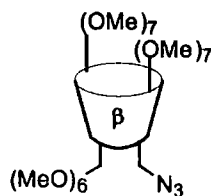
$\delta_{\text{H}}(\text{CD}_3\text{OD})$: 5.30-5.10 (m, 7H, C(1)-H), 3.95-2.95 (m, 105H), of which 3.34 (s), 3.48 (s) and 3.61 (s) are for OCH_3 groups and 3.11 (s) is for one SO_2CH_3 group.

$\delta_{\text{C}}(\text{CD}_3\text{OD})$: 98.5-97.6 (m, inc 98.4, 98.1, 98.0, 97.9, 97.8), 82.1-81.2 (m, inc 81.9, 81.7, 81.6, 81.4), 79.8-78.6 (m, inc 79.7, 79.3, 79.2, 78.9, 78.7), 71.3-70.7 (m, inc 71.2, 71.1, 71.0, 70.8), 69.7, 69.5, 60.5-60.1 (m, inc 60.4, 60.3), 58.0-57.2 (m, inc 57.9, 57.8, 57.6, 57.5, 57.4), 36.0, 31.2.

ν_{max} : 2926, 2830, 1466, 1366, 1140, 1106, 1034, 976, 862, 754, 704, 528 cm^{-1} .

Found: C: 50.4%, H: 7.10%, S: 2.14%. $C_{63}H_{111}O_{37}S$ requires C: 50.7%, H: 7.56%, S: 2.15%.

6^A-Azido-6^A-deoxy-heptakis-(2,3-di-O-methyl)-6^B,6^C,6^D,6^E,6^F,6^G-hexa-O-methyl- β -cyclodextrin (27).



Method 1

An attempt to prepare mono-6-azido-6-deoxy-per-O-methyl- β -cyclodextrin (**27**) was made following the procedure described by Perly et al.⁴ Mono-6-azido-6-deoxy- β -cyclodextrin (**10**) (0.25 g, 0.21 mmol) was dried under vacuum for 18 hours. The solid was then stirred in suspension with powdered potassium hydroxide (0.36 g) and Aliquat 336 (0.01 g) in dimethyl sulphate (1 cm³) for 18 hours at room temperature. Further dimethyl sulphate (2 cm³) was then added and the suspension stirred for a further 24 hours at room temperature. The dimethyl sulphate was removed by evaporation under reduced pressure (20 mmHg, 40°C) and the remaining solid treated with dichloromethane (50 cm³). Solvent was removed under reduced pressure to give a yellow oil (0.16 g). Analysis of the oil by electrospray mass spectrometry suggested the presence of mono-6-azido-6-deoxy-per-O-methyl- β -cyclodextrin (**10**) in negligible quantities along with various partially methylated compounds. This analysis was confirmed by ¹H NMR which shows the presence of only one O-Me peak in significant quantities).

m/e (ES⁺): 1202, 1232, 1246, 1271, 1277, 1352, 1359, 1373, 1387, 1429, 1447, 1457.

Method 2

Mono-6-azido-6-deoxy- β -cyclodextrin (**10**) (0.40 g, 0.34 mmol) and 18-crown-6 (0.004 g) were dried under vacuum for 18 hours then dissolved in dry DMF (20 cm³). Sodium hydride (0.5 g, 21 mmol) was added and after stirring the solution for 1 hour, methyl iodide (2 cm³, 32 mmol) was added over a period of 1 hour. The mixture was stirred at 50°C for 7 days. Further additions of sodium hydride (0.15 g, 6 mmol) and methyl iodide (1 cm³, 16 mmol) were subsequently made on the 2nd, 3rd and 4th days. After 7 days the solution was analysed by electrospray mass spectrometry which showed the presence of mono-6-azido-6-deoxy-per-O-methyl- β -cyclodextrin (**27**) and no detectable mono-6-azido-6-deoxy- β -cyclodextrin (**10**) or per-O-methyl- β -cyclodextrin (**5**). The solution was then quenched with the addition of methanol (10 cm³) and filtered, the solid being washed with further methanol (30 cm³). The solvents were removed under reduced pressure (20 mmHg, 30°C) to give an orange solid.

The orange solid was treated with dichloromethane (100 cm³) and water (100 cm³) and the organic phase separated and washed with water (3 x 30 cm³). Sodium chloride (20 g) was then dissolved in the combined aqueous phases and the aqueous solution washed with dichloromethane (50 cm³). The combined organic phases were dried (K₂CO₃), filtered and solvent removed under reduced pressure to yield a deep yellow oil.

TLC (10:1 CHCl₃:MeOH, silica) analysis of the oil revealed one major component (R_f=0.70) and one minor component (R_f=0.50).

Purification by column chromatography (1% MeOH/CHCl₃, silica) gave a yellow oil (0.11 g, 0.076 mmol, 22 %).

Method 3

Mono-6-O-methanesulfonyl-6-deoxy-per-O-methyl- β -cyclodextrin (**30**) (0.88 g, 0.59 mmol) was dried under vacuum for 18 hours then dissolved in dry DMF (30 cm³) and lithium azide (0.31 g, 6.3 mmol) added. The solution was heated to

100°C for 18 hours and solvent removed under reduced pressure to yield a brown solid. The brown solid was dissolved in water (50 cm³) and extracted into chloroform (3 x 60 cm³). The combined organic phases were dried (K₂CO₃), filtered and solvent removed under reduced pressure to yield a yellow solid (0.53 g, 0.365 mmol, 62 %).

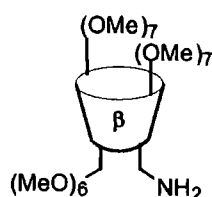
R_f=0.70 (10:1 CHCl₃:MeOH, silica).

m/e (ES⁺): 1458 [M+NH₄]⁺.

mp: 77-79°C (lit. 87-90°C).⁶

δ_H(CD₃OD): 5.15-4.95 (m, 7H, C(1)-H), 3.95-2.95 (m, 102H), of which 3.28 (s), 3.41 (s) and 3.54 (s) are for OCH₃ groups.

6^A-Amino-6^A-deoxy-heptakis-(2,3-di-O-methyl)-6^B,6^C,6^D,6^E,6^F,6^G-hexa-O-methyl-β-cyclodextrin (31).



Method 1

Mono-6-azido-6-deoxy-per-O-methyl-β-cyclodextrin (**27**) (0.11 g, 0.074 mmol) and triphenylphosphine (0.11 g, 0.41 mmol) were dissolved with stirring in DMF (3 cm³). Aqueous ammonia solution (0.25 cm³, ~35 %) was added and a subsequent addition (0.25 cm³) was made after 30 minutes. The solution was stirred at room temperature for 20 hours, added to water (40 cm³) and extracted into chloroform (4 x 60 cm³). The combined organic extracts were dried (K₂CO₃), filtered and solvent removed under reduced pressure to yield mono-6-amino-6-deoxy-per-O-methyl-β-cyclodextrin (**31**) as a deep yellow solid (0.137 g). Analysis by electrospray mass spectrometry showed complete conversion to the desired product. Analysis by NMR indicated that the solid was contaminated with triphenylphosphine, but it was taken on for further reaction without intermediate purification.

Method 2

Mono-6-amino-6-deoxy--per-O-methyl- β -cyclodextrin (**31**) was prepared following the procedure described by Bradshaw *et al.*⁶ Mono-6-azido-6-deoxy-per-O-methyl- β -cyclodextrin (**27**) (0.55 g, 0.38 mmol) was dissolved in ethanol (10 cm³) in the presence of platinum oxide (0.02 g). The solution was then shaken under hydrogen (50 psi) at room temperature. After 4 days analysis by electrospray mass spectrometry indicated that complete conversion to the desired compound had occurred. The solution was filtered and solvent removed under reduced pressure to yield a colourless crystalline solid (0.52 g, 0.37 mmol, 96 %).

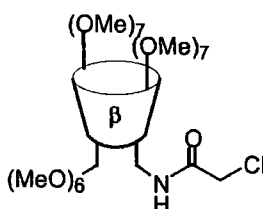
R_f=0.20 (10:1 CHCl₃:MeOH, silica).

m/e (ES⁺): 1414 [M+H]⁺.

mp: 91-93°C (lit. 91-93°C).⁶

δ_{H} (CDCl₃): 5.12 (d, J=3.4, 7H, C(1)-H), 3.95-2.95 (m, 104H), of which 3.38 (s), 3.50 (s) and 3.64 (s) are for OCH₃ groups.

6^A-(Chloromethylcarbamoyl)-6^A-deoxy-heptakis-(2,3-di-O-methyl)-6^B,6^C,6^D,6^E,6^F,6^G-hexa-O-methyl- β -cyclodextrin (32**).**



Mono-6-amino-6-deoxy-per-O-methyl- β -cyclodextrin (**31**) (3.2 g, 2.26 mmol) and triethylamine (0.34 g, 3.36 mmol) were dissolved in ether (100 cm³) and cooled to -30°C. Chloroacetylchloride (**33**) (0.38 g, 3.36 mmol) was added and the solution stirred at -30°C for 1 hour and at room temperature for a further hour. The solvent was removed under reduced pressure to yield an orange solid which was purified by column chromatography (CH₂Cl₂, then 5% MeOH/CH₂Cl₂, silica) to yield a glassy yellow solid (2.93 g, 1.97 mmol, 87 %).

$R_f=0.73$ (10:1 CHCl_3 :MeOH, silica).

m/e (ES-): 1524 [$\text{M}+\text{Cl}$ ($2\times^{35}\text{Cl}$)], 1525, 1526, 1527, 1528, 1529.

mp: 85-87°C.

δ_{H} (CD_3OD): 5.12 (d, $J=3.4$, 7H, C(1)-H), 4.09 (s, 2H, CH_2Cl), 4.00-2.95 (m, 102H), of which 3.34 (s), 3.48 (s) and 3.61 (s) are for OCH_3 groups.

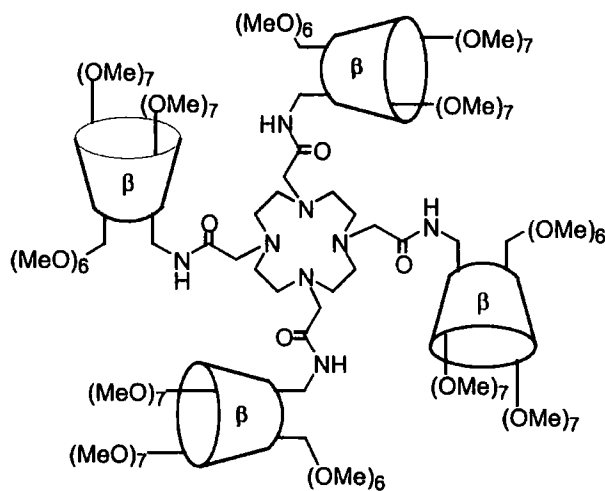
δ_{C} (CD_3OD): 99.5 (C(1)), 83.5, 83.2, 80.8, 72.8, 72.3, 61.8 (O- $\underline{\text{C}}\text{H}_3$), 59.4 (O- $\underline{\text{C}}\text{H}_3$), 59.0 (O- $\underline{\text{C}}\text{H}_3$).

^{13}C NMR partial analysis is consistent with a lack of C_7 symmetry within the molecule.

ν_{max} : 2930, 2830, 1690 (C=O), 1156, 1030, 968, cm^{-1} .

Found: C: 51.3%, H: 7.60%, N: 0.71%, Cl: 2.69%. $\text{C}_{64}\text{H}_{112}\text{O}_{35}\text{NCl}$ requires C: 51.6%, H: 7.57%, N: 0.94%, Cl: 2.38%.

1, 4, 7, 10-tetrakis-[6^A-deoxy-heptakis-(2,3-di-O-methyl)-6^B,6^C,6^D,6^E,6^F,6^G-hexa-O-methyl- β -cyclodextrin-6^A-acetamido]-1, 4, 7, 10-tetraazacyclododecane (25).



1,4,7,10-tetraazacyclododecane (**34**) (0.026 g, 0.15 mmol), potassium carbonate (0.10 g, 0.72 mmol) and potassium iodide (1 crystal, cat.) were dissolved in anhydrous DMF (1 cm^3) and heated to 60°C. Mono-6-(chloromethylcarbamoyl)-6-deoxy-per-O-methyl- β -cyclodextrin (**32**) (1.00 g, 0.67 mmol), dissolved in further DMF (1 cm^3), was added and the solution stirred at 60°C for 5 days. The solvent was removed under reduced pressure and the solid residue dissolved in water (10 cm^3) and placed in benzoylated dialysis tubing. The sealed tubing was placed in water

(2000 cm³) and allowed to stand. After 2 days the solution within the tubing was removed and solvent removed under reduced pressure.

Purification by column chromatography (98% CH₂Cl₂, 1.8% MeOH, 0.2% NH₃, rising to 95% CH₂Cl₂, 4.5% MeOH, 0.5% NH₃, silica) gave the tetraamide as a glassy yellow solid (0.16 g, 0.027 mmol, 18 % yield)

R_f=0.20 (90% CH₂Cl₂, 9% MeOH, 1% NH₃, silica).

m/e (ES⁺): 2024 [M+Y]³⁺. Ytterbium nitrate was added to improve ionisation of the 3⁺ ion.

(MALDI-TOF): 5987 [M+H]⁺.

mp: 132-136°C.

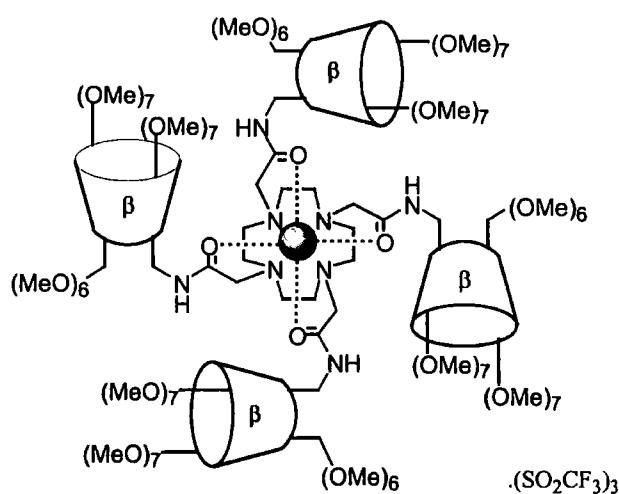
δ_H(CDCl₃): 5.35-5.00 (m, 28H, C(1)-H), 4.05-2.50 (m, 436H), of which 3.37 (s), 3.48 (s) and 3.62 (s) are for OCH₃ groups.

δ_C(CD₃OD): 100-97 (C(1)), including 99.0, 82.5-79, including 83.0, 82.6, 80.4, 79.7, 74-70, including 72.2, 71.8, 63-57, including 61.3, 60.9, 58.9, 58.5.

¹³C spectra consistent with lack of C₇ symmetry within the molecule.

Found: C: 50.0%, H: 7.44%, N: 1.95%. C₂₆₄H₄₆₄O₁₄₀N₈.18H₂O requires C: 50.2%, H: 7.98%, N: 1.77%.

Lanthanide complexes of ligand (25).



[Eu.25]³⁺

The ligand (**25**) (0.052 g, 8.7 mmol) was dissolved in anhydrous, freshly distilled, acetonitrile (1 cm³). Europium trifluoromethanesulfonate (0.008 g, 12.6 mmol) was added and the solution stirred at 70°C for 24 hours. Solvent was removed under reduced pressure, the solid residue was taken up in water (3 cm³) and purified through benzoylated dialysis tubing for 3 days. Solvent was removed under reduced pressure.

Column chromatography using a 0.5cm depth of silica (100% CH₂Cl₂, then 90% CH₂Cl₂, 9% MeOH, 1% NH₃, silica) gave the complex as a white solid (0.022 g, 3.3 mmol, 39 %).

Analysis by uv absorption showed the presence of unknown chromophores at 260nm and 340nm. The complex was dissolved in an aqueous solution of tetraethylammonium perchlorate (4 x 10⁻³M, 5 cm³) and placed in benzoylated dialysis tubing. The sealed tubing was placed in an aqueous solution of tetraethylammonium perchlorate (4 x 10⁻³M, 1000 cm³) and stirred for 3 days. The solution within the tubing was then removed and solvent removed under reduced pressure. Analysis by uv absorption showed the presence of no significant chromophore within the range 250-600nm.

m/e (ES⁺): 3070 [M.Eu+H]²⁺, 3146 [M.Eu+SO₃CF₃]²⁺.

mp: 130-133°C

δ_H(CD₃OD): 23.1 (s, 4H, H_{ax}), 9.0-1.0 (m, 438H), 0.0 (s, 2H, C(6^A)H₂), -3.8 (s, 4H, H_{eq}), -4.2 (s, 4H, H'_{ax}), -8.8 (s, 4H, H'_{eq}), -9.3 (s, 4H, CHCO), -12.0 (s, 4H, CH'CO).

¹H spectra consistent with a lack of C₇ symmetry within the complex and with line broadening due to presence of coordinated Eu³⁺ ion.

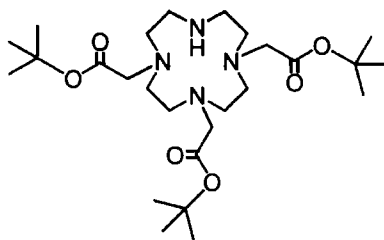
[Tb.25]³⁺.

The terbium complex was prepared and isolated in a similar manner to that described above for the europium complex, from the ligand **(16)** (0.050 g, 8.3 mmol) and terbium trifluoromethanesulfonate (0.008 g, 13.2 mmol). (Yield=0.045 g, 82 %).

m/e (ES⁺): 3074 [M.Eu+H]²⁺.

mp: 149-151°C.

1, 4, 7-Tris(*t*-butoxycarbonylmethyl)-1, 4, 7, 10-tetraazacyclododecane (35).



1, 4, 7-Tris(*t*-butoxycarbonylmethyl)-1, 4, 7, 10-tetraazacyclododecane **(35)** was prepared as described by Woods.⁷ 1, 4, 7, 10-tetraazacyclododecane **(34)** (1.13 g, 6.7 mmol) and sodium hydrogen carbonate (2.20 g, 26.2 mmol) were dissolved in freshly distilled acetonitrile (10 cm³), degassed and chilled (2°C). A solution of *t*-butylbromoacetate **(36)** (3.0 cm³, 18.2 mmol) in freshly distilled, degassed acetonitrile (30 cm³) was added by cannula transfer and the solution stirred at room temperature. After 18 hours solvent was removed under reduced pressure and the resulting solid purified by column chromatography (CH₂Cl₂, then 30%THF/CH₂Cl₂, then 5%MeOH, 5% NH₃, 30% CH₂Cl₂, 60% THF, silica) to give a white crystalline solid (1.06 g, 2.1 mmol, 33 %).

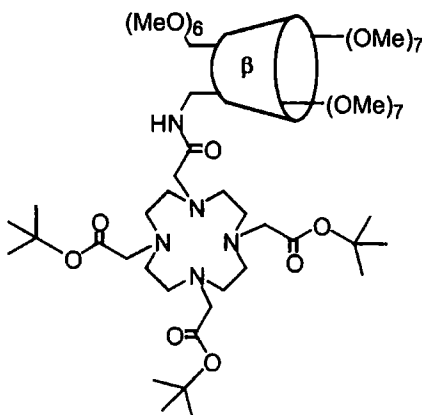
R_f=0.47 (5% MeOH, 5% NH₃ (aq), 30%CH₂Cl₂, 60% THF, silica).

m/e (ES⁺): 515 [M+H]²⁺.

δ_H(CDCl₃): 3.34 (s, 4H, -CH₂CO₂R), 3.26 (s, 2H, -CH₂CO₂R), 2.95 (br m, 16H, CH₂ cyclen ring), 1.42 (s, 27H, -C(CH₃)₃).⁷

$\delta_{\text{C}}(\text{CDCl}_3)$: 172.2 (2 x $-\text{CO}_2\text{R}$), 171.4 ($-\text{CO}_2\text{R}$), 83.8 ($\text{C}(\text{CH}_3)_3$), 83.6 (2 x $\text{C}(\text{CH}_3)_3$), 60.4 (CH_2 cyclen ring), 53.6 (CH_2 cyclen ring), 53.1 (CH_2 cyclen ring), 51.2 ($-\text{CH}_2\text{CO}_2\text{R}$), 50.4 ($-\text{CH}_2\text{CO}_2\text{R}$), 49.5 (CH_2 cyclen ring), 30.2 (9 x CH_3).⁷

1-[6^A-Deoxy-heptakis-(2,3-di-O-methyl)-6^B,6^C,6^D,6^E,6^F,6^G-hexa-O-methyl- β -cyclodextrin-6^A-acetamido]-4, 7, 10-tris(*t*-butoxycarbonylmethyl)-1, 4, 7, 10-tetraazacyclododecane (37).



1, 4, 7-Tris(*t*-butoxycarbonylmethyl)-1, 4, 7, 10-tetraazacyclododecane (**35**) (0.54 g, 1.0 mmol) and caesium carbonate (0.66 g, 2.0 mmol) were stirred under argon in freshly distilled acetonitrile (20 cm³) for 5 minutes. Mono-6-(chloromethylcarbomoyl)-6-deoxy-per-O-methyl- β -cyclodextrin (**32**) (1.55 g, 1.0 mmol) was added and the solution stirred at 50°C for 3 days. Solvent was removed under reduced pressure and the resulting solid purified by column chromatography (CH_2Cl_2 to 4%MeOH/ CH_2Cl_2 , silica) to give an off-white solid (0.914 g, 0.46 mmol, 45 %).

$R_f=0.18$ (10% MeOH/ CH_2Cl_2 , silica).

m/e (ES⁺): 1004 [$\text{M}+2\text{NH}_4$]²⁺.

m/e (MALDI-TOF⁺): 2007 [$\text{M}+\text{K}$]⁺.

mp: 118-120°C.

$\delta_{\text{H}}(\text{CDCl}_3)$: 5.1-5.0 (m, 7H, C(1)-H), 4.0-3.0 (m, 127H, of which 3.60, 3.58, 3.47, 3.46 and 3.35 are for OCH_3 groups), 1.43 (s, 18H, $\text{C}(\text{CH}_3)_3$), 1.41 (s, 9H, $\text{C}(\text{CH}_3)_3$).

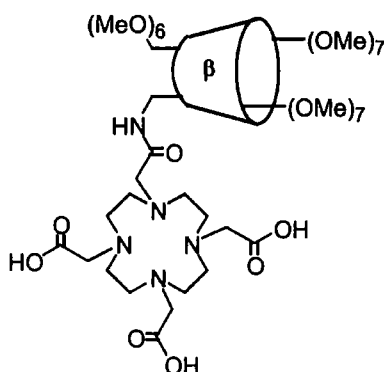
$\delta_{\text{C}}(\text{CDCl}_3)$: 172.3 ($\text{C}(\text{O})\text{O}^t\text{Bu}$), 171.8 ($\text{C}(\text{O})\text{O}^t\text{Bu}$), 99.0-97.9 (C(1), including 99.0, 98.9, 98.8, 98.6, 98.0), 82.4-79.6 (including 82.3, 82.1, 82.0, 81.9, 81.7, 81.5, 81.4,

80.6, 80.3, 80.0, 79.9, 79.6), 71.3-70.8 (including 71.3, 71.2, 71.0, 70.9, 70.8), 61.5-61.0 (including 61.5, 61.4, 61.3, 61.2, 61.1), 59.8, 59.0-58.1 (including 59.0, 58.9, 58.8, 58.5, 58.3, 58.2, 58.1), 55.7, 28.0, 27.8.

ν_{\max} : 2906, 2832, 1725, 1154, 1093, 1011 cm^{-1} .

Found: C: 50.2%, H: 7.83%, N: 2.86%. $\text{C}_{90}\text{H}_{161}\text{N}_5\text{O}_{41} \cdot 3\text{CH}_2\text{Cl}_2$ requires C: 50.2%, H: 7.57%, N: 3.15%.

1-[6^A-Deoxy-heptakis-(2,3-di-O-methyl)-6^B,6^C,6^D,6^E,6^F,6^G-hexa-O-methyl- β -cyclodextrin-6^A-acetamido]-4, 7, 10-tris(carboxymethyl)-1, 4, 7, 10-tetraazacyclododecane (26).



1-[6^A-deoxy-heptakis-(2,3-di-O-methyl)-6^B,6^C,6^D,6^E,6^F,6^G-hexa-O-methyl- β -cyclodextrin-6^A-acetamido]-4, 7, 10-tris(*t*-butoxycarbonylmethyl)-1, 4, 7, 10-tetraazacyclododecane (**37**) (0.89 g, 0.45 mmol) was dissolved in trifluoroacetic acid (10 cm^3) and stirred at room temperature for 24 hours. Solvent was removed under reduced pressure to yield an off-white solid (0.81 g, 0.45 mmol, 100 %).

$R_f=0.00$ (10% MeOH/ CH_2Cl_2 , silica).

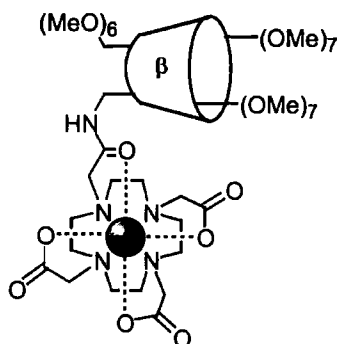
m/e (MALDI-TOF+): 1801 $[\text{M}+\text{H}]^+$, 1823 $[\text{M}+\text{Na}]^+$, 1839 $[\text{M}+\text{K}]^+$.

mp: 87-94°C.

δ_{H} (CDCl_3): 4.90-5.70 (m, 7H, C(1)-H), 2.90-4.30 (m, 130H) of which 3.64 (s), 3.50 (s) and 3.32 (s) are for OCH_3 groups.

ν_{\max} : 2934, 2042, 1736, 1676 (C=O), 1466, 1364, 1151, 1090, 1030, 970, 916, 796 cm^{-1} .

Lanthanide complexes of ligand 1-[6^A-deoxy-heptakis-(2,3-di-O-methyl)-6^B,6^C,6^D,6^E,6^F,6^G-hexa-O-methyl- β -cyclodextrin-6^A-acetamido]- 4, 7, 10-tris(carboxymethyl)-1, 4, 7, 10-tetraazacyclododecane (26).



[Tb.26].

1-[6^A-Deoxy-heptakis-(2,3-di-O-methyl)-6^B,6^C,6^D,6^E,6^F,6^G-hexa-O-methyl- β -cyclodextrin-6^A-acetamido]- 4, 7, 10-tris(carboxymethyl)-1, 4, 7, 10-tetraazacyclododecane (**26**) (0.33 g, 0.18 mmol) was dissolved in Purite water (10 cm³) and the pH adjusted to 4.2 with the addition of 0.1M aqueous potassium hydroxide solution. Terbium nitrate pentahydrate (0.25 g, 0.59 mmol) was added and the solution readjusted to a pH of 4.8. The solution was stirred at 60°C for 18 hours, poured into methanol (20 cm³) and extracted into dichloromethane (2 x 50 cm³). Solvent was removed to yield a pale yellow solid (0.29 g, 0.15 mmol, 79 %).

m/e (MALDI-TOF+): 1980 [M+Na]⁺.

mp: 180-182°C.

δ_{H} (CD₃OD, 20°C, 65MHz): 310-210 (br m, 4H, NCHCO), 170-120 (br m, 4H, H'_{ax}), 70-40 (br m, 4H, NCH'CO), 50- -20 (m, 110H), -40- -160 (m, 8H, H_{eq} and H'_{eq}), -370- -440 (br m, 4H, H_{ax}).

[Eu.26].

1-[6^A-Deoxy-heptakis-(2,3-di-O-methyl)-6^B,6^C,6^D,6^E,6^F,6^G-hexa-O-methyl- β -cyclodextrin-6^A-acetamido]- 4, 7, 10- tris(carboxymethyl)-1, 4, 7, 10-tetraazacyclododecane (**26**) (0.15 g, 0.08 mmol) was dissolved in Purite water

(8 cm³) and the pH adjusted to 4.2 with the addition of 0.1M aqueous potassium hydroxide solution. Europium nitrate pentahydrate (0.12 g, 0.28 mmol) was added and the solution readjusted to a pH of 5.3. The solution was stirred at 60°C for 18 hours, poured into methanol (20 cm³) and extracted into dichloromethane (2 x 50 cm³). Solvent was removed to yield a white crystalline solid (0.09 g, 0.04 mmol, 55 %).

m/e (MALDI-TOF+): 1973 [M+Na]⁺, 1989 [M+K]⁺.

mp: 164-166°C.

δ_{H} (CD₃OD, 20°C): 39.2 (s, 0.5H, H_{ax}), 38.8 (s, 0.5H, H_{ax}), 36.2 (s, 0.5H, H_{ax}), 36.0 (s, 0.5H, H_{ax}), 35.0 (s, 1H, H_{ax}), 34.0 (s, 1H, H_{ax}), 10.0-0.0 (m, 110H), 0- -8 (m, 8H, H_{eq} and H'_{eq}), -10.9 (s, 0.5H, CHCO), -11.3 (s, 0.5H, CHCO), -12.5- -15.5 (m, 4H, H'_{ax}), -17.0 (s, 0.5, CH'CO), -17.3 (s, 0.5, CH'CO), -17.5- -19.1 (m, 6H, CHCO and CH'CO).

[Gd.26].

1-[6^A-Deoxy-heptakis-(2,3-di-O-methyl)-6^B,6^C,6^D,6^E,6^F,6^G-hexa-O-methyl- β -cyclodextrin-6^A-acetamido]- 4, 7, 10- tris(carboxymethyl)-1, 4, 7, 10-tetraazacyclododecane (**26**) (0.37 g, 0.20 mmol) was dissolved in Purite water (10 cm³) and the pH adjusted to 4.5 with the addition of 0.1M aqueous potassium hydroxide solution. Gadolinium nitrate hexahydrate (0.24 g, 0.53 mmol) was added and the solution readjusted to a pH of 5.0. The solution was stirred at 60°C for 18 hours, filtered and partitioned between water and dichloromethane. The aqueous fraction was removed and solvent removed under reduced pressure. The residual solid was taken up in minimum water and purified by dialysis (2000 MWCO filter) for 2 days. Solvent was removed under reduced pressure to yield a white glassy solid (0.175 g, 0.09 mmol, 44 %).

m/e (ES⁺, H₂O): 978 [M+2H]²⁺, 985 [M+H+NH₄]²⁺.

mp: 242°C (dec.).

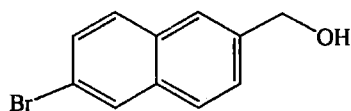
[Yb.26].

1-[6^A-Deoxy-heptakis-(2,3-di-O-methyl)-6^B,6^C,6^D,6^E,6^F,6^G-hexa-O-methyl- β -cyclodextrin-6^A-acetamido]-4,7,10-tri-acetic acid-1,4,7,10-tetraazacyclododecane (**26**) (0.36 g, 0.20 mmol) was dissolved in Purite water (5 cm³) and the pH adjusted to 4.2 with the addition of 0.1M aqueous potassium hydroxide solution. Ytterbium nitrate pentahydrate (0.50 g, 1.11 mmol) was added and the solution readjusted to a pH of 4.8. The solution was stirred at 60°C for 18 hours, filtered and partitioned between water and dichloromethane. The aqueous fraction was removed and solvent removed under reduced pressure. The residual solid was taken up in minimum water and purified by dialysis (1000 MWCO filter) for 2 days. Solvent was removed under reduced pressure to yield a white glassy solid (0.318 g, 0.16 mmol, 81 %).

m/e (ES⁺, H₂O): 1998 [M+NH₄], 994 [M+H+NH₄]²⁺.

mp: 210°C (dec.).

δ_{H} (CD₃OD, 20°C, 65MHz): 140-120 (br m, 4H, H_{ax}), 36- -16 (m, 118H, of which 4.88 (s), 3.46 (s) and 3.30 (s) are for OCH₃), -22- -60 (br m, H'_{ax}, 4H), -60- -95 (br m, 8H, CH₂CO).

5.3 Experimental for Chapter 3.**6-(2-Bromonaphthyl)methanol (62).**

2-Bromo-6-naphthoic acid (**61**) (5.24 g, 20.9 mmol) was dissolved in anhydrous THF (200 cm³) and chilled to 0°C under argon. Borane-dimethyl sulfide complex (5.61 g, 73.8 mmol) was added and the solution stirred at 0°C for 2 hours and at room temperature for a further 24 hours. Residual borane was quenched with the cautious addition of methanol (30 cm³) and solvent removed under reduced pressure. The resulting solid was taken up in HCl solution (300 cm³, 1M in methanol) and stirred

under reflux for 12 hours. The solution was cooled and solvent removed under reduced pressure. The resulting solid was recrystallised from aqueous methanol to give a white crystalline solid (4.19 g, 17.7 mmol, 85 %).

$R_f=0.45$ (10% MeOH/CH₂Cl₂, silica).

m/e (EI⁺): 236 [M]⁺.

mp: 122-125°C.

δ_H (CDCl₃): 8.00 (d, $J=1.6$, 1H, C(1)-H), 7.79 (s, 1H, C(5)-H), 7.75 (d, $J=8.4$, 1H, C(8)-H), 7.70 (d, $J=9.0$, 1H, C(4)-H), 7.55 (dd, $J_1=8.7$, $J_2=2.1$, 1H, C(3)-H), 7.30 (dd, $J_1=8.5$, $J_2=1.6$, 1H, C(7)-H), 4.85 (s, 2H, CH₂-OH), 1.82 (br s, 1H, CH₂-OH).

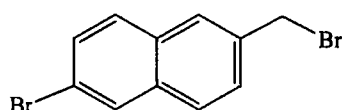
δ_C (CDCl₃): 139.0 (C(2)), 134.2 (C(9)), 132.0 (C(10)), 130.0 (C(1)), 129.8, 129.8, 127.0 (C(8)), 126.4 (C(7)), 125.5 (C(5)), 120.1 (C(6)), 65.5 (Ar-CH₂OH).

ν_{max} : 3500-3000 (br, OH), 2918, 2855, 1588, 1498, 1460, 1357, 1252, 1163, 1127, 1013, 883, 822, 741, 639, 481, cm⁻¹.

Found: C: 55.5%, H: 3.69%, Br: 33.8%. C₁₁H₉BrO requires C: 55.7%, H: 3.83%, Br: 33.7%.

λ_{max} (CH₃OH): 277nm, $\epsilon = 2130M^{-1}cm^{-1}$.

2-Bromo-6-bromomethylnaphthalene (63).



6-(2-Bromonaphthyl)methanol (**62**) (1.94 g, 8.2 mmol) was dissolved in a solution of HBr in acetic acid (33 %, 50 cm³) and stirred under reflux for 1 hour. Solvent was removed under reduced pressure, aliquots (3 x 50 cm³) of toluene being added to aid removal of residual acetic acid by formation of an azeotrope. The resulting solid was taken up in dichloromethane (100 cm³) and washed with potassium hydroxide solution (1M, 50 cm³) and water (50 cm³). The organic fraction was removed and solvent removed under reduced pressure to give a brown solid (2.36 g, 7.9 mmol, 96 %).

$R_f=0.61$ (25% $\text{CH}_2\text{Cl}_2/n$ -Hexane, silica).

m/e (EI+): 298 $[\text{M}]^+$.

mp: 108-112°C (lit. 124-125).⁸

$\delta_{\text{H}}(\text{CDCl}_3)$: 7.98 (d, $J=1.5$, 1H, C(1)-H), 7.78 (s, 1H, C(5)-H), 7.72 (d, $J=8.7$, 1H, C(8)-H), 7.66 (d, $J=9.0$, 1H, C(4)-H), 7.60-7.50 (m, 2H), 4.63 (s, 2H, $\text{CH}_2\text{-Br}$).

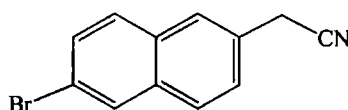
$\delta_{\text{C}}(\text{CDCl}_3)$: 135.9 (C(2)), 134.3 (C(9)), 131.8 (C(10)), 130.1 (C(1)), 130.0, 129.8, 128.1 (C(8)), 128.1 (C(7)), 128.0 (C(5)), 120.9 (C(6)), 33.9 (Ar- CH_2Br).

ν_{max} : 2956, 2922, 2850 (C-H), 1776, 1558 (Ar-H), 1493, 1464, 1436, 1336, 1251, 1209, 1195, 1131, 1059, 897, 886, 822, 806, 734, 666, 595, 478, cm^{-1} .

Found: C: 44.0%, H: 2.92%, Br: 50.8%. $\text{C}_{11}\text{H}_8\text{Br}_2 \cdot 2 \frac{1}{2} \text{CH}_3\text{OH}$ requires C: 43.8%, H: 3.09%, Br: 51.1%.

λ_{max} (CH_3OH): 280nm, $\epsilon = 7660\text{M}^{-1}\text{cm}^{-1}$.

6-(2-Bromonaphthyl)acetonitrile (64).



2-Bromo-6-bromomethylnaphthalene (**63**) (1.66 g, 5.5 mmol) and sodium cyanide (0.36 g, 7.3 mmol) were stirred in anhydrous dimethyl sulfoxide (20 cm^3) at 60°C for 18 hours. The solution was poured into water (50 cm^3) and extracted into dichloromethane (3 x 50 cm^3). The combined organic extracts were washed with water (50 cm^3) and solvent removed under reduced pressure. The resulting solid was purified by chromatatron chromatography (2mm silica plate, 30% $\text{CH}_2\text{Cl}_2/n$ -Hexane) to give a yellow crystalline solid (1.08 g, 4.38 mmol, 79 %).

$R_f=0.15$ (50% $\text{CH}_2\text{Cl}_2/n$ -Hexane, silica).

m/e (EI+): 245 $[\text{M}]^+$.

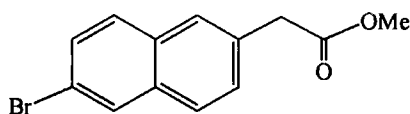
$\delta_{\text{H}}(\text{CDCl}_3)$: 7.99 (d, 1H, $J=6$, C(1)-H), 7.78 (s, 1H, C(5)-H), 7.75 (d, 1H, $J=8.7$, C(8)-H), 7.69 (d, 1H, $J=8.7$, C(4)-H), 7.58 (dd, 1H, $J_1=8.7$, $J_2=1.8$, C(3)-H), 7.40 (dd, 1H, $J_1=8.4$, $J_2=1.8$, C(7)-H), 3.89 (s, 2H, Ar- CH_2CN).

$\delta_{\text{C}}(\text{CDCl}_3)$: 132.6 (C(2)), 130.6 (C(9)), 129.9 (C(10)), 129.1 (C(1)), 128.7, 128.2, 127.1 (C(8)), 125.7 (C(7)), 125.5 (C(5)), 122.9 (C(6)), 119.5 (C \equiv N), 22.8 (Ar-CH₂CN).

Satisfactory elemental analysis was not obtained for this compound.

ν_{max} : 3069, 2947, 2913, 2247 (C=N), 1948, 1758, 1684, 1582, 1500, 1459, 1398, 1337, 1256, 1052, 923, 867, 821, 766, 740, 644, 475 cm⁻¹.

6-(2-Bromonaphthyl)acetic acid methyl ester (65).



6-(2-Bromonaphthyl)acetonitrile (**64**) (2.25 g, 9.1 mmol) was dissolved in anhydrous methanol (250 cm³) and HCl (g) bubbled through the solution for 1 hour. The solution was boiled under reflux for 20 hours under argon then solvent was removed under reduced pressure. The resulting solid was taken up in dichloromethane (100 cm³), washed with aqueous HCl solution (1M, 50 cm³) and solvent removed under reduced pressure to yield a yellow solid (2.26 g, 8.1 mmol, 89 %).

R_f = 0.38 (CH₂Cl₂, silica).

m/e (EI⁺): 278 [M]⁺.

mp: 52-54°C (lit 67-69).⁸

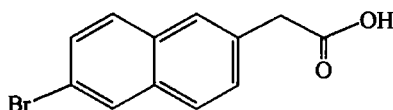
$\delta_{\text{H}}(\text{CDCl}_3)$: 7.98 (d, 1H, $J=1.5$, C(1)-H), 7.72 (d, 1H, $J=8.7$, C(8)-H), 7.71 (s, 1H, C(5)-H), 7.67 (d, 1H, $J=8.7$, C(4)-H), 7.54 (dd, 1H, $J_1=8.9$, $J_2=2.0$, C(3)-H), 7.45 (dd, 1H, $J_1=8.4$, $J_2=1.8$, C(7)-H), 3.78 (s, 2H, Ar-CH₂-CO₂Me), 3.72 (s, 3H, CO₂CH₃).

$\delta_{\text{C}}(\text{CDCl}_3)$: 172.0 (CO₂Me), 133.8 (C(2)), 132.3 (C(9)), 132.1 (C(10)), 129.9 (C(1)), 129.8, 129.6, 128.7 (C(8)), 128.2 (C(7)), 127.6 (C(5)), 120.0 (C(6)), 52.4 (CO₂CH₃), 41.5 (Ar-CH₂-CO₂Me).

ν_{max} : 2961, 2927, 2848, 1734 (C=O), 1584, 1494, 1432, 1311, 1246, 1196, 1006, 885, 807, 724, 638, 472 cm⁻¹.

Satisfactory elemental analysis was not obtained for this compound.

λ_{max} (CH₃OH): 276nm, $\epsilon = 2990\text{M}^{-1}\text{cm}^{-1}$.

6-(2-Bromonaphthyl) acetic acid (66).

6-(2-(Bromonaphthyl)acetic acid methyl ester (**65**) (0.08 g, 0.29 mmol) was dissolved in a solution of methanol (10 cm³) and aqueous sodium hydroxide (1M, 10 cm³) and stirred at room temperature for 24 hours. The pH of the solution was lowered to approximately 1 by the addition of concentrated aqueous hydrochloric acid (0.5 cm³), the solution was then extracted into dichloromethane (3 x 20 cm³). Solvent was removed under reduced pressure to yield a yellow crystalline solid (0.07 g, 0.26 mmol, 92 %).

$R_f = 0.59$ (10% MeOH/CH₂Cl₂, silica).

m/e (EI⁺): 264 [M]⁺.

Found (EI⁺): 265.9759. C₁₂H₉⁸¹BrO₂ requires 265.9766.*

mp: 160-164°C (lit 175-176).⁸

δ_H (CDCl₃): 8.01 (s, 1H, C(1)-H), 7.78-7.69 (m, 3H, Ar-H), 7.52 (dd, 1H, J₁=8.9, J₂=1.6, C(3)-H), 7.45 (d, 1H, J=8.4, C(7)-H), 3.82 (s, 2H, Ar-CH₂-CO₂H).

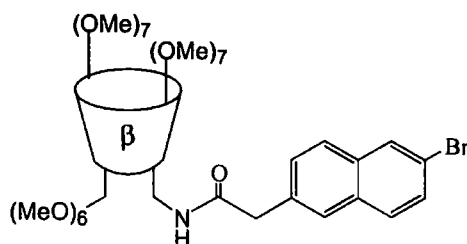
δ_C (CD₃OD): 174.0 (CH₂C=O), 133.8 (C(2)), 133.3 (C(9)), 132.2 (C(10)), 129.5 (C(1)), 129.4, 129.2, 128.7 (C(8)), 127.8 (C(7)), 127.0 (C(5)), 119.3 (C(6)), 40.8 (CH₂CO₂H).

ν_{max} : 3400-2800 (br, OH), 2928, 2852, 1693 (C=O), 1588, 1498, 1462, 1321, 1253, 1229, 1198, 1063, 877, 810, 481 cm⁻¹.

λ_{max} (THF): 276nm, $\epsilon = 3390M^{-1}cm^{-1}$.

* ⁸¹Br isotope measured due to interference by reference compound at m/z 264.

6^A-[6²-(2⁷-Bromonaphthyl)methylcarbamoyl]-6^A-deoxy-heptakis-(2,3-di-O-methyl)-6^B,6^C,6^D,6^E,6^F,6^G-hexa-O-methyl-β-cyclodextrin (57).



6-2-(Bromonaphthyl)acetic acid (**66**) (0.50 g, 1.89 mmol) was dissolved in oxalyl chloride (10 cm³). Dimethylformamide (1 drop) was added and the solution stirred under argon at room temperature for 2 hours. Oxalyl chloride was removed under reduced pressure and the residual solid dissolved in dichloromethane (20 cm³) and added to a chilled (~0°C) solution of mono-6-amino-6-deoxy-per-O-methyl-β-cyclodextrin (**31**) (1.00 g, 0.71 mmol) and potassium carbonate (0.30 g, 2.2 mmol) in dichloromethane (5 cm³). The solution was allowed to warm to room temperature and stirred under argon. After 18 hours solvent was removed under reduced pressure. The residual solid was purified by column chromatography to give a white solid (0.21 g, 0.17 mmol, 18 %).

R_f = 0.36 (10% MeOH/CH₂Cl₂, silica).

m/e (ES⁺): 1684 [M+Na]⁺, 853 [M+2Na]²⁺.

mp: 56-58°C.

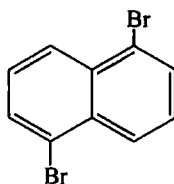
δ_H(CDCl₃): 7.95 (d, 1H, J=2.0, C(1')-H), 7.70 (d, 1H, J=8.2, C(8')-H), 7.67 (s, 1H, C(5')-H), 7.64 (d, 1H, J=8.8, C(4')-H), 7.52 (dd, 1H, J₁=8.8, J₂=2.0, C(3')-H), 7.40 (dd, 1H, J₁=8.2, J₂=1.8, C(7')-H), 5.20-4.70 (m, 7H, C(1)-H), 4.0-3.0 (m, 105H, of which 3.66 (s), 3.52 (s) and 3.39 (s) are for O-CH₃).

δ_C(CDCl₃): 170.8 (CONH), 133.7, 133.6, 132.2, 130.0 (C(1') and C(3')), 129.5 (C(4')), 128.6 (C(7')), 128.2 (C(5')), 127.9 (C(8')), 120.1 (C(2')), 100-98 (m, , inc 99.3, 99.2, C(1)-H), 83-80 (m, inc 82.3, 82.0, 80.5), 72-70 (m, inc 71.3, 71.1), 62-58 (m, inc 61.7, 59.3, 59.2, 58.6), 44.2 (CH₂NHCO), 40.3 (ArCH₂-).

ν_{max}: 2922, 2886, 2832, 1660 (C=O), 1442, 1139, 1017, 967, 908, 854, 727 cm⁻¹.

Satisfactory elemental analysis was not obtained for this compound.

λ_{max} (MeOH): 278nm, ε = 6970M⁻¹cm⁻¹.

1,5-Dibromonaphthalene (68).**Method 1**

1,5-Dibromonaphthalene (**68**) was prepared as described by Hodgson and Whitehurst.⁹ 1,5-Diaminonaphthalene (**69**) (5.80 g, 36 mmol) was dissolved in sulfuric acid (200 cm³, 50 % in water) and chilled to -20°C (CO₂/propan-2-ol). Sodium nitrite (9.09 g, 130 mmol) in water (50 cm³) was added and the solution stirred at -20°C for 30 minutes. Copper bromide (20.4 g, 140 mmol) in hydrobromic acid (100 cm³) was added and the solution allowed to warm to room temperature. Small aliquots of diethyl ether were added to reduce foaming. The solution was heated to 50°C for 1 hour then chilled to 0°C. Potassium hydroxide pellets were added until the pH of the solution exceeded 8, the temperature being maintained below 10°C. The precipitate formed was collected by vacuum filtration and the residual solid washed with hot tetrahydrofuran (~2000 cm³) until the extracts were colourless. Solvent was removed from the combined washes under reduced pressure and the resulting solid washed with hot dichloromethane (~1000 cm³) until the washing were colourless. Solvent was removed from the combined washes under reduced pressure and the residue purified by column chromatography (10% CH₂Cl₂/*n*-hexane, silica) to yield 1,5-dibromonaphthalene (**68**) as a yellow solid (7.06 g, 24.7 mmol, 67 %).

Method 2

1,5-Dibromonaphthalene (**68**) was also prepared by adaptation of a procedure described by Schaefer and Higgins.¹⁰ Dibromotriphenyl phosphorane (**72**) (25.1 g, 59.5 mmol) dissolved under argon in acetonitrile (100 cm³). 1,5-Dinaphthol (**71**) (4.50 g, 28 mmol) was added and the solution heated to 80°C for 1 hour. Solvent was removed under water aspirator pressure and the residual solid heated to *circa* 350°C

by use of a Woods metal bath until evolution of hydrogen bromide had ceased (*circa* 30 minutes). The molten residue was poured into a shallow basin to solidify, crushed to a fine powder and extracted into *n*-hexane (300 cm³) by Soxhlet extraction. Solvent was removed under reduced pressure and the residual solid purified by column chromatography (*n*-Hexane, silica) and recrystallised from boiling ethanol to give 1,5-dibromonaphthalene (**68**) as a white crystalline solid (2.29 g, 8.0 mmol, 28 %).

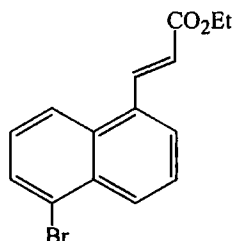
$R_f=0.29$ (*n*-Hexane, silica).

m/e (EI⁺): 284 [M]⁺.

δ_H (CD₃OD): 8.27 (d, 2H, $J=9$, C(4)-*H*), 7.85 (d, 2H, $J=7.5$, C(2)-*H*), 7.44 (dd, 2H, $J_1=8.4$, $J_2=7.5$, C(3)-*H*).¹¹

δ_C (CD₃OD): 133.0 (C(9)), 130.9 (C(2)), 127.4 (C(3)), 127.3 (C(4)), 123.0 (C(1)).¹²

Trans-ethyl-3'-[5-(1-bromonaphthyl)]propenoate (**75**).



1,5-Dibromonaphthalene (**68**) (2.29 g, 8.0 mmol), tri-*o*-tolylphosphine (0.14 g, 0.46 mmol) and palladium acetate (0.028 g, 0.13 mmol) were placed under argon and triethylamine (25 cm³) added. Ethyl acrylate (**74**) (1.11 g, 11.1 mmol) was added and the solution stirred under argon at 100°C for 18 hours. Solvent was removed under reduced pressure, the residual solid was taken up in dichloromethane (50 cm³) and washed with hydrobromic acid (1M, 50 cm³). Solvent was removed under reduced pressure and the resulting solid was purified by column chromatography (*n*-hexane - 30%CH₂Cl₂/*n*-hexane, silica) to give a white solid (1.13 g, 3.7 mmol, 46 %). Unreacted 1,5-dibromonaphthalene (**68**) was also recovered as a white crystalline solid (1.08g, 3.8mmol, 47%).

$R_f=0.23$ (50% $\text{CH}_2\text{Cl}_2/n$ -hexane, silica).

m/e (EI+): 304 [M]⁺.

Found (EI+): 304.0104. $\text{C}_{15}\text{H}_{13}\text{BrO}_2$ requires 304.0099.

mp: 50-51°C.

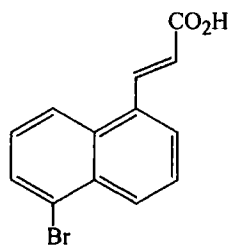
δ_{H} (CD_2Cl_2): 8.44 (d, 1H, $J=15.6$, ArCH=CH-), 8.32 (d, 1H, $J=8.4$, C(4)-H), 8.17 (d, 1H, $J=8.7$, C(8)-H), 7.84 (d, 1H, $J=7.2$, C(6)-H), 7.80 (d, 1H, $J=7.5$, C(2)-H), 7.60 (t, 1H, $J=8.0$, C(3)-H), 7.41 (t, 1H, $J=8.1$, C(7)-H), 6.51 (d, 1H, $J=15.9$, ArCH=CH-), 4.26 (q, 2H, $J=7.1$, OCH_2CH_3), 1.33 (t, 3H, $J=7.1$, OCH_2CH_3).

δ_{C} (CD_2Cl_2): 166.7 (C(5)), 141.2 (ArCH=CH₂-), 133.0, 132.9, 132.5 (C(1)), 130.8 (C(6)), 129.6 (C(4)), 127.3, 127.2, 126.2 (C(2)), 123.8 (C(8)), 122.4 (ArCH=CH₂-), 61.0 (OCH_2CH_3), 14.5 (CH_2CH_3).

ν_{max} : 3049, 2994, 1714 (C=O), 1631 (C=C), 1564, 1294, 1243, 1182, 1158, 1100, 975, 860, 775, 617, 539, 439 cm^{-1} .

λ_{max} (CH_3OH): 322nm, $\epsilon = 7310 \text{ M}^{-1}\text{cm}^{-1}$.

Trans-3'-[5-(1-bromonaphthyl)]propenoic acid (76).



Trans-ethyl- 3-[5-(1-bromonaphthyl)]propenoate (75) (0.89 g, 2.9 mmol) was dissolved in methanol (50 cm^3) and aqueous sodium hydroxide (20 cm^3 , 2M) added, followed by THF (20 cm^3) to ensure that a single phase formed. The solution was stirred for 18 hours at room temperature, chilled and acidified by the cautious addition of aqueous hydrochloric acid (5M). The resulting precipitate was collected by vacuum filtration and dried to give trans-3'-[5-(1-bromonaphthyl)]propenoic acid (76) as a white crystalline solid (0.77 g, 2.8 mmol, 95 %).

$R_f=0.19$ (10% THF/ CH_2Cl_2 , silica).

m/e (EI+): 276 [M]⁺.

Found (EI+): 275.9790. $\text{C}_{13}\text{H}_9\text{BrO}_2$ requires 275.9786.

mp: 251-255°C (lit. 269-270°C)¹³.

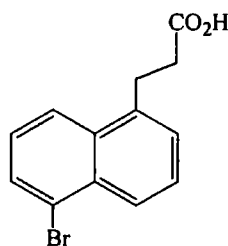
δ_{H} (d⁸-THF): 8.47 (d, 1H, J=16.0, ArCH=CH-), 8.32 (d, 1H, J=8.5, C(4)-H), 8.25 (d, 1H, J=8.5, C(8)-H), 7.93 (d, 1H, J=7.5, C(6)-H), 7.88 (d, 1H, J=7.5, C(2)-H), 7.65 (t, 1H, J=8.0, C(3)-H), 7.46 (t, 1H, J=8.0, C(7)-H), 6.57 (d, 1H, J=15.5, ArCH=CH).

δ_{C} (d⁸-THF): 164.8, 138.6 (ArCH=CH₂-), 131.2, 131.1, 130.5, 128.7 (C(2)), 127.1 (C(4)), 125.3, 125.2, 124.1 (C(6)), 121.8 (C(8)), 121.5, 120.9 (ArCH=CH₂).

ν_{max} : 3100-2400 (br, OH), 1678 (C=O), 1624 (C=C), 1557, 1499, 1427, 1319, 1252, 1207, 1099, 1032, 929, 866, 768, 709, 624 cm⁻¹.

λ_{max} (THF): 318nm, ϵ =20,350 M⁻¹cm⁻¹.

3'-[5-(1-Bromonaphthyl)]propanoic acid (78).



Trans-3'-[5-(1-bromonaphthyl)]propanoic acid (76) (0.44 g, 1.57 mmol) was dissolved in methanol (10 cm³) in the presence of triethylamine (1 cm³). The solution was flushed with hydrogen and (2S, 4S)-(-)-2,4-bis(diphenylphosphino)pentane(norbornadiene) rhodium (1) hexafluorophosphate (77) (0.022 g, 28 μ mol) added. The solution was shaken under hydrogen (40 psi) for 24 hours. Solvent was removed under reduced pressure and the resulting solid taken up in aqueous sodium hydroxide (0.1M, 10 cm³). The solution was taken to pH 1 by the addition of aqueous hydrochloric acid (0.1M) and the resulting precipitate collected by vacuum filtration and purified by column chromatography to give a white solid (0.259 g, 0.93 mmol, 59 %).

R_{f} =0.26 (10% THF/CH₂Cl₂, silica).

m/e (EI+): 278 [M]⁺.

Found (EI+): 277.9939. C₁₃H₁₁BrO₂ requires 277.9942.

mp: 160-163°C (lit. 170-171°C)¹⁴.

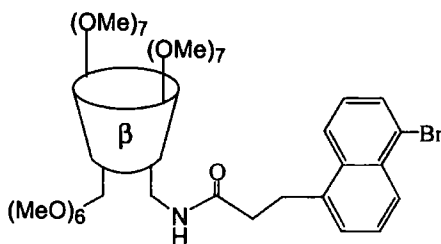
δ_{H} (d^8 -THF): 8.01 (d, 2H, $J=8.5$, C(4)-*H* & C(8)-*H*), 7.69 (d, 1H, $J=7.5$, C(2)-*H*), 7.39 (t, 1H, $J=7.5$, C(7)-*H*), 7.36 (d, 1H, $J=6.0$, C(6)-*H*), 7.28 (t, 1H, $J=7.8$, C(3)-*H*), 3.28 (t, 1H, $J=8.0$, ArCH₂-), 2.55 (t, 2H, $J=8.0$, -CH₂CO₂H).

δ_{C} (d^8 -THF): 173.1 (C=O), 138.2, 137.4, 133.4, 132.5, 129.9 (C(2)), 127.1, 126.3 (C(3)), 125.9, 125.2, 123.9, 34.6 (ArCH₂-), 28.2 (-CH₂CO₂H).

ν_{max} : 3000-2400 (br, OH), 2949, 2913, 1700 (C=O), 1429, 1389, 1297, 1216, 1193, 1152, 1012, 931, 858, 768, 609 cm⁻¹.

λ_{max} (THF): 291nm, $\epsilon = 9400\text{M}^{-1}\text{cm}^{-1}$.

6^A-[5²-(1²-Bromonaphthyl)ethylcarbamoyl]-6^A-deoxy-heptakis-(2,3-di-O-methyl)-6^B,6^C,6^D,6^E,6^F,6^G-hexa-O-methyl- β -cyclodextrin (58).



3'-[5-(1-Bromonaphthyl)]propanoic acid (**78**) (0.108 g, 0.387 mmol), mono-amino-per-O-methyl- β -cyclodextrin (**31**) (0.477 g, 0.337 mmol), EDC (0.12 g, 0.63 mmol), DMAP (0.10 g, 0.82 mmol) and 1-hydroxybenzotriazole (0.10 g, 0.74 mmol) were stirred in dichloromethane (10 cm³) under argon for 18 hours. Solvent was removed under reduced pressure. The residual solid was purified by column chromatography (CH₂Cl₂, to 2% MeOH/CH₂Cl₂, silica) to yield a glassy white solid (0.45 g, 0.82 mmol, 79 %).

$R_f=0.35$ (10% MeOH/CH₂Cl₂, silica).

m/e (ES⁺): 1692 [M+NH₄]⁺, 847 [M+H+NH₄]²⁺.

Found (ES⁺): 1691.7143. C₇₅H₁₂₀BrNO₃₅ requires 1691.7168.

mp: 58-60°C

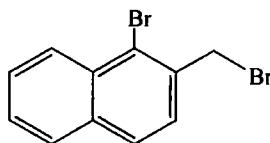
δ_{H} (CD₃OD): 8.21 (d, 1H, $J=10.0$, C(4')-*H*), 8.19 (d, 1H, $J=10.0$, C(8')-*H*), 7.88 (d, 1H, $J=7.2$, C(2')-*H*), 7.60 (t, 1H, $J=7.8$, C(7')-*H*), 7.52 (d, 1H, $J=6.8$, C(6')-*H*), 7.47 (t, 1H, $J=7.8$, C(3')-*H*), 5.3-5.1 (m, 7H, C(1)-*H*), 4.1-3.1 (m, 105H, of which 3.67 and 3.55 are for OCH₃ groups), 2.72 (t, 2H, $J=7.4$, ArCH₂-).

δ_c (CD₃OD): 174.6 (CONH), 139.1, 134.2, 133.5, 131.0 (C(2')), 128.2, 128.1, 127.5 (C(3')), 127.0 (C(8')), 124.9 (C(4')), 124.5, 100-98 (m, inc 99.5, 99.4, 99.3, C(1)-H), 84-78 (m, inc 83.2, 83.1, 82.8, 81.0, 80.6), 73-71 (m, inc 72.6, 72.3, 72.2), 63-58 (m, inc 61.8, 61.7, 59.7, 59.4, 59.1, 59.0), 41.5 (CH₂NHCO), 38.0 (ArCH₂-), 29.9 (-CH₂CONH).

ν_{\max} : 2922, 2895, 2823, 1669 (C=O), 1456, 1193, 1139, 1085, 1021, 967, 908, 854, 781, 754, 700, 668 cm⁻¹.

λ_{\max} (CH₃OH): 291 nm, $\epsilon=8415\text{M}^{-1}\text{cm}^{-1}$.

1-Bromo-2-bromomethylnaphthalene (80).



1-Bromo-2-bromomethylnaphthalene (**80**) was prepared following the procedure described by Adams and Binder.¹⁵ 1-Bromo-2-methylnaphthalene (**79**) (27.28 g, 110 mmol) and N-bromosuccinimide (21.3 g, 120 mmol) were dissolved in CCl₄ (300 cm³) under argon. Benzoyl peroxide (~0.1 g, cat.) was added and the solution heated to reflux for 18 hours. The solution was filtered and the solid residues washed with CCl₄ (20 cm³). Solvent was removed from the combined filtrates to give a yellow solid. The solid was filtered through a 1 cm silica plug (50% CH₂Cl₂/*n*-hexane) and recrystallised from 50% CH₂Cl₂/*n*-hexane to give a pale yellow crystalline solid (20.7 g, 69 mmol, 56 %).

$R_f=0.22$ (10% CH₂Cl₂/*n*-hexane, silica).

$m/e=298$ [M]⁺, 219 [M-Br]⁺.

Found (EI+): 297.8990. C₁₁H₈Br₂ requires 297.8993.

mp: 101-103°C (lit. 107-109)¹⁶.

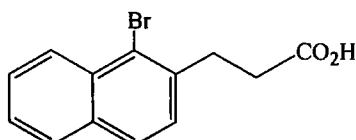
δ_H (CDCl₃): 8.34 (d, J=8.5, C(8)-H), 7.82 (d, J=8.0, C(5)-H), 7.79 (d, J=8.5, C(4)-H), 7.63 (ddd, J₁=8.4, J₂=6.8, J₃=1.6, C(7)-H), 7.55 (ddd, J₁=7.8, J₂=7.3, J₃=0.5, C(6)-H), 7.53 (d, J=8.0, C(3)-H), 4.88 (s, 2H, Ar-CH₂Br).

δ_c (CD₂Cl₂): 135.3, 134.4, 132.7, 128.6 (C(4)), 128.4 (C(5)), 128.1 (C(7)), 127.9 (C(8)), 127.7 (C(3)), 127.5 (C(6)), 125.0 (C(1)), 35.2 (Ar-CH₂Br).

ν_{\max} : 3738, 3646, 1552, 1500, 1437, 1327, 1256, 1194, 975, 865, 801, 749, 663, 576, 524, 495, 431, 403 cm^{-1} .

λ_{\max} (CH₃OH): 235nm, $\epsilon = 50,030 \text{ M}^{-1}\text{cm}^{-1}$; 286nm, $\epsilon = 5735 \text{ M}^{-1}\text{cm}^{-1}$.

3'-[2-(1-Bromonaphthyl)]propanoic acid (84).



Sodium ethoxide was generated by dissolving sodium (0.16 g, 6.96 mmol) in freshly distilled ethanol (20 cm^3) and stirring under argon at room temperature for 1 hour. Diethyl malonate (**81**) (1.06 g, 6.59 mmol) was added and the solution stirred for a further 30 minutes. 1-Bromo-2-bromomethylnaphthalene (**80**) was added and the solution stirred at room temperature for 18 hours. Suspended solid was removed by vacuum filtration and solvent removed under reduced pressure. The residual solid was purified by column chromatography (CH₂Cl₂, silica) to give the diester (**82**) as a white solid (1.46 g, 3.85 mmol, 56 %).

$R_f = 0.12$ (50% *n*-Hexane/CH₂Cl₂, silica).

m/e (ES⁺): 395 [M+NH₄]⁺, 379 [M+H]⁺.

The diester (**82**) was taken up in ethanol (50 cm^3) and aqueous sodium hydroxide (100 cm^3 , 2M) added. The solution was heated to reflux for 5 hours, chilled and taken to pH1 by the careful addition of HBr (48% in H₂O). The resulting diacid (**83**) was extracted into toluene (200 cm^3), solvent was removed under reduced pressure to yield a white solid.

$R_f = 0.00$ (10%MeOH/CH₂Cl₂, silica).

The diacid (**83**) was heated under vacuum by use of a Woods metal bath for 15 minutes. The resulting melt was allowed to cool and dissolved in THF (150 cm^3), filtered and solvent removed under reduced pressure. The resulting solid was partitioned between dichloromethane (150 cm^3) and aqueous sodium hydroxide

(100 cm³, 1M), filtered and the aqueous layer removed, chilled and taken to pH1 by the careful addition of aqueous hydrobromic acid (48%). The resulting precipitate was collected by vacuum filtration and dried to yield the acid as a yellow solid (0.64 g, 2.29 mmol, 35 % from 1-bromo-2-bromomethylnaphthalene (**80**)).

$R_f=0.53$ (10% THF/CH₂Cl₂, silica).

m/e (EI+): 278 [M]⁺, 199 [M-Br]⁺.

Found (EI+): 277.9943. C₁₃H₁₁BrO₂ requires 277.9942.

mp: 108-110°C (lit. 123-124°C)¹⁷.

δ_H (CDCl₃): 8.32 (d, 1H, J=8.4, C(8)-H), 7.82 (d, 1H, J=8.1, C(5)-H), 7.77 (d, 1H, J=8.4, C(4)-H), 7.60 (t, 1H, J=7.2, C(7)-H), 7.51 (t, 1H, J=7.5, C(6)-H), 7.41 (d, 1H, J=8.4, C(3)-H), 3.33 (t, 2H, J=7.8, ArCH₂R), 2.80 (t, 2H, J=7.8, -CH₂CO₂H).

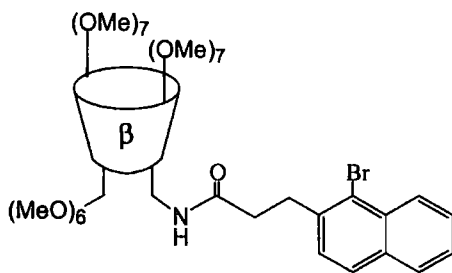
δ_C (CDCl₃): 177.3 (C=O), 137.5 (C(2)), 133.4, 132.5, 128.0 (C(3)), 127.9 (C(5)), 127.8 (C(4)), 127.5, 127.2 (C(8)), 126.2, 123.9, 33.7 (CH₂CO₂H), 32.4 (Ar-CH₂R).

ν_{max} : 3400-2900 (br), 1710 (C=O), 1595, 1412, 1287, 1220, 917, 820, 753, 671, 522 cm⁻¹.

Found: C: 55.1%, H:3.88%, Br: 28.2%. C₁₃H₁₁BrO₂.H₂O requires C: 55.1%, H: 4.08%, Br: 28.2%.

λ_{max} (THF): 288nm, $\epsilon = 6790M^{-1}cm^{-1}$.

6^A-[2'-(1'-Bromonaphthyl)ethylcarbamoyl]-6^A-deoxy-heptakis-(2,3-di-O-methyl)-6^B,6^C,6^D,6^E,6^F,6^G-hexa-O-methyl- β -cyclodextrin (59**).**



3'-[2-(1-Bromonaphthyl)]propanoic acid (**84**) (0.140 g, 0.502 mmol), mono-amino-per-O-methyl- β -cyclodextrin (**31**) (0.450 g, 0.319 mmol), EDC (0.185 g, 0.96 mmol), DMAP (0.14 g, 1.15 mmol) and 1-hydroxybenzotriazole (0.11 g, 0.82 mmol) were stirred in dichloromethane (5 cm³) under argon for 18 hours. The

solution was taken up in further dichloromethane (50 cm³), washed with water (20 cm³) and aqueous sodium hydroxide (20 cm³, 1M) and solvent removed under reduced pressure. The residual solid was purified by column chromatography (5% MeOH, 1% Et₃N, 94% CH₂Cl₂, silica) and dialysis (1000 MWCO filter) to yield a glassy white solid (0.29 g, 0.17 mmol, 54 %).

R_F=0.35 (10% MeOH/CH₂Cl₂, silica).

m/e (ES⁺): 1692 [M+NH₄]⁺.

mp: 64-66°C

δ_H (CD₃OD): 8.31 (d, 1H, J=8.4, C(8')-H), 7.90 (d, 1H, J=8.0, C(5')-H), 7.87 (d, 1H, J=8.4, C(4')-H), 7.64 (t, 1H, J=7.8), 7.56 (t, 1H, J=7.4), 7.49 (d, 1H, J=8.4, C(3')-H), 5.3-5.0 (m, 7H, C(1)-H), 4.1-3.0 (m, 103H, of which 3.66, 3.65 and 3.54 are for OCH₃ groups), 2.62 (t, 2H, J=7.5, ArCH₂-), 2.28 (t, 2H, J=7.5, -CH₂CO-).

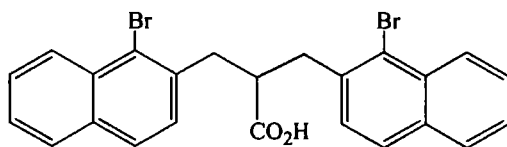
δ_C (CD₃OD): 173.2 (C=O), 138.7, 133.7, 132.6, 128.2, 128.1, 128.0, 127.6, 126.8, 126.2, 123.2, 99-98 (m, inc 98.5, 98.4, C(1)-H), 83-78 (m, inc 82.2, 82.1), 72-69 (m, inc 71.6, 71.2), 61-56 (m, inc 60.7, 58.3, 57.9), 40.6 (CH₂NHCO), 35.9 (ArCH₂-), 33.2 (-CH₂CONH).

ν_{max}: 2916, 2812, 1669 (C=O), 1446, 1363, 1016, 964, 855, 751, 669 cm⁻¹.

Found: C: 54.2%, H: 7.43%, N: 1.02%, Br: 4.10%. C₇₅H₁₂₀NBrO₃₅ requires C: 53.8%, H: 7.22%, N: 0.84%, Br: 4.76%.

λ_{max} (CH₃OH): 286nm, ε=5960M⁻¹cm⁻¹.

2'-[2-(1-Bromonaphthyl)methyl]-3'-[2-(1-bromonaphthyl)]-1'-propanoic acid (85).



Sodium ethoxide was generated by dissolving sodium (0.20 g, 8.70 mmol) in freshly distilled ethanol (20 cm³) and stirring under argon at room temperature for 1 hour. Diethyl malonate (**81**) (0.53 g, 3.30 mmol) was added and the solution stirred for a further 30 minutes. 1-Bromo-2-bromomethylnaphthalene (**80**) was added and the solution stirred at room temperature for 18 hours. Solvent was removed under reduced pressure, the residual solid was dissolved in ethanol (100 cm³) and aqueous

sodium hydroxide (2M, 100 cm³). The solution was heated to 100°C for 18 hours, chilled to 0°C and taken to a pH of 2 by the careful addition of hydrobromic acid (48 % aqueous). The solution was extracted into dichloromethane (2x200 cm³), solvent was removed under reduced pressure. The residual solid was purified by recrystallisation from boiling toluene to give the acid as fine colourless crystals (0.59 g, 1.18 mmol, 35 %).

$R_f=0.43$ (10% THF/CH₂Cl₂, silica).

m/e (EI+): 496 [M]⁺.

Found (EI+): 495.9668. C₂₄H₁₈Br₂O₂ requires 495.9674.

mp: 202-204°C

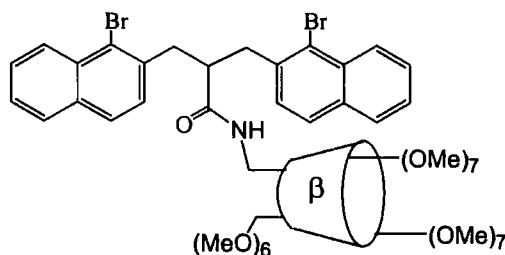
δ_H (d⁸-THF): 8.14 (dd, 2H, $J_1=8.5$, $J_2=0.5$, C(8)-H), 7.70 (dd, 2H, $J_1=7.5$, $J_2=0.5$, C(5)-H), 7.65 (d, 2H, $J_1=8.0$, C(4)-H), 7.43 (ddd, 2H, $J_1=8.4$, $J_2=7.0$, $J_3=1.5$, C(7)-H), 7.38-7.33 (m, 4H, Ar-H), 3.73-3.60 (m, 1H, CH₂CO₂H), 3.38-3.20 (m, 4H, ArCH₂R).

δ_C (d⁸-THF): 175.5 (C=O), 138.1 (C(2)), 134.5, 133.4, 129.7 (C(3)), 128.8 (C(5)), 128.1 (C(4)), 128.0, 127.8 (C(8)), 126.8, 124.9, 46.8 (CHCO₂H), 40.4 (Ar-CH₂R).

ν_{max} : 2980, 2922, 1700 (C=O), 1648, 1450, 1408, 1229, 1172, 1023, 825, 806, 739, 643, 522 cm⁻¹.

λ_{max} (THF): 289nm, $\epsilon = 11,000\text{M}^{-1}\text{cm}^{-1}$.

6^A-{1^{''},3^{''}-Bis-[2[']-(1[']-bromonaphthyl)]-2^{''}-butylcarbamoyl}-6^A-deoxy-heptakis-(2,3-di-O-methyl)-6^B,6^C,6^D,6^E,6^F,6^G-hexa-O-methyl- β -cyclodextrin (60).



2'-[2-(1-Bromonaphthyl)methyl]-3'-[2-(1-bromonaphthyl)]-1'-propanoic acid (**85**) (0.193 g, 0.388 mmol), mono-amino-per-O-methyl- β -cyclodextrin (**31**) (0.495 g, 0.350 mmol), EDC (0.10 g, 0.52 mmol), DMAP (0.07 g, 0.57 mmol) and 1-hydroxybenzotriazole (0.07 g, 0.52 mmol) were stirred in dichloromethane (10 cm³) under argon for 18 hours. Purification by column chromatography (CH₂Cl₂ to 3%

MeOH/CH₂Cl₂, silica) gave the amide (**60**) as a glassy white solid (0.54 g, 0.28 mmol, 81 %).

R_f=0.65 (10% MeOH/CH₂Cl₂, silica).

m/e (ES⁺): 1915 [M+Na]⁺, 968 [M+2Na]²⁺.

mp: 100-102°C.

δ_H (CDCl₃): 8.22 (d, 1H, J=8.4, C(8')-H), 8.20 (d, 1H, J=8.4, C(8')-H), 7.75 (d, 1H, J=7.5, C(5')-H), 7.73 (d, 2H, J=8.1, C(4')-H & C(5')-H), 7.66 (d, 1H, J=8.4, C(4')-H), 7.60-7.51 (m, 2H, C(7')-H), 7.51-7.37 (m, 2H, C(6')-H), 7.41 (d, 1H, J=8.4, C(3')-H), 7.40 (d, 1H, J=8.4, C(3')-H), 5.6-4.6 (m, 7H, C(1)-H), 3.9-2.4 (m, 108H, of which 3.59, 3.46 and 3.33 are for OCH₃ groups).

δ_C (CDCl₃): 173.9 (CONH), 137.2, 137.1, 133.4, 133.3, 132.4, 129.2, 129.1, 128.9, 128.8, 128.3, 128.0, 127.3, 127.1, 127.0, 126.1, 125.9, 124.3, 124.1, 99.2-98.0 (m, inc 99.0, 98.9, 98.8, 98.7, 98.4, 98.3, 98.2, C(1)-H), 82.5-79.0 (m, inc 82.0, 81.7, 80.9, 80.3, 80.1, 79.9, 79.7, 79.2), 72.0-69.0 (m, inc 71.3, 71.1, 70.9, 69.4), 61.8-60.8 (m, inc 61.3, 61.0), 59.5-58.0 (m, inc 58.9, 58.8, 58.6, 58.3), 48.4 (-CH₂CONH), 40.3, 40.0, 39.7.

ν_{max}: 2922, 2823, 1669 (C=O), 1451, 1189, 1139, 1085, 1017, 967, 913, 854, 813, 749, 700 cm⁻¹.

Found: C: 53.9%, H: 6.79%, N: 0.72%, Br: 8.64%. C₈₆H₁₂₇NBr₂O₃₅.H₂O requires C: 54.0%, H: 6.80%, N: 0.73%, Br: 8.35%.

λ_{max} (CH₃OH): 277nm, ε=10,076M⁻¹cm⁻¹, 287nm, ε=10,787M⁻¹cm⁻¹.

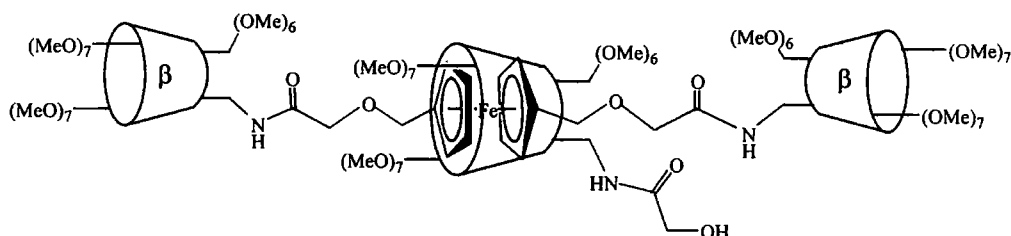
5.4 Experimental for Chapter 3.

Methyl cyclodextrin rotaxane and thread (**92** & **95**).

1, 1'- Bis(hydroxymethyl)ferrocene (**96**) (0.10 g, 0.40 mmol) was dissolved in anhydrous tetrahydrofuran (10 cm³) under argon and chilled to -70°C. Sodium hydride (0.30 g, 12.5 mmol) was added and the solution allowed to warm to room temperature and stirred for 1 hour. The solution was chilled to -70°C and mono-6-(chloromethylcarbonyl)-6-deoxy-per-O-methyl-β-cyclodextrin (**32**) (1.36g, 0.91mmol) in anhydrous tetrahydrofuran (10 cm³) added. The solution was allowed

to warm to room temperature and stirred under argon for 3 days. Solvent was removed under reduced to pressure, the residual solid was purified by preparative HPLC (Hypersil semiprep column, 95% MeOH/ H₂O) to give the rotaxane (**95**) (0.16 g, 0.034 mmol, 11%, $\tau_r=11.2$ min) and the thread (**92**) (0.24 g, 0.076 mmol, 19%, $\tau_r=5.7$ min) as pale yellow solids.

Rotaxane (**95**).



$R_f=0.73$ (10% MeOH/CH₂Cl₂, silica).

m/e (MALDI-TOF+, Linear): 4641 [M]⁺, 4623 [M-H₂O]⁺ (C₂₀₄H₃₅₁FeN₃O₁₀₈ requires 4630).

mp: 108-110°C.

δ_H (CD₃OD): 5.40-5.10 (m, 21H, C(1)-H), 4.44 (s, 4H, Fc-H), 4.33 (m, 4H, Fc-H), 4.26 (s, 4H, Fc-H), 4.188-3.10 (m, 317H, of which 3.63, 3.49 and 3.37 are for OCH₃).

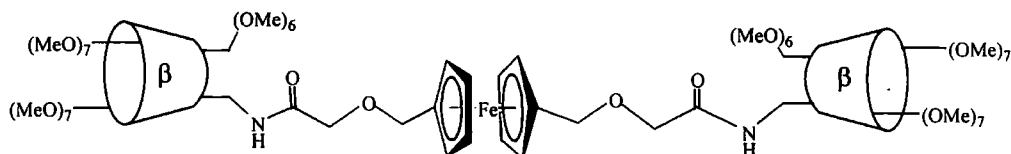
δ_C (CD₃OD): 100-99 (m, C(1)-H), 84-79, 73-69 (m, inc Fc peaks), 62-58 (m).

λ_{max} (CH₃OH): 433nm, $\epsilon = 229M^{-1}cm^{-1}$.

Found: C: 51.9%, H: 7.42%, N: 0.88%. C₂₀₄H₃₅₁FeN₃O₁₀₈.(H₂O)₄

requires C: 51.9%, H: 7.64%, N: 0.89%.

Thread (**92**).



$R_f=0.73$ (10% MeOH/CH₂Cl₂, silica).

m/e (MALDI-TOF+, Linear): 3173 [M]⁺ (C₁₄₀H₂₃₈FeN₂O₇₂ requires 3157).

mp: 95-98°C.

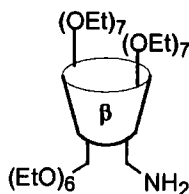
δ_{H} (CD₃OD): 5.30-5.10 (m, 14H, C(1)-H), 4.50-4.18 (m, 12H, Fc-H), 4.50-4.18 (m, 212H, inc OCH₃).

δ_{C} (CD₃OD): 100-99 (m, C(1)-H), 84-79, 73-69 (m, inc Fc peaks), 63-56 (m).

Found: C: 49.9%, H: 7.22%, N: 1.23%. C₁₄₀H₂₃₈FeN₂O₇₂·(H₂O)₈

requires C: 49.9%, H: 7.82%, N: 1.66%.

6^A-Amino-6^A-deoxy-heptakis-(2,3-di-O-ethyl)-6^B,6^C,6^D,6^E,6^F,6^G-hexa-O-ethyl- β -cyclodextrin (98).



Mono-6-azido-6-deoxy- β -cyclodextrin (**10**) (3.34 g, 2.88 mmol) was dissolved in anhydrous DMF (150 cm³) under argon. Sodium hydride (6.5 g, 270 mmol) was added in small portions over 1 hour and the solution stirred at room temperature for a further hour. Ethyl bromide (32 g, 295 mmol) was added dropwise and the solution stirred for 4 days at room temperature. Excess sodium hydride was quenched by the addition of methanol (100 cm³) and solvents removed under reduced pressure. The residual solid was partitioned between aqueous lithium chloride solution (300 cm³) and *n*-hexane (500 cm³). The hexane fraction was collected and solvent removed under reduced pressure to give mono-6-azido-6-deoxy-per-O-ethyl- β -cyclodextrin (**97**) as a pale yellow solid (4.85 g), which was used without further purification.

Mono-6-azido-6-deoxy-per-O-ethyl- β -cyclodextrin (**97**) was dissolved in ethanol (150 cm³) and hydrazine (1.9 g, 37 mmol) and palladium hydroxide (1% on carbon, 0.13 g) added. The solution was heated to reflux for 36 hours then filtered hot through a bed of celite and solvent removed under reduced pressure. The residual solid was purified by column chromatography (5% MeOH/CH₂Cl₂, silica) to give a white solid (3.09 g, 1.8 mmol, 63 %).

R_f=0.32 (10% MeOH/CH₂Cl₂, silica).

m/e (ES⁺): 1694 [M+H]⁺, 864 [M+2(NH₄)]²⁺.

mp: 60-61°C.

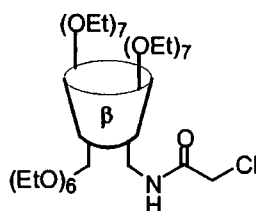
δ_H (CD₂Cl₂): 5.30-5.05 (m, 7H, C(1)-H), 4.10-2.90 (m, 83H), 1.30-1.05 (m, 60H, -OCH₂CH₃), 1.90 (br s, 2H, -NH₂).

δ_C (CD₂Cl₂): 99.9-98.3 (m, inc 98.8, 98.7, 98.6, C(1)), 81.0-78.0 (m, inc 80.6, 80.4, 80.0, 79.4, 79.2, 78.8, 78.6, 78.3), 72.3, 71.9-71.4 (m, inc 71.7), 70.0-68.8 (m, inc 69.8, 69.2, 69.0, 68.9), 67.3, 67.3, 67.1-66.7 (m, inc 66.8), 42.8 (C-NH₂), 15.87 (CH₂CH₃), 15.47 (CH₂CH₃).

ν_{\max} : 2972, 2928, 2869, 2360, 2340, 1376, 1351, 1141, 1105, 1024, 951, 884 cm⁻¹.

Found: C: 57.6%, H: 9.05%, N: 1.10%. (C₈₂H₁₅₁O₃₄N)₄.CH₂Cl₂ requires C: 57.6%, H: 8.90%, N: 0.81%.

6^A-(Chloromethylcarbamoyl)-6^A-deoxy-heptakis-(2,3-di-O-ethyl)-6^B,6^C,6^D,6^E,6^F,6^G-hexa-O-ethyl-β-cyclodextrin (99).



Mono-6-amino-6-deoxy-per-O-ethyl-β-cyclodextrin (**98**) (2.65 g, 1.56 mmol) and triethylamine (0.73 g, 7.2 mmol) were dissolved in freshly distilled ether (50 cm³) under argon and cooled to -50°C. Chloroacetylchloride (**33**) (1.42 g, 13 mmol) was added and the solution stirred at -50°C for 1 hour and at room temperature for a further hour. Methanol (50 cm³) was added and the solvent removed under reduced pressure. The resulting solid was purified by filtration through a 1cm silica plug (10% MeOH/CH₂Cl₂, silica) to give a pale yellow solid (2.68 g, 1.51 mmol, 97 % yield).

R_f =0.64 (10% MeOH/CH₂Cl₂, silica).

m/e (ES⁺): 1787 [M+NH₄]⁺, 903 [M+2(NH₄)]²⁺.

mp: 60-62°C

δ_H (CD₃OD): 5.3-5.1 (m, 7H, C(1)-H), 4.08 (s, 1H, COCH₂Cl), 4.00-3.10 (m, 83H), 1.3-1.1 (m, 60H, -OCH₂CH₃).

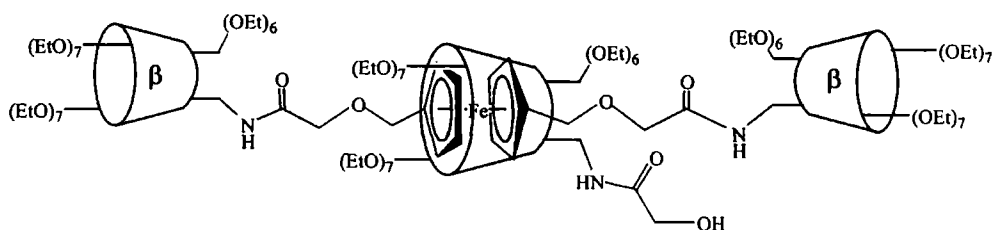
$\delta_{\text{C}}(\text{CD}_3\text{OD})$: 169.8 (NH-CO-), 101-99 (m, inc 100.2, 100.1, 99.7, C(1)), 83-79 (m, inc 82.5, 82.4, 81.8, 81.0, 80.6, 80.4, 80.0), 74-70 (m, inc 73.8, 73.5, 72.3, 71.5, 70.8, 70.1), 69-68 (m, inc 68.7), 44.2 (CH₂Cl), 42.9 (CH₂NHCO), 18-16 (m, inc 17.0, 16.9, 16.6, 16.5, CH₂CH₃).

ν_{max} : 2974, 2929, 2867, 1676 (C=O), 1531, 1443, 1378, 1141, 1103, 1025, 951, 885, 765, 701 cm⁻¹.

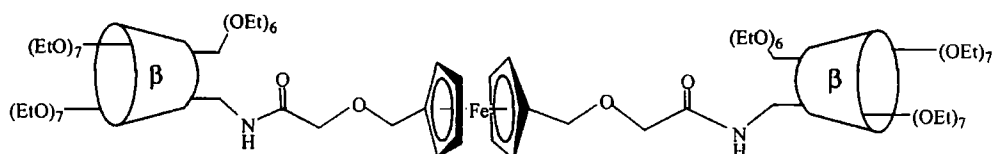
Satisfactory elemental analysis was not obtained for this compound.

Ethyl cyclodextrin rotaxane and thread (93 & 100).

Rotaxane (100).



Thread (93).



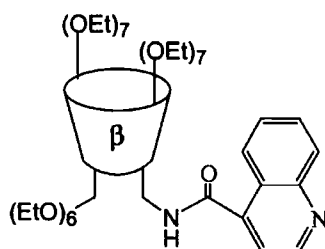
1, 1'- Bis(hydroxymethyl)ferrocene (**96**) (0.049 g, 0.20 mmol) and mono-6-(chloromethylcarbamoyl)-6-deoxy-per-O-ethyl- β -cyclodextrin (**99**) (1.03 g, 0.58 mmol) were dissolved in anhydrous tetrahydrofuran (10 cm³) under argon and stirred at -70°C for 30 minutes. Sodium hydride (0.50 g, 12.5 mmol, 60% in mineral oil) was added and the solution stirred at -70°C for 1 hour, then allowed to warm to room temperature and stirred for a further 2 days. Solvent was removed under reduced to pressure, the residual solid was purified by column chromatography (5% MeOH/CH₂Cl₂, silica) to give a mixture of the rotaxane (**100**) and thread (**93**) as a pale yellow solid (0.68 g).

$R_f=0.64$ (10% MeOH/CH₂Cl₂, silica).

m/e (MALDI-TOF+, Linear): 5464 [M]⁺ ((100) C₂₆₄H₄₆₉FeN₃O₁₀₇ requires 5466),
3716 [M]⁺ ((93) C₁₈₀H₃₁₆FeN₂O₇₂ requires 3714).

δ_H (CDCl₃): 5.30-5.10 (m, C(1)-H), 4.30-4.10 (m, Fc-H), 4.10-3.10 (m, inc
OCH₂CH₃), 1.30-1.10 (m, OCH₂CH₃).

**6^A-(4'-Quinolylcarbamoyl)-6^A-deoxy-heptakis-(2,3-di-O-ethyl)-
6^B,6^C,6^D,6^E,6^F,6^G-hexa-O-ethyl- β -cyclodextrin (94).**



Quinoline-4-carboxylic acid (101) (0.020 g, 0.116 mmol), 1-hydroxybenzotriazole (0.020 g, 0.148 mmol), EDC (0.040 g, 0.209 mmol) and DMAP (0.040 g, 0.327 mmol) were dissolved in dichloromethane (3 cm³) and stirred at room temperature for 30 minutes. Mono-amino-per-O-ethyl- β -cyclodextrin (0.20 g, 0.12 mmol) was added and the solution stirred under argon for a further 18 hours. The solution was taken up in further dichloromethane (50 cm³), washed with water (15 cm³) and aqueous sodium hydroxide (15 cm³, 1M) and solvent removed under reduced pressure. The residual solid was purified by column chromatography (3% MeOH, 1% Et₃N, 96% CH₂Cl₂, silica) to give a glassy white solid (0.172 g, 0.092 mmol, 80 %).

$R_f=0.68$ (15%MeOH, 5%Et₃N, 80% CH₂Cl₂, silica).

m/e (ES+): 1867 [M+NH₄]⁺, 934 [M+H+NH₄]²⁺.

mp: 74-76°C.

δ_H (CD₃OD): 8.96 (d, 1H, J=4, C(3')-H), 8.27 (d, 1H, J=8, C(8')-H), 8.13 (d, 1H, J=8, C(5')-H), 7.87 (td, 1H, J₁=8, J₂=1, C(7')-H), 7.71 (td, 1H, J₁=8, J₂=1, C(6')-H), 7.60 (d, 1H, J=4, C(2')-H), 5.4-5.1 (m, 7H, C(1)-H), 4.1-3.1 (m, 83H), 1.3-1.1 (m, 60H, -CH₃).

δ_C (CD₃OD): 168.6 (NHCO), 149.9 (C(3')), 148.0, 143.6, 130.4, 128.7 (C(5')), 127.7 (C(7')), 125.6, 124.9, (C(8')), 119.1, 119.0, 97-97 (m, inc 98.2, C(1)), 81-77 (m, inc 80.6, 80.2, 80.0, 78.2), 72-68 (m, inc 71.4, 69.5, 68.8), 67-66 (m, inc 66.7, 66.6, 66.5), 40.5 (CH₂NHCO), 15.1-14 (m, inc 15.0, 14.6, 14.5, -CH₃).

ν_{\max} : 2958, 2864, 1669 (C=O), 436, 1374, 1099, 1021, 881, 694, 497 cm⁻¹.

Found: C: 59.2%, H:8.45%, N:1.51%. C₉₂H₁₅₆N₂O₃₅.CH₃OH requires C: 59.3%, H: 8.57%, N:1.49%.

λ_{\max} (CH₃OH): 284nm, ϵ =6540 M⁻¹cm⁻¹.

5.5 References.

- ¹ S. E. Brown, J. H. Coates, D. R. Coghlan, C. J. Easton, S. J. van Eyk, W. Janowski, A. Lepore, S. F. Lincoln, Y. Luo, B. L. May, D. S. Schiesser, P. Wang, M. L. Williams, *Aust. J. Chem.*, 1993, **46**, 953.
- ² N. Zhong, H.-S. Byun, R. Bittman, *Tett. Lett.*, 1998, **39**, 2919.
- ³ R.P. Bonomo, V. Cucinotta, F. D'Alessandro, G. Impellizzeri, G. Maccarrone, G. Vecchio, E. Rizzarelli, *Inorg. Chem.*, 1991, **30**, 2708.
- ⁴ H. Parrot-Lopez, F. Djedaani, B. Perly, A.W. Coleman, H. Galons, M. Miocque, *Tetrahedron Lett.*, 1990, **31**, 1999.
- ⁵ Z. Chen, J. S. Bradshaw, M. L. Lee, *Tetrahedron Lett.*, 1996, **37**, 6831.
- ⁶ G. Yi, W. Li, J. S. Bradshaw, A. Malik, M. L. Lee, *J. Heterocyclic Chem.*, 1995, **32**, 1715.
- ⁷ M. Woods, Ph. D. Thesis, University of Durham, 1998.
- ⁸ R. G. Jones, Q. F. Soper, O. K. Behrens, J. W. Corse, *J. Am. Chem. Soc.*, 1948, **70**, 2843.
- ⁹ H. H. Hodgson, J. S. Whitehurst, *J. Chem. Soc.*, 1947, 80.
- ¹⁰ J. P. Schaefer, J. Higgins, *J. Org. Chem.*, 1967, **32**, 1607.
- ¹¹ A. Dastan, M. N. Tahir, D. Úlkú, P. B. Sheulin, M. Balci, *J. Org. Chem.*, 1997, **62**, 4018.
- ¹² Carbon-13 NMR Spectroscopy, H.-O. Kalinowski, S. Berger, S. Brown, John Wiley & Sons, 1988, p344.
- ¹³ J. Ruggli, R. Preuss, *Helv. Chim. Acta*, 1941, **24**, 1345.

-
- ¹⁴ P. Dizabo, M.-F. Mouneyrac, *Bull. Soc. Chim. Fr.*, 1968, 2957.
- ¹⁵ R. Adams, L. O. Binder, *J. Am. Chem. Soc.*, 1941, **63**, 2771.
- ¹⁶ J. J. Cornejo, S. Ghodsi, R. D. Johnson, R. Woodling, B. Rickman, *J. Org. Chem.*, 1983, **48**, 3869.
- ¹⁷ L. A. Carpino, Y. -Z. Lin, *J. Org. Chem.*, 1990, **55**, 247.

Appendices

Appendix A. Calculation of Binding Constants by Benesi-Hildebrand Analysis.

Binding between a cyclodextrin and a luminescent guest can be monitored by perturbations in luminescent emission intensity. The 1:1 binding constant (K_{11}) can be calculated from the magnitude of change of emission intensity with the change in concentration of the guest.¹

The complex (HG) between the cyclodextrin host (H) and the luminescent guest (G) is formed by an equilibrium process, for a two state, or 1:1 system the equilibrium is described as shown in equation 1.

Equation 1.



The stability of the complex can be described in terms of the formation constant, K_f or K_{11} , or a dissociation constant K_d as:

Equation 2.

$$K_f = \frac{[HG]}{[H][G]}$$

where K_d is the reciprocal of K_f :

Equation 3.

$$K_d = \frac{[H][G]}{[HG]}$$

The value of K_f is typically found by using the Benesi-Hildebrand equation.² If the system is considered to be a 1:1 complex with the cyclodextrin in an excess of

¹ Adapted from; K. A. Connors, *Binding Constants, The Measurement of Molecular Complex Stability*, John Wiley and Sons, New York, 1987.

² H. A. Benesi, J. J. Hildebrand, *J. Am. Chem. Soc.*, 1949, 71, 2703.

concentration over the guest, and both host and guest in dilute solution (ie $A_{ex} < 0.1$) so that $I_f \propto I_0$,* in the absence of the guest, the emission intensity of the host (I_H) at a given wavelength is:

Equation 4.

$$I_H = aI_0\Phi_H[H]_t$$

where Φ_H is the extinction coefficient for uncomplexed host, $[H]_t$ is the total concentration of the host, a is a constant and I_0 is the intensity of excitation. In the presence of the guest the total emission intensity (I_{HG}) becomes:

Equation 5.

$$I_{HG} = aI_0\Phi_H[H] + aI_0\Phi_{HG}[HG]$$

where Φ_{HG} is the quantum yield for emission from complexed host due to energy transfer from the complexed guest and $[H]$ is concentration of free host. Combining this with the mass balance:

$$[H]_t = [H] + [HG]$$

we obtain:

Equation 6.

$$I_{HG} = aI_0\Phi_H[H]_t + aI_0\Delta\Phi_{HG}[HG]$$

where

$$\Delta\Phi_{HG} = \Phi_{HG} - \Phi_H$$

Given that $\Delta I = I_{HG} - I_H$ and together with the definition of K_f (equation 2) and equations 4 and 6 we obtain:

* Where A_{ex} is the absorbance at the excitation wavelength and I_f is the intensity of fluorescent emission.

Equation 7.

$$\Delta I = I_{HG} - I_H = \alpha I_0 K_f \Delta \Phi_{HG} [H] [G]$$

The mass balance for the host can be written as:

Equation 8.

$$[H] = \frac{[H]_t}{1 + K_f [G]}$$

which, upon substitution in equation 7 gives:

Equation 9.

$$\frac{\Delta I}{\alpha I_0} = \frac{[H]_t K_f \Delta \Phi_{HG} [G]}{1 + K_f [G]}$$

which can be linearised and inverted to give the Benesi-Hildebrand equation.

Equation 10.

$$\frac{\alpha I_0}{\Delta I} = \frac{1}{[H]_t K_f \Delta \Phi_{HG} [G]} + \frac{1}{[H]_t \Delta \Phi_{HG}}$$

Hence a plot of $1/\Delta I$ versus $1/[G]$ gives a straight line graph, and allows the calculation of K_f .

Appendix B. Research Colloquia and Lectures.

The author attended the following colloquia between October 1996 and September 1999.

1996

- October 14 Professor A. R. Katritzky, University of Gainesville, University of Florida, USA
Recent Advances in Benzotriazole Mediated Synthetic Methodology
- October 16 Professor Ojima, Guggenheim Fellow, State University of New York at Stony Brook
Silylformylation and Silylcarbocyclisations in Organic Synthesis
- October 22 Professor Lutz Gade, Univ. Wurzburg, Germany
Organic transformations with Early-Late Heterobimetallics: Synergism and Selectivity
- October 22 Professor B. J. Tighe, Department of Molecular Sciences and Chemistry, University of Aston
Making Polymers for Biomedical Application - can we meet Nature's Challenge?
(Joint lecture with the Institute of Materials)
- November 13 Dr G. Resnati, Milan
Perfluorinated Oxaziridines: Mild Yet Powerful Oxidising Agents
- November 27 Dr Richard Templer, Imperial College, London
Molecular Tubes and Sponges
- December 3 Professor D. Phillips, Imperial College, London
"A Little Light Relief" -

1997

- January 15 Dr V. K. Aggarwal, University of Sheffield
Sulfur Mediated Asymmetric Synthesis
- January 16 Dr Sally Brooker, University of Otago, NZ
Macrocycles: Exciting yet Controlled Thiolate Coordination
Chemistry
- January 22 Dr Neil Cooley, BP Chemicals, Sunbury
Synthesis and Properties of Alternating Polyketones
- February 12 Dr Geert-Jan Boons, University of Birmingham
New Developments in Carbohydrate Chemistry
- February 26 Dr Tony Ryan, UMIST
Making Hairpins from Rings and Chains
- March 4 Professor C. W. Rees, Imperial College
Some Very Heterocyclic Chemistry
- March 5 Dr. J. Staunton FRS, Cambridge University
Tinkering with biosynthesis: towards a new generation of antibiotics
- October 8 Professor E Atkins, Department of Physics, University of Bristol
Advances in the control of architecture for polyamides: from nylons
to genetically engineered silks to monodisperse oligoamides
- October 23 Professor M R Bryce, University of Durham, Inaugural Lecture
New Tetrathiafulvalene Derivatives in Molecular, Supramolecular and
Macromolecular Chemistry: controlling the electronic properties of
organic solids

- October 29 Professor R Peacock, University of Glasgow
Probing chirality with circular dichroism
- October 28 Professor A P de Silva, The Queen's University, Belfast
Luminescent signalling systems"
- November 5 Dr M Hii, Oxford University
Studies of the Heck reaction
- November 11 Professor V Gibson, Imperial College, London
Metallocene polymerisation
- November 12 Dr J Frey, Department of Chemistry, Southampton University
Spectroscopy of liquid interfaces: from bio-organic chemistry to
atmospheric chemistry
- November 20 Dr L Spiccia, Monash University, Melbourne, Australia
Polynuclear metal complexes
- November 25 Dr R Withnall, University of Greenwich
Illuminated molecules and manuscripts
- November 26 Professor R W Richards, University of Durham, Inaugural Lecture
A random walk in polymer science
- December 2 Dr C J Ludman, University of Durham
Explosions
- December 3 Professor A P Davis, Department. of Chemistry, Trinity College
Dublin.
Steroid-based frameworks for supramolecular chemistry

1998

- January 14 Professor D Andrews, University of East Anglia
Energy transfer and optical harmonics in molecular systems
- February 3 Dr J Beacham, ICI Technology
The chemical industry in the 21st century
- February 18 Professor G Hancock, Oxford University
Surprises in the photochemistry of tropospheric ozone
- February 24 Professor R Ramage, University of Edinburgh
The synthesis and folding of proteins
- October 21 Professor P Unwin, Department of Chemistry, Warwick University
Dynamic Electrochemistry: Small is Beautiful
- October 23 Professor J C Scaiano, Department of Chemistry, University of
Ottawa, Canada
In Search of Hypervalent Free Radicals, RSC Endowed Lecture
- October 27 Professor A Unsworth, University of Durham
What's a joint like this doing in a nice girl like you?
In association with The North East Polymer Association
- October 28 Professor J P S Badyal, Department of Chemistry, University of
Durham
Tailoring Solid Surfaces, Inaugural Lecture
- November 4 Dr N Kaltsoyannis, Department of Chemistry, UCL, London
Computational Adventures in d & f Element Chemistry
- November 11 Dr M Wills, Department of Chemistry, University of Warwick
New Methodology for the Asymmetric Transfer Hydrogen of Ketones

- November 12 Professor S Loeb, University of Windsor, Ontario, Canada
From Macrocycles to Metallo-Supramolecular Chemistry
- November 17 Dr J McFarlane University of Glasgow.
Nothing but Sex and Sudden Death!
- November 18 Dr R Cameron, Department of Materials Science & Metallurgy,
Cambridge University
Biodegradable Polymers
- November 24 Dr B G Davis, Department of Chemistry, University of Durham
Sugars and Enzymes
- December 1 Professor N Billingham, University of Sussex
Plastics in the Environment - Boon or Bane
In association with The North East Polymer Association.
- 1999**
- January 19 Dr J Mann, University of Reading
The Elusive Magic Bullet and Attempts to find it?
- January 20 Dr A Jones, Department of Chemistry, University of Edinburgh
Luminescence of Large Molecules: from Conducting Polymers to
Coral Reefs
- February 9 Professor D J Cole-Hamilton, St. Andrews University
Chemistry and the Future of life on Earth
- February 17 Dr B Horrocks, Department of Chemistry, Newcastle University
Microelectrode techniques for the Study of Enzymes and Nucleic
Acids at Interfaces

May 11 Dr John Sodeau, University of East Anglia
Ozone Holes and Ozone Hills

Appendix C. Conferences.

The author attended the following meetings.

Stereochemistry at Sheffield, University of Sheffield, December 1996.

RSC Dalton Regional Scottish Meeting, University of Edinburgh, February 1997.

21st Century Heterocyclic Chemistry, University of Sunderland, May 1997.

RSC Young Chemists Symposium * and Autumn Meeting *, University of Aberdeen, September 1997.

Stereochemistry at Sheffield, University of Sheffield, December 1997.

RSC Macrocyclic and Supramolecular Chemistry Group, Annual Meeting, University of Nottingham, January 1998.*

RSC Young Chemists Symposium * and National Congress *, University of Durham, April 1998.

XXIII International Symposium on Macrocyclic Chemistry, Turtle Bay Hilton, Oahu, Hawaii, June 1998.*

New Horizons in Industrial and Environmental Sensing, University of Durham, September-October 1997.

ICI Poster Presentation, University of Durham, December 1997* (1st prize winner)

RSC Macrocyclic and Supramolecular Chemistry Group, Annual Meeting,
University of Surrey, January 1999.*

* Indicates poster presentation.

